ISSN: 2764-5886

Volume 5· Nº 1 · March 2022

Journal of Bioengineering, Technologies and Health

An Official Publication of
SENAI CIMATEC

ISSN: 2764-5886

Volume 5 • Number 1 • March 2022

JOURNAL OF BIOENGINEERING TECHNOLOGIES AND HEALTH

An Official Publication of SENAI CIMATEC

PUBLISHED BY SENAI CIMATEC

Sistema FIEB | SENAI CIMATEC
PELO FUTURO DA INOVAÇÃO

March 2022
Printed in Brazil

JOURNAL OF BIOENGINEERING, TECHNOLOGIES AND HEALTH

An Official Publication of SENAI CIMATEC

JOURNAL OF BIOENGINEERING AND TECHNOLOGY APPLIED TO HEALTH

Volume 5 • Number 1 *March 2022*

SUMMARY

Editorial

Original Articles

Review Articles

The Journal of Bioengineering, Technologies and Health (JBTH) is an official publication of the SENAI CIMATEC (Serviço Nacional de Aprendizagem Industrial - Centro Integrado de Manufatura e Tecnologia). It is published quarterly (March - June - September - December) in English by SENAI CIMATEC – Avenida Orlando Gomes, 1845, Piatã, Zip Code: 41650-010, Salvador-Bahia-Brazil; phone: (55 71) 3879-5501. The editorial offices are at SENAI CIMATEC.

Editorial Office

Correspondence concerning subscriptions, advertisements, claims for missing issues, changes of address, and communications to the editors should be addressed to the Deputy Editor, Dr. Roberto Badaró, SENAI CIMATEC (Journal of Bioengineering, Technologies and Health – JBTH) – Avenida Orlando Gomes, 1845, Piatã, Zip code: 41650-010, Salvador-Bahia-Brazil; phone: (55 71) 3879-5501; or sent by e-mail: jbth@fieb.org.br / jbth.cimatec@gmail.com.

Permissions

COVER: Robot checking brain, test result with computer interface, futuristic human brain analysis, innovative technology in science and medicine concept. Photo: istock gallery.

Postmaster

Send address changes to JBTH, Avenida Orlando Gomes, 1845, Piatã, Zip Code: 41650-010, Salvador-Bahia-Brazil.

Information by JBTH-SENAI CIMATEC

Address: Avenida Orlando Gomes, 1845, Piatã, Zip Code: 41650-010, Salvador-Bahia-Brazil
Home-page: www.jbth.com.br
E-mail: jbth@fieb.org.br / jbth.cimatec@gmail.com
Phone: (55 71) 3879-5501 / 3879-5500 / 3879-9500

DOI:10.34178/jbth.v5i1

New Approaches of JBTH

Roberto Badaró[1*], Luciana Bastianelli[2]
Director of ISI SENAI CIMATEC; Managing Editor JBTH

The Journal of Bioengineering and Technology Applied to Health (JBTH), an official publication of SENAI CIMATEC, was launched in 2018 to provide an opportunity to researchers and scientists to explore the advanced and latest research developments, advancement discoveries, and applications in the field of bioengineering and technologies applied to health. It aimed to create a Brazilian Journal of reference for the national and international scientific world, supporting its proposal for the quality of the selected articles and the editions.

Over the years, JBTH has maintained these projected expectations through the quality standard of journals published in print and online, in addition to the gradual increase in the number of articles, the maintenance of periodicity and indexing of the Journal (Research Gate by Elsevier, Latindex, Ulrich's Database, Google Scholar, CAS, CAB, DOAJ, Scielo and Lilacs, the last two still being analyzed).

However, due to the increase in the number of articles denied by the JBTH that included in their scope several areas related to engineering and bioengineering, chemistry, and technologies, but not directly linked to the health area, many highly relevant papers had to be out of the Journal. As one of the important responsibilities of the Editorial Board is to evaluate the scope of the papers, they have stressed how significant the other areas of SENAI CIMATEC advances are to scientific discovery and development and decided to extend the scope of JBTH to include papers that provide the engineerings, bioengineering, technologies, chemistry, and related areas, but not linked just for health.

In this sense, we have already received many strong submissions in many fields we expected. Now, the Journal reflects the evolution we have seen. We ensure it remains relevant and interesting to our readers and researchers. We've had March and part of April issues ready for publication.However, not to lose the indexes DOI, and Crossref, the acronym, and the website remained the same, changing only the name, the editorial board, and the scope of the Journal. Therefore, the Journal is now called "**The Journal of Bioengineering, Technologies, and Health (JBTH)**".

Received on 10 January 2022; revised 17 February 2022.
Address for correspondence: Dr. Roberto Badaró. Av. Orlando Gomes, 1845 - Piatã, Salvador - BA- Brazil. Zipcode: 41650-010. E-mail: rbadaro884@gmail.com / badaro@fieb.org.br. DOI 10.34178/jbth.v5i1.186.

J Bioeng. Tech. Health 2022;5(1):1-2.

Nevertheless, this is not a formal change in policy that will shift the editorial process going forward. It is an expansion of its scope, which continues to strictly follow the already established standards of an international publication. The papers should still be submitted as regular manuscripts and follow the same preparation guidelines as before.The expansion of new horizons for the JBTH aims at a broad, inter and multidisciplinary audience of academic and industry researchers actively involved in research, and will directly imply a greater production of articles submitted to the Journal. The successive step for next year is to make JBTH bimonthly and index it in Scopus and Pubmed/Medline.

Heterologous Expression, Purification, and Immune-Based Assay Application of Soluble SARS-CoV-2 Nucleocapsid Protein

Vinicius Rocha[1]*, Mariana Bandeira[1], Eduarda Lima[1], Cássio Meira[1,2], Breno Cardim[1,2], Emanuelle Santos[1], Milena Soares[1,2]

[1]Institute of Technology and Health, SENAI CIMATEC;

[2]Gonçalo Moniz Institute Oswaldo Cruz Foundation (FIOCRUZ); Salvador, Bahia, Brazil

The serological monitoring of SARS-CoV-2 infection using the measurement of IgG is an important tool to determine the number of infected people in a population, and the disease spreading. One of the most important proteins from SARS-CoV-2 applied to immune-based assays is the nucleocapsid protein, also known as N protein. This is an abundant protein in the pathogen and exerts important functions in viral viability and replication. Moreover, protein N is highly immunogenic. The use of N protein as a recombinant protein is difficult since this biomolecule is mainly produced inside inclusion bodies in *Escherichia coli*. In this work, we present a simple and easy method for the expression and purification of soluble his-tagged N protein, suitable for serological assays, such as ELISA. ELISA assays using this recombinant protein presented 100% of specificity and 86% of sensitivity. The protocol for expression and purification of this recombinant protein can be applied in low infrastructure laboratories, without equipment dedicated to protein expression. This work may help other research groups to develop serological assays to monitor antibody production against SARS-CoV-2.

Keywords: SARS-CoV-2. ELISA. Protein N. Recombinant Protein. Purification.

Abbreviations: COVID-19: Corona Virus Disease-19; Protein N: Nucleocapsid protein; IgG: Immunoglobulin G; *E. coli*: *Escherichia coli*; ELISA: Enzyme-Linked ImmunoSorbent Assay; RT-qPCR: Reverse transcriptase-quantitative polymerase chain reaction; CLIA: Chemiluminescent Immunoassay; SARS-CoV-2: Severe Acute Respiratory Syndrome Coronavirus 2; WHO: World Health Organization; LB: Luria-Bertani; TB: Terrific Broth; IPTG: Isopropyl β-D-1-thiogalactopyranoside; RPM: Rotation per minute; PBS: Phosphate buffer saline; pH: Hydrogen potential; DTT: Ditiotreitol; EDTA: Ethylenediaminetetraacetic acid; SDS-PAGE: Sodium dodecyl sulfate-polyacrylamide gel electrophoresis; HRP: Horseradish peroxidase; TBS: Tris-buffered saline; TMB: tetramethylbenzidine; ROC: Receiver Operator Characteristic; kDa: kilodaltons; GFP-6His: 6-histidine tagged green fluorescent protein; OD: Optical density; IMAC: Immobilized metal affinity chromatography.

The novel coronavirus (SARS-CoV-2), is one of the highly pathogenic β-coronaviruses [1] and causes COVID-19. It was initially identified in Wuhan province, China, in December 2019, and declared an international health emergency on January 30, 2020, by the World Health Organization (WHO) [2]. Since its emergence in Asia, it has spread to all continents, affecting countries around the world. Moreover, it has led well-structured health systems to collapse due to the exponential increase in hospitalizations as a result of its high transmissibility potential [3].

Received on 18 December 2021; revised 23 February 2022.
Address for correspondence: Vinicius Pinto Costa Rocha. Av. Orlando Gomes, 1845 - Piatã, Salvador - BA- Brazil. Zipcode: 41650-010. E-mail: vinicius.rocha@fieb.org.br.
DOI 10.34178/jbth.v5i1.187.

J Bioeng. Tech. Health 2022;5(1):3-10.

Given the accelerated spread and symptoms common to other diseases, early diagnosis of COVID-19 has become a critical step to treat infected patients, control and monitor disease transmission, and practice social isolation [1]. The direct detection of the virus is possible by molecular diagnostic performed through reverse transcriptase-quantitative polymerase chain reaction (RT-qPCR) [4]. However, this diagnostic method is not compatible with mass testing of the population and does not match the point of care features. To solve this issue and provide a mass population diagnostic screening, serological tests are being used due to their easy manipulation and lower cost. Thus, the need for studies about the coronavirus and its markers grew so that there was development, production, and application of mass tests for disease detection as a strategy to prevent the further spread of the virus [5, 6].

The main component of a serological test kit is the target for antibody recognition during the assay, usually being a recombinant protein or fragments of the full-length polypeptide. One of the main proteins encoded in the SARS-CoV-2 genome and one of the most conserved among coronaviruses is the nucleocapsid protein, or N protein [7, 8]. This protein participates directly in infection in the cell by playing a key role during viral self-assembly and viral genome packaging [7, 9]. Its participation during infection and its high expression makes the N protein immunogenic and highly abundant in the infected cell, turning it into an important disease marker antigen [7, 8, 10].

SARS-CoV-2 N protein is an important target to pursue and has become a major ally of researchers in the development of diagnostic tests and the rapid, accurate, and simple screening for coronavirus contamination, either through antigen or specific antibody detection [9]. The N protein recombinant production and its antigenic potential for application in serological diagnostics have been previously explored [11].

The N protein produced in *E. coli* has been applied in serological diagnostics. However, such recombinant productions are either from inclusion bodies [12], as a fragment [11] or expressed using robust approaches to increase protein solubility [13]. Thus, the present work aims to express and purify the recombinant native and soluble N protein for use in serological tests, such as ELISA (enzyme-Linked ImmunoSorbent Assay) and CLIA (Chemiluminescent Immunoassay), to effectively and accurately detect the presence of antibodies against SARS-CoV-2. To accomplish this goal, we used the pET21a vector and a codon-optimized sequence for *E. coli* expression, producing a recombinant protein fused to a 6-histidine tag at the C-terminal domain. Using this construct, we set up a protocol for protein expression and purification using current reagents and avoiding the requirement of robust equipment and chromatographic columns.

The method applied in this work does not require expensive and robust equipment and can be easily replicated in laboratories with minimal infrastructure to produce recombinant proteins. The study was conducted according to the guidelines of the Declaration of Helsinki, and approved by the Ethics Committee of the integrated campus of manufacturing and technology (CIMATEC – Salvador, BA, Brazil) (approval number 4.334.505). This research received funding from SENAI National Department (SENAI DN – Grant Number 329266).

The *E. coli* soluble fraction lysate was incubated with the Ni-NTA agarose beads, the material was collected in an empty column to retain the immobilized phase. The beads were exhaustively washed with 50 mM imidazole to remove the low-biding contaminants, followed by serial elution with imidazole at 250 and 500 mM. Figure 1A shows the SDS-PAGE containing the diluted soluble fraction (1) and elution of soluble N protein of SARS-CoV-2 (2-5). The first incubation of the beads with the 250 mM imidazole solution gave us a small amount of recombinant protein (2) around 48 kDa. However, most of the N protein was eluted in the second wash with 250 mM imidazole solution (3). The elution with 500 mM of imidazole removed the remaining protein still adhered to the surface of the beads (4 and 5). All the aliquots were pooled and submitted to concentration and buffer exchange (6), followed by storage at -80° C. It is noteworthy that buffer exchange is pivotal for protein stabilization in solution since freeze and thawing in absence of glycerol rendered low-quality protein, based on downstream immunoassay performed (data not shown).

To confirm the presence of a recombinant 6-histidine tagged protein, we performed western blotting targeting the histidine tag in the C-terminal end. The eluted samples (1 and 2) were detected at around 48 kDa. As a positive control, we used a 6-histidine tagged green fluorescent protein (GFP-6His) detected at 30 kDa (3) (Figure 1B). To confirm if the soluble recombinant protein would be suitable for immune-based assays, we performed western blotting using convalescent sera collected

fourteen days after SARS-CoV-2 RNA detection by RT-qPCR. The convalescent sera were able to recognize the 48 kDa recombinant protein, corresponding to the viral N protein (Figure 1C).

An ELISA assay was standardized using the soluble recombinant N protein, based on the need to develop a specific and sensitive immune-based assay to detect antibodies as earlier as possible in the sera of patients. The astringent cut-off was derived from the mean plus three standard deviations of the OD values detected in 63 negative serum samples. The mean OD values from positive samples collected either 7 or 14 days after positive RT-qPCR results, were significantly higher than OD from negative samples (Figure 2). Using the cut-off value of 0.11, it was possible to detect anti-N protein IgG in 25 from 29 positive samples selected after 14 days of positive PCR diagnostic, resulting in a sensitivity of 86% (Figure 3). Regarding the positive samples selected from patients after 7 days of positive RT-qPCR results, IgG was detected in 29 out of 49 patients, rendering a sensitivity of 59%. The assay presented a specificity of 100% since any negative serum samples generated OD values above 0.11. The calculated ROC curve presented the AUC equal to 0.9637 (95% confidence interval 0.9329 to 0.9945) and 0.9918 (95% confidence interval 0.9794 to 1.000) for patient samples collected 7 and 14 days after positive RT-qPCR result, respectively. Moreover, the p values found were below 0.0001 for both RT-qPCR positive sample groups. For comparison, most of the samples were also submitted to ELISA using a commercial N protein as a coating antigen. Thirty-three from 35 samples collected after 14 days of symptoms onset was positive rendering a sensitivity of 95%. All the 48 samples collected from patients after 7 days of symptoms onset were detected above the cut-off (0.07), rendering a sensitivity of 100%. None of the negative samples were detected as positive (100% specificity).

Indirect diagnosis by antibody detection is important to understand the immunological response against the pathogen and the spread of COVID-19. In addition, it is an important tool to measure the pandemic control by vaccination. Moreover, serological diagnostics are essential to identify individuals who are immune and theoretically protected from infection of severe disease, either after natural infection or by vaccination [14-16].

Figure 1. Analysis of recombinant protein by SDS-PAGE and western blotting.

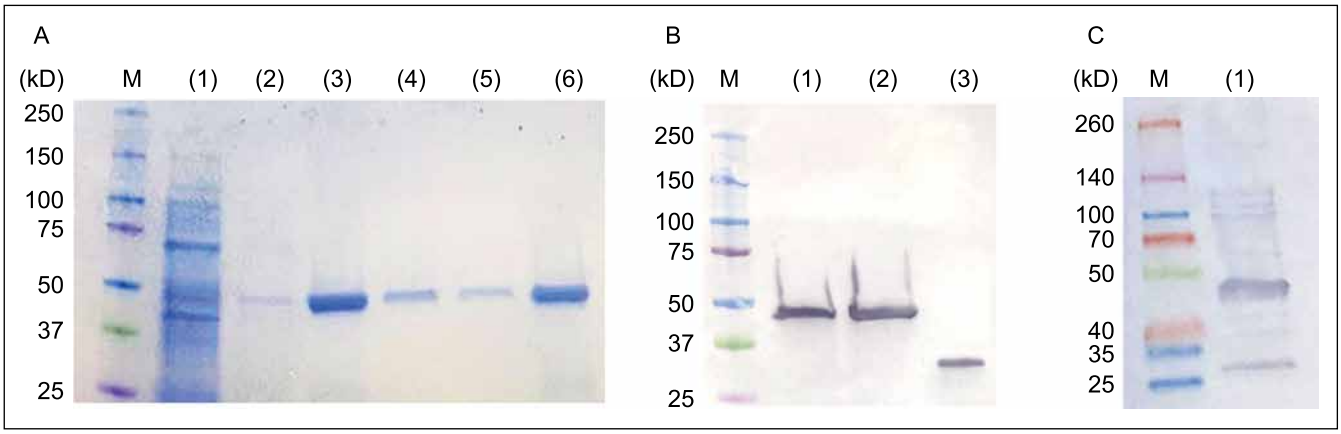

Soluble recombinant N protein from SARS-CoV-2 was expressed in *E. coli* and purified from the soluble fraction by IMAC. (A) SDS-PAGE showing the soluble fraction (1) and eluted protein at 48kDa (2-5) and pooled elutions. (B) western blotting targeting the his-tagged recombinant protein (1-2) at 48kDa and his-tagged GFP as positive control (3) at 30kDa. (C) western blotting targeting the recombinant N protein by convalescent serum 14 days after symptoms onset (1).kDa- kilodalton; M-Modecular weight marker.

Figure 2. ELISA to detect antibodies against N protein from SARS-CoV-2.

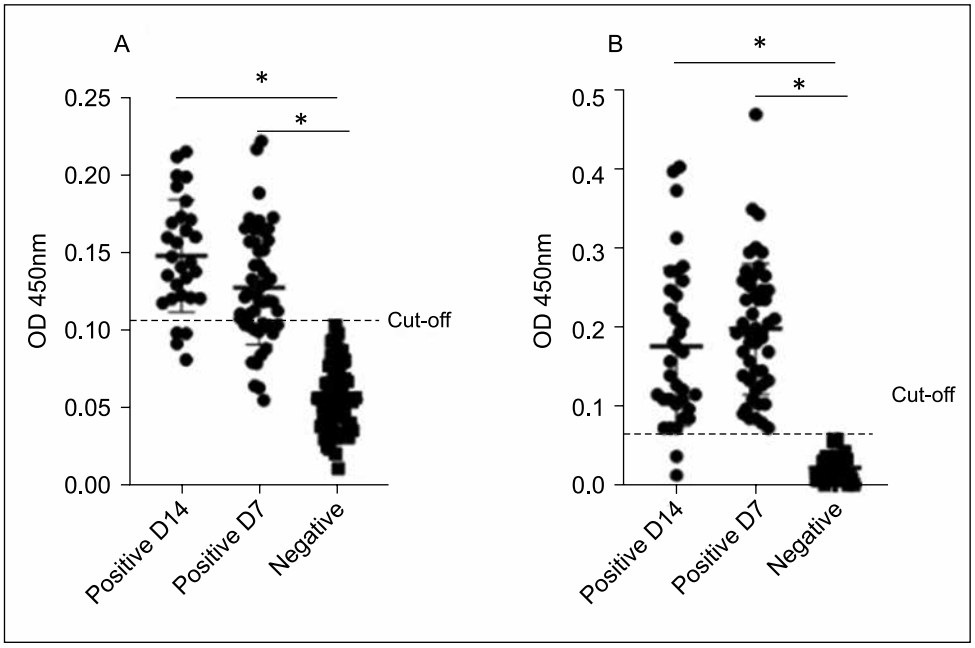

An ELISA assay was designed to search antibodies in convalescent serum from patients after 7 or 14 days after symptoms onset. The recombinant soluble N protein was used as coating antigen (A), and a commercial one as a quality control (B), both at 2μg/mL and 100ηg/well. The negative samples were used to calculate de cut-off as the mean OD plus three times the standard deviation (mean OD+3SD). OD - Optical density.

Figure 3. ROC curve generated with positive and negative samples determined by the ELISA.

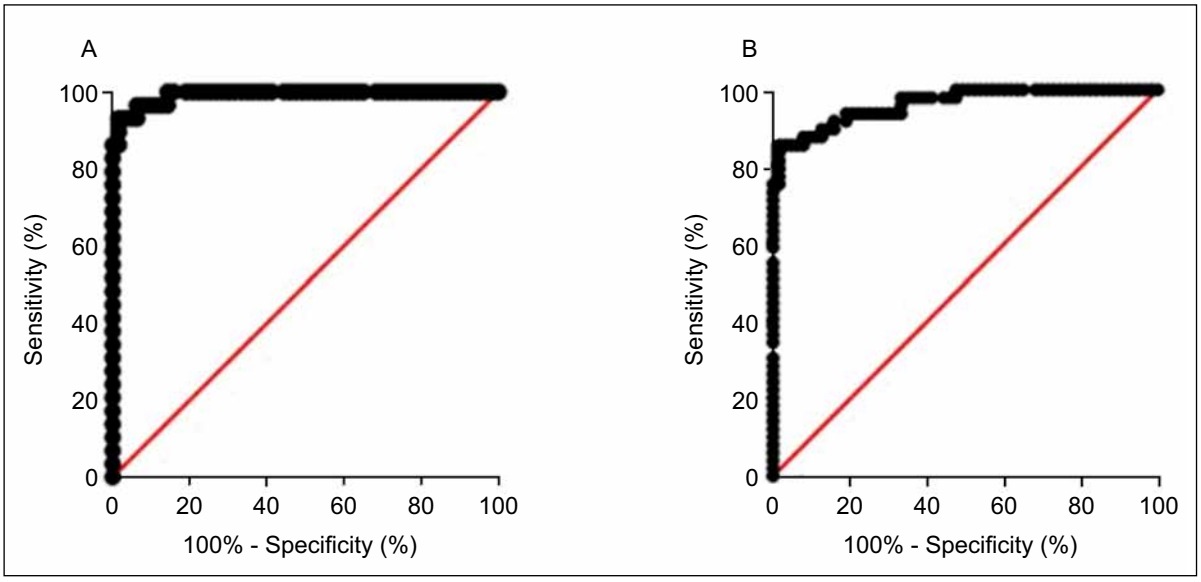

ROC curve was calculated using Graph Pad Prims version 8.0.1. The AUC determined was 0.9637 (95% confidence interval 0.9329 to 0.9945) and 0.9918 (95% confidence interval 0.9794 to 1.000) for patient samples collected 7 (A) and 14 (B) days after positive RT-qPCR result, respectively. The *p* values found were 0.0001.

In this study, we described the expression and purification of soluble N protein from SARS-CoV-2, as well as the validation of the recombinant protein in immune-based assays. Protein purification by immobilized metal affinity chromatography (IMAC) using nickel was standardized most entirely, making it possible to be performed in low infrastructure laboratories. The purified soluble protein was able to be recognized by convalescent serum and has been applied in ELISA assays to detect antibodies against SARS-CoV-2. It is noteworthy that commercial N recombinant protein used as quality control generates an ELISA assay which has better performance. However, the purchased protein is expensive and is sold in low amounts, meaning that not all laboratories will be able to buy and apply the protein in the routine serological assay. Moreover, the estimated time to import the reagent is too long and expensive, as well. The ELISAs performed in this work demonstrated that the antibodies produced by patients infected with SARS-CoV-2 showed reactivity against the recombinant N protein produced in *E. coli*. This data suggests that the antigenic conformation of the recombinant protein expressed is maintained as being suitable for antibody recognition. During the performance of the serological assay, this similarity is crucial to obtaining reliable results, since it not only confirms the immunogenic potential of N protein but also reaffirms the application of the recombinant protein in other serological tests. Moreover, this recombinant protein presented 100% of specificity and did not cross-react with human sera collected before and during the pandemic, in SARS-CoV-2 negative individuals. It also reinforces the fact that the expressed soluble protein keeps its native conformation after storage and manipulation during the assay.

The sensitivity of the ELISA using convalescent serum from patients 7 and 14 days after symptoms onset agrees with data reported by meta-analysis studies and similar assays in the literature [17-19]. The sensitivity of the ELISA for the detection of anti-SARS-CoV-2 antibodies depends on the time of blood taken after the beginning of the symptoms, the immunocompetence of the individual, and the severity of the clinical case [19]. The immune response and the production of antibodies may not be sufficient to be detected in the early stages of infection, decreasing the sensitivity of the test, which limits its applicability at this time point [19]. According to a previous report, the titer of specific IgG and the switch from IgM to IgG increases from the second or third week of infection [15]. This may explain the low sensitivity in the detection of IgG antibodies from samples after 7 days compared to the greater sensitivity observed in the detection of antibodies using convalescent sera collected after 14 days of infection.

In addition, studies have shown that individuals who had mild symptoms or were asymptomatic produce little or no antibodies to the disease. It has been suggested that before the adaptive immune system produces antibodies, the innate immune system acts by eliminating the virus [16, 19, 20]. These data demonstrate that the use of serological methods for the diagnosis of COVID-19 has limitations and requires proper interpretation of the results. The final result of serological diagnostics will depend on factors inherent to the protein used, disease severity, and the time of symptoms onset.

However, it is important to note that studies have shown that IgM antibody levels throughout infection are not well described, and are unreliable for detecting the acute phase of the disease [16]. Furthermore, meta-analysis studies of serologic diagnostics have concluded that immunoglobulin type (IgM/ IgG) was not associated with diagnostic accuracy. In the same study, comparisons of sensitivity in ELISA tests using IgM and IgG, demonstrated a higher sensitivity, in general, using IgG [17]. The limitation of this approach relies on the kinetics of antibody production during the infection.

Overall, this work demonstrated that SARS-CoV-2 N protein can be produced and purified from the soluble fraction of *E. coli*, rendering a tool for serological assays. The use of the soluble

protein may be useful for crystallography studies, antibody development, phage display, and other techniques that can improve the fight against COVID-19.

The non-detection of IgM antibodies is one of the limitations of the study. The variations of antibodies in individuals upon infection become another limiting factor. In this case, it is not possible to make sure that the measurement of IgG levels is related to a past or recent infection. However, the fact that IgG can become detectable three days after the onset of symptoms or at least 7 to 10 days after infection suggests both situations are possible even without the determination of IgM in the samples [16].

Acknowledgments

Authors thank the SENAI National Department and CIMATEC for the infrastructure and financial support provided.

References

1. Hosseini S E, Kashani R N, Nikzad H, Azadbakht J, Brafani HH, Kashani HH. The novel coronavirus Disease-2019 (COVID-19): Mechanism of action, detection, and recent therapeutic strategies. Virology 2020;551:1–9.
2. Velavan TP, Meyer CG. The COVID-19 epidemic. Trop Med Int Health. 2020;25(3):278-280.
3. de Wit E, van Doremalen N, Falzarano D, Munster VJ. SARS and MERS: recent insights into emerging coronaviruses. Nat Rev Microbiol. 2016;14(8):523-534.
4. Corman VM, Landt O, Kaiser M, Molenkamp R, Meijer A, Chu KWD et al. Detection of 2019 novel coronavirus (2019-nCoV) by real-time RT-PCR. Eurosurveillance 2020;25:8.
5. Chau CH, Strope JD, Figg WD. COVID-19 Clinical diagnostics and testing technology. Pharmacotherapy. 2020; 40(8):857-868.
6. Silva RGLD, Chammas R, Plonski GA, Goldbaum M, Ferreira LCS, Novaes HMD. University participation in the production of molecular diagnostic tests for the novel coronavirus in Brazil: the response to health challenges. A participação da universidade na produção de testes diagnósticos moleculares do novo coronavírus no Brasil: resposta aos desafios sanitários. Cad Saude Publica. 2020;36(6):e00115520.
7. Carlson CR, Asfaha JB, Ghent CM, Howard CJ, Hartooni N, Safari M et al. Phosphoregulation of phase separation by the SARS-CoV-2 N protein suggests a biophysical basis for its dual functions. Mol Cell. 2020;80(6):1092-1103.
8. Lin Y, Shen X, Yang RF, Li YX, Ji YY, He YY et al. Identification of an epitope of SARS-coronavirus nucleocapsid protein. Cell Res. 2003;13(3):141-145.
9. Liu W, Liu L, Kou G, Zheng Y, Ding Y, Ni W et al. Evaluation of nucleocapsid and spike protein-based enzyme-linked immunosorbent assays for detecting antibodies against SARS-CoV-2. J Clin Microbiol. 2020;58(6): e00461-20.
10. Che XY, Hao W, Wang Y, Di B, Yin K, Xu Y et al. Nucleocapsid protein as an early diagnostic marker for SARS. Emerg Infect Dis. 2004;10(11):1947-1949.
11. Djukic T, Mladenovic M, Stanic-Vucinic D, Radosavljevic J, Smiljanic K, Sabljic L et al. Expression, purification and immunological characterization of recombinant nucleocapsid protein fragment from SARS-CoV-2. Virology 2021;557:15-22.
12. Li G, Li W, Fang X, Song X, Teng S, Ren Z et al. Expression and purification of recombinant SARS-CoV-2 nucleocapsid protein in inclusion bodies and its application in serological detection. Protein Expr Purif. 2021;186:105908.
13. Klausberger M, Duerkop M, Haslacher H, Wozniak-Knopp G, Cserjan-Puschmann M, Perkmann T. A comprehensive antigen production and characterisation study for easy-to-implement, specific and quantitative SARS-CoV-2 serotests. EBioMedicine 2021;67:103348.
14. Castro R, Luz PM, Wakimoto MD, Veloso V G, Grinsztejn B, Perazzo H. COVID-19: A meta-analysis of diagnostic test accuracy of commercial assays registered in Brazil. The Brazilian Journal of Infectious Diseases 2020;24:180-187.
15. Sethuraman N, Jeremiah SS, Ryo A. Interpreting diagnostic tests for SARS-CoV-2. JAMA 2020;323: 2249-2251.
16. Younes N, Al-Saqed D W, Al-Jighefee H, Younes S, Al-Jamal O, Daas HI et al. Challenges in laboratory diagnosis of the novel coronavirus SARS-CoV-2. Viruses 2020;12(6):582.
17. Bastos ML, Tavaziva G, Abidi SK, Campbell JR, Haraoui L-P, Johnston JC et al. Diagnostic accuracy of serological tests for COVID-19: systematic review and meta-analysis. BMJ (Clinical research ed.). 2020;370: 13.
18. Deeks JJ, Dinnes J, Takwoingi Y, Davenport C, Spijker R, Taylor-Phillips S. Antibody tests for identification of current and past infection with SARS-CoV-2. Cochrane Database Syst Rev. 2020;6:306.

19. Meireles LG, Silva AMF, Carvalho CA, Kesper N, Jr AJG, Soares C et al. Natural *versus* recombinant viral antigens in SARS-CoV-2 serology: Challenges in optimizing laboratory diagnosis of COVID-19. Clinics (Sao Paulo, Brazil) 2020;75:7.
20. Melgaço JG, Azamor T, Ano Bom APD. Protective immunity after COVID-19 has been questioned: What can we do without SARS-CoV-2-IgG detection? Cellular Immunology 2020;353:104-114.

Materials and Methods

Cloning of the Nucleocapsid Protein Gene

The SARS-CoV-2 N protein was cloned by inserting the optimized coding sequence in the pET21a(+) vector (FastBio, São Paulo, Brazil). *E. coli* (DE3) pRARE2 were transformed by heat shock with the recombinant plasmid and the transformants were selected in Luria-Bertani (LB) Agar (Sigma Aldrich, St. Louis, MO, USA) plates containing 100 µg/mL ampicillin and 34 µg/mL chloramphenicol (both from Sigma Aldrich). The recombinant protein was produced fused to a C-terminal histidine tag.

Induction of Recombinant N Protein Expression in *E. coli*

The selected *E. coli* clones were cultured in 5 mL of LB medium (Tryptone 10 g/L, Yeast extract 5 g/L, NaCl 10 g/L) containing ampicillin at 100 µg/mL and 34 µg/mL chloramphenicol under 150 rpm orbital shaking at 37°C for 16 hours (Jeio Tech - Shaker incubated, SIF-500R, Yuseong-gu, Korea). Subsequently, 50 mL of phosphate buffer (0.17 M KH2PO4, 0.72 M K2HPO4) was poured into 450 mL of TB (Terrific Broth) medium (Yeast Extract 24 g/L, Tryptone 20 g/L, Glycerol 4 mL/L), containing the abovementioned antibiotics. Then, the entire volume of pre-inoculum (5 mL) was transferred to the solution and incubated at 37°C under 150 rpm agitation until it reached an optical density at 600 ηm of 1.5. Upon reaching the optical density, IPTG (Isopropyl β-D-1-thiogalactopyranoside – Invitrogen, Waltham, MA, USA) was added at a final concentration of 0.5 mM for the induction of recombinant protein expression. After the addition of IPTG, the culture was incubated at 18° C under 150 rpm orbital shaking for 16 hours.

Purification of Soluble Recombinant N Protein by Affinity Chromatography

After protein expression, the culture was centrifuged at 4° C, 4000 rpm, for 20 minutes. The cells were then resuspended and lysed in lysis buffer (PBS buffer with dithiothreitol 1 mM, protease inhibitor cocktail, lysozyme 200 µg/mL, DNAse 2 mM – all reagents from Sigma Aldrich), followed by sonication. The sonication was performed at 40% amplitude in 4 cycles of 15-second pulse and 30-second rest and repeated three times separately, 12 cycles in total (Qsonica LLC, Newtown, CT, USA). After sonication, 0.01% triton X-100 (Sigma-Aldrich) was added and the sample was submitted to the vortex for 5 minutes. Then, the lysate was centrifuged at 4°C, 18,000 g for 10 minutes.

Subsequently, the lysate was incubated with the Ni-NTA Agarose (Qiagen, Hilden, Germany) beads at 4°C, 60 rpm, for 2 h for protein binding. After this period, the sample with the beads was placed into the column for packing. After this step, the column was washed thoroughly with 20 column volumes (40 mL) with wash buffer (25 mM Tris (pH 7.4), 500 mM NaCl, 1 mM DTT, 5% Glycerol, 50 mM Imidazole), followed by elution with 1mL of elution buffer 1 (25 mM Tris pH 7.4, 200 mM NaCl, 1 mM DTT, 5% glycerol, 250 mM imidazole), twice. Subsequently, the remaining protein was eluted again with elution buffer 2 (25 mM Tris pH 7.4, 200 mM NaCl, 1 mM DTT, 5% glycerol, 500 mM imidazole), twice. The concentration of the purified protein solution was determined using the NanoDrop and Qubit protein BR assay kit (Invitrogen).

The collected fractions were mixed and submitted to a centrifugal ultrafiltration concentrator (10 kDa, Merck, Darmestadium, Germany) with storage buffer (200 mM Tris pH 8.0, 0.1 mM EDTA, 500 mM NaCl, 10% glycerol) at 4° C, 4,000 rpm for 20 minutes, twice, to achieve the highest concentration of purified recombinant protein, obtaining about 3 mL of protein in storage buffer.

Analysis by SDS-PAGE and Western Blotting

The eluted fractions and the concentrated protein were analyzed by SDS-PAGE and the sample was separated by electrophoresis in a 10% gel stained by Coomassie Brilliant Blue R-250 (Bio-Rad; Hercules, CA, USA). The presence of recombinant protein was analyzed by Western blotting, using rabbit anti-histidine polyclonal and anti-rabbit IgG-HRP antibodies (Santa Cruz, Dallas, TX, USA). In addition, a western blotting assay with the protein was performed with convalescent sera from COVID-19 positive and negative patients.

After electrophoresis, the separated samples on the gel were transferred to a nitrocellulose membrane under constant amperage of 250 mA for 1 hour. After transfer, the membrane was blocked with Tris-buffered saline (TBS) containing 5% skim milk and incubated for 1 hour at room temperature. The membrane was washed three times with TBS 0.1% tween-20 (Sigma Aldrich) (TBS-T) and TBS respectively. After washing, the primary rabbit anti-histidine polyclonal antibody (Santa Cruz) was diluted 1:500 in 2% skim milk in TBS solution and added to the membrane, followed by overnight incubation and three washes with TBS-T and TBS 1X. Next, the presence of a recombinant

his-tagged protein was revealed by incubation with an anti-rabbit IgG-HRP conjugated antibody (1:5000; Santa Cruz) and Opti-4CN Substrate Kit (Bio-Rad).

In another assay, the anti-histidine polyclonal antibody was replaced by COVID-19 convalescent human serum (1:2000) and a negative serum sample. The membranes were incubated overnight at 4°C, followed by 3 times washes with TBS-T and TBS 1X. The material was incubated with secondary anti-human IgG-HRP antibody (Santa Cruz) 1:5000 diluted in TBS plus 2% skim milk and incubated for 1 hour at room temperature. After the period, the membrane was washed again and incubated with Opti-4CN Substrate Kit (Bio-Rad).

Enzyme-linked immunosorbent assay (ELISA)

To perform the ELISA, a 96-well plate was sensitized with 50 µL of a 2 µg/mL recombinant N protein solution (100 ηg/well) diluted in phosphate-buffered saline (PBS) and incubated at 4° C overnight. For quality control, a commercially available N recombinant protein (Invitrogen) was also used. The plate was washed three times with PBS containing 0.05% Tween 20 (wash solution) and blocked with 200 µL per well of the blocking solution of PBS containing 3% skim milk and incubated at room temperature for 1 hour. Serum samples from RT-qPCR positive and negative patients were diluted at a ratio of 1:50 in a blocking solution with 1% skim milk. After the incubation time, the diluted samples were added to the plate and incubated at room temperature for 2 hours. After that, the plate was washed and the secondary anti-human-HRP (peroxidase) IgG antibody (Bio-Rad) diluted at a 1:5000 ratio was added and incubated for 1 hour at room temperature. Finally, TMB substrate was added (Scienco, Santa Catarina, Brazil) for 2 minutes, followed by phosphoric acid (1M) to stop the reaction. The plate was read on the (Multiskan FC; Skanit Software 6.0.2 for Microplate readers, Thermo Scientific, Waltham, MA, EUA), at 450 nm.

Statistical Analysis

The statistical analysis was performed in Graph Pad Prism version 8.0.1 (San Diego, CA, USA). To test the normal distribution of data, the Kolmogorov-Smirnov test was applied. Statistical difference between controls and positive samples with normal distribution was determined by the T-test ($p< 0.05$). The Receiver Operator Characteristic (ROC) curve and area under the curve were also calculated based on positive and negative samples. Sensitivity was calculated based on positive samples diagnosed by RT-qPCR and positive samples determined by the developed assay. Specificity was calculated based on negative samples collected before and during the COVID-19 pandemic, also diagnosed by RT-qPCR, and the negatives samples determined by the developed assay.

Learning Proposal for Cybersecurity for Industrial Control Systems Based on Problems and Established by a 4.0 Didactic Advanced-Manufacturing-Plant

Bruno Santos Junqueira[1*], Marvim Vinicius Souza de Souza[1], Victor Bittencourt Lima[1], Wallace Souza Faria de Jesus Gonçalves[2], Herman Augusto Lepikson[2]

[1]Center of Competence in Advanced Manufacturing, SENAI CIMATEC; [2]Automation Department, SENAI CIMATEC; Salvador, Bahia, Brazil

Researches data indicate that the search for cybersecurity professionals to protect industrial control systems (ICS) in Brazil is increasing, mainly because of the rise in cyber-attacks directed at the industry. However, we observed a deficiency of professionals with the required competence in ICS cybersecurity, which involves technology-information fields (IT) and operational technology (OT). On the other hand, there is a lack of educational institutions with the right strategies for training professionals who master the technologies for ICS protection. This paper presents a strategy through procedures to address this lack by evaluating scenarios of practices for the development of competencies in ICS cybersecurity through the problem-based learning (PBL) methodology. The scenarios combine theory and practice involved in solving ICS cybersecurity problems, using PBL with the support of SENAI CIMATEC's 4.0 Advanced Manufacturing Plant (AMP).

Keywords: Cybersecurity. Industry. Scenarios. Practices. Problem-Based.

Abbreviations: PLC: Programmable Logic Controller; IDS: Intrusion Detection System; IPS: Instrusion Prevention System.

Introduction

Cybersecurity has been gaining prominence in managerial and governmental agendas. Industry 4.0 is an inevitable tendency. It comprises a type of industrialization where intelligent machines, storage systems, and production facilities are integrated end-to-end, by cyber-physical systems (CPS) capable of autonomously exchanging information, triggering actions, and controlling themselves independently [1]. All this integration is supported by nine enabling technologies: Internet of Things (IoT) and Industrial IoT (IIoT); cybersecurity; extended reality; big data analytics; autonomous robots; additive manufacturing; simulation and digital twins; systems integration; and cloud computing. In the era of Industry 4.0, where working machines are connected to the network and with each other using smart devices and operating in the cloud, the scale and variety of cyber-attacks have grown exponentially [2].

Within Industry 4.0, the emergence of cyber risks marks the presence of CPS in industrial environments, where vulnerabilities and threats can critically impact business models and lead to a loss of competitiveness. A study carried out by Tüv [3] states that 61% of manufacturing industries struggle in mitigating cyber risks, and only 34 % of all cyberattacks in the operational environment are detected. These data refer to all harmful attacks, including attacks coming from information technology (IT) systems, as some of them may result in intruders attacking the operational technology (OT) systems present in the operating network through the corporate network [3].

Cyber risks deman that cybersecurity strategies shall be integrated with organizational initiatives, information, and communication technologies, aiming to ensure the security of data, knowledge, and performance of the production value chain. Consequently, research and education in the cybersecurity area of Industrial Control Systems (ICS) and Supervisory Control and Data Acquisition (SCADA) systems have attracted the interest of several institutions around the world through the

Received on 12 December 2021; revised 10 February 2022.
Address for correspondence: Bruno Santos Junqueira. Av. Orlando Gomes, 1845 - Piatã, Salvador - BA- Brazil. Zipcode: 41650-010. E-mail: brunosjunq@gmail.com. DOI 10.34178/jbth.v5i1.188.

J Bioeng. Tech. Health 2022;5(1):11-17.

high industrial demand for cybersecurity training for such systems in recent years [4].

In Brazil, seeking to achieve the Industry 4.0 model, industries prioritize the pillars of Systems Integration, Data Analysis, and IoT [5]. However, according to ISC2 [6] there is still a growing demand for qualified professionals with knowledge related to ICS cybersecurity. But regular, traditional courses are not well fitted to cope with some learning needed for this specialization, considering that hands-on practice is essential to deal with the nuances posed by the diverse cyber-attack specificities in ICS. The best fit for this purpose is active-based learning techniques, in which problem-based learning (PBL) has the advantage of bringing the necessary practice to the specific student problem. The creation of scenarios and routines enabled by PBL allows the insertion of students in situations involving cybersecurity problems associated with ICS in procedures. In PBL, students work together to analyze and solve problems and communicate, evaluate, and integrate information from diverse sources [7]. However, to be an efficient method, it should have an environment for hands-on practices that represents an industrial plant. In this context, SENAI CIMATEC, to contribute to industrial-technological advancement, was the first institution to integrate ICS cybersecurity in Brazil into its Advanced Manufacturing Plant (AMP). So, this research proposes scenarios of practices through learning based on current problems, which will be solved in AMP by adding ICS cybersecurity competence.

Materials and Methods

We used a method based on three steps to develop the ICS cybersecurity training scenarios considering Industry 4.0 environments (Figure 1).

Basic documental research and analysis of similar approaches were carried out to check the scenarios and practices already developed. After that, we assessed the learning requirements linked to cybersecurity technologies applied in Industry 4.0. Finally, we established the scenarios and indicated the practices and problems based on research related to cybersecurity in Industry 4.0.

Search and Analysis of Similar Approaches

Laboratories for security experiments and cybersecurity training exist in various manifestations. The traditional approach is a dedicated computer lab for IT security training [8]. In this kind of lab, a two teams approach, like red and blue, is followed, where a group of people is authorized and organized to emulate attacks or exploitation capabilities. There is also a high industry demand for cybersecurity training for ICS and SCADA systems. However, many existing research centers are limited by the lack of testbeds or models capable of representing actual instantiations of ICS applications and an inability to observe an entire SCADA system. The reasons are usually high costs and limited space for such laboratories [4]. The lack of ICS cybersecurity training strategies in educational institutions in Brazil is also associated with these reasons. Another is the lack of competent professionals to give a specific discipline to this topic. We chose PBL based on risks and benefits. As a benefit, we have a student-centered approach, which collaborates to greater understanding, interdisciplinarity, and the development of necessary lifelong skills. In contrast, as risks, creating suitable problem scenarios can be

Figure 1. The method used for scenario development.

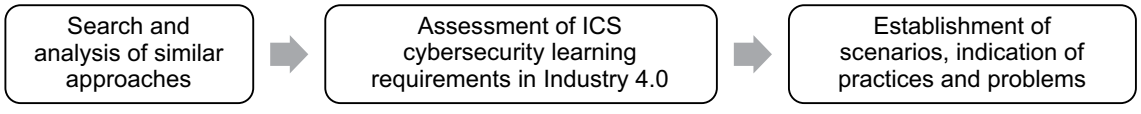

difficult, and PBL may require more study time, taking away time from other subjects, developing anxiety because learning certainly will be messier, needing one instructor, or more, to guide the students. PBL has already been used to improve the efficiency of cybersecurity education, helping students to develop a wide range of skills in technical aspects, teamwork, making judgments, and developing as lifelong learners [9]. In contrast to traditional learning, in PBL a scenario-based problem is presented to a student, who must seek what they need to learn to solve practical problems that would likely appear during their professional life [10] (Figure 2).

Assessment of ICS Cybersecurity Learning Requirements in Industry 4.0

For the AMP to be used as a cybersecurity laboratory in the context of Industry 4.0, it is necessary to verify which technologies should be addressed in the scenarios. The general security requirements for ICS can be divided into three categories: network protection, authentication and authorization, and secure communication [11]. Based on these requirements, we raised specific conditions for the protection of ICS in Industry 4.0 using ICS cybersecurity standards.

With the adoption of Industry 4.0 technologies, the Industry 3.0 pyramid model became obsolete. So, the interdependence between hierarchical levels of communication is no longer a crucial factor, and the connectivity between the factory floor (field level) and the systems present at corporative levels gets relevant. Thus, a pillar model is consolidated, where systems at the field level and their industrial assets are constantly interacting as CPS to improve the performance of processes (Figure 3) [12].

As a consequence of this interaction, in addition to the industrial floor or field assets, data is stored in systems of the corporate level such as Enterprise Resource Planning (ERP), Plant Information Management (PIMS), and Manufacturing Execution (MES) that are also critical and must be protected.

Establishment of Scenarios, Indication of Practices, and Problems

We analyzed data from research and problems related to cybersecurity in Industry 4.0 to establish the scenarios and indicate practices and problems. ICS cybersecurity problems can be divided into three classes: people, process, and technology [13]. The technology problems are linked to the safety of the control and network components of an ICS [11]. Moreover, the top three industrial threats are phishing and social engineering, ransomware, and DNS-based DoS attacks. Besides, 57 % of the experts say that renewable and cutting-edge technologies present in Industry 4.0 are increasing the risks of cyber-attacks [3].

In addition to surveys data on cybersecurity problems, to create the scenarios it is necessary to take into account a classification referring to the needs of the labor market in the area of ICS cybersecurity. IT cybersecurity can be divided into seven categories, 33 specialty areas, and 52 work roles [14]. We didn't find a similar classification for the OT context, so it was used as a reference. Also, to address the problems involving knowledge in

Figure 2. Traditional learning x problem-based learning [10].

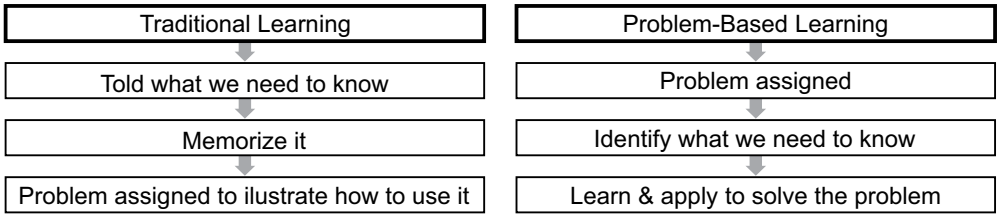

Figure 3. Pillar model of Industry 4.0 automation [12].

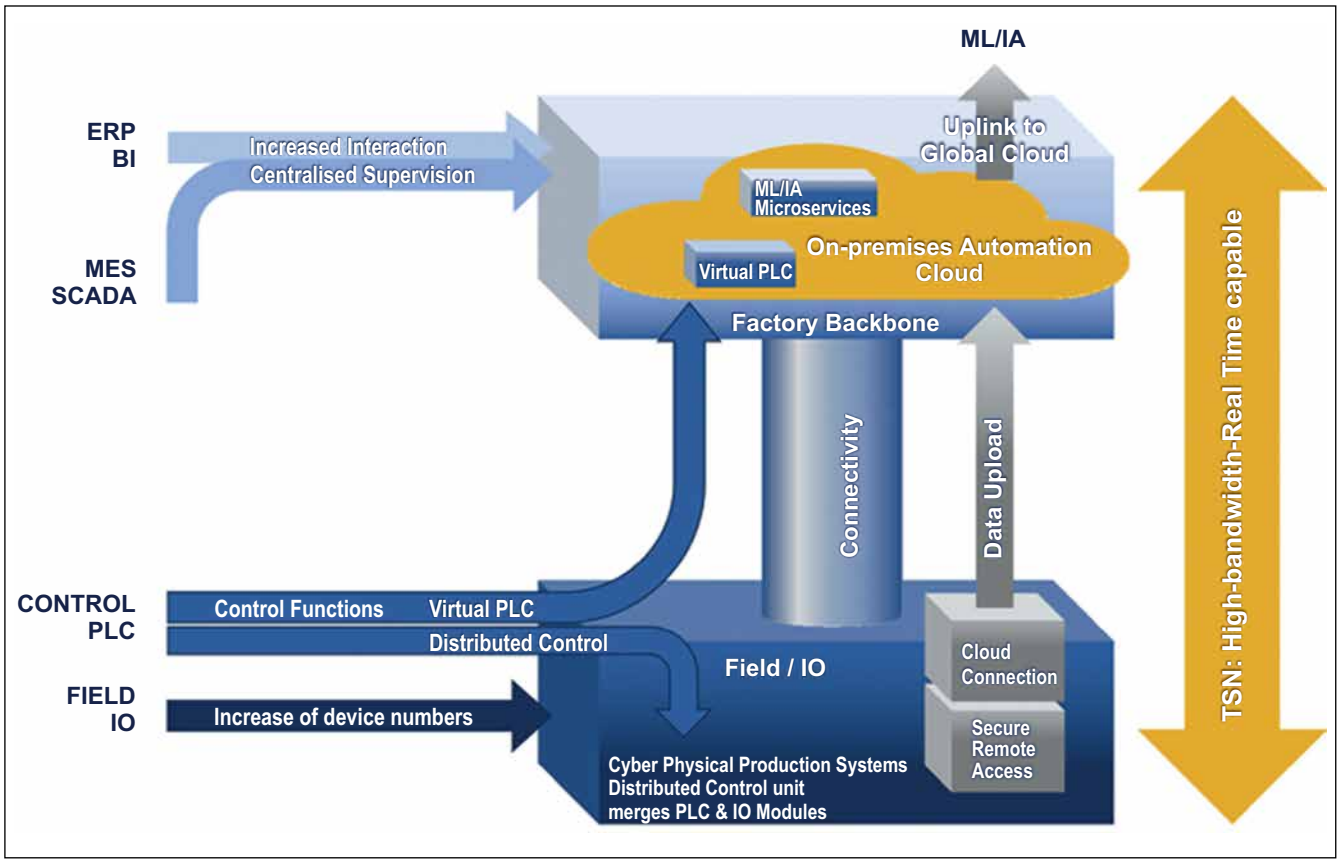

ICS needed for the labor market, the results of a survey carried out by Filkins and colleagues [15] were taken into account, which pointed out that process and technology practices can be more useful to people's development.

Results and Discussion

The scenarios were assembled and practices and problems were indicated through the proposed method. The resources needed to carry out the practices and solve the problems through PBL were raised. And, we discussed the method of evaluating the performance of students participating in the practices.

Scenarios, Practices, and Problems

At the end of the research and similar analysis, the scenarios are needed to (Figure 4): a. develop or securely provision industrial cybersecurity projects from scratch [14,16], b. operate and maintain ICS cybersecurity technologies [14,16] and c. gather information about security breaches in ICS to see what damage is possible in the event of an attack, which is a common practice in IT cybersecurity known as pentesting (vulnerability testing), enabling to see how to protect and defend the infrastructure [14,17].

For Industry 4.0, data analysis and integration between the floor or field and management systems are currently done through software solutions provided by third-party vendors or commercial-off-the-shelf device integrations [13]. It can cause several problems brought by the lack of security integrated into some solutions. It reveals the need for two additional scenarios: d. secure integration of devices and systems, because of the need to collect and operate data and devices in industry 4.0; and e. governance, which aims to address the need for IT and OT alignment to oversee and govern security

Figure 4. Proposed scenarios and practices.

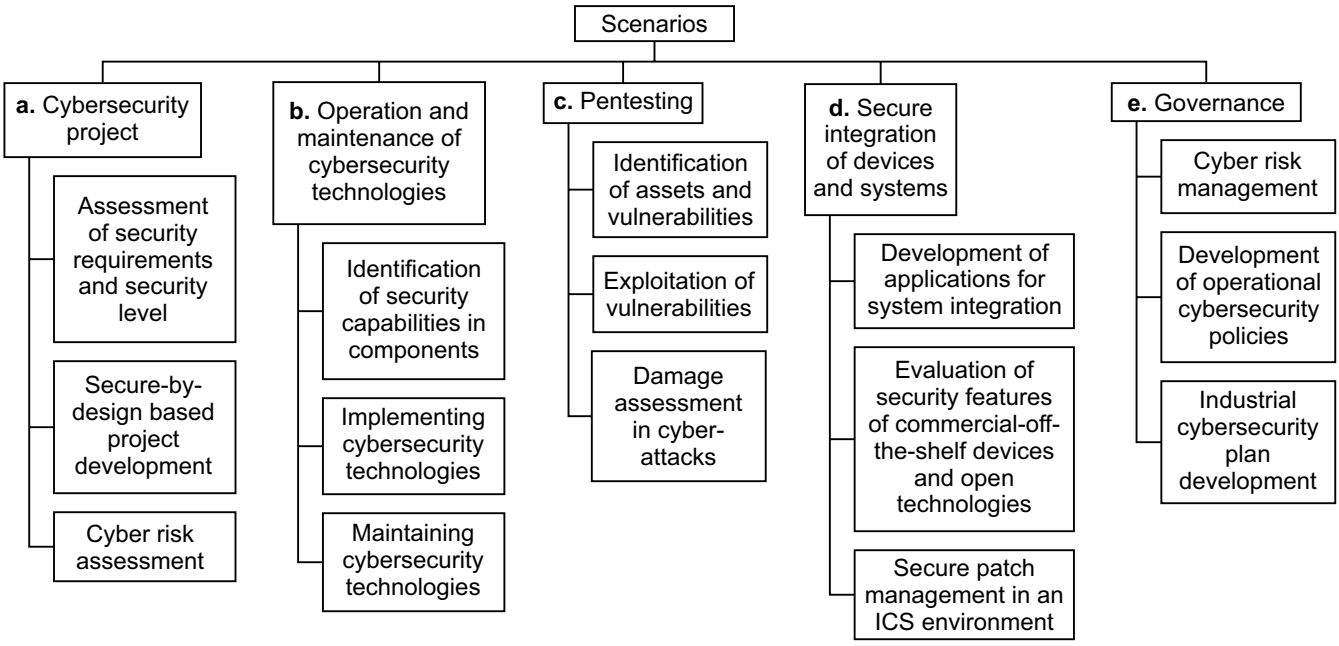

breaches, which according to 63 % of security experts, is one of the reasons for the increase of risk [3,14].

In addition, the use of parts of the IEC 62443 [18] or other standards families, can assist in the development of problems associated with the practices. So, already existing requirements and recommendations to ensure ICS cybersecurity can be followed by students.

Application at SENAI CIMATEC AMP

SENAI CIMATEC's AMP integrates several Industry 4.0 technologies, being an environment prepared to receive professionals of all technical levels. The manufacturing process present in this plant consists of manufacturing 25 and 40 mm pneumatic cylinder bases, where the raw material is turned, milled, and later sent to modular process stations [19]. In the context of this process, each scenario and practice will be applied, seeking to solve problems in specific parts of the AMP.

First, in scenario a., an insecure topology configuration implemented in the AMP can serve as a basis for a new secure topology by inserting cybersecurity technologies into the previous one. In the case of scenario b., technologies already implemented can be re-implemented or updated, leading students to seek the necessary information to carry out this process. In scenario c., students can use the computers in the lab to connect to a virtualized network or even the network with the lab devices to gain practical experience in industrial network pentesting. In scenario d., practices can be done where commercial-off-the-shelf devices and open technologies must be evaluated and tested to verify their safety. And finally, in scenario e., students can split into multidisciplinary teams to use a risk analysis methodology to assess possible cyber risks involving the AMP.

Resources

To enable PBL and evaluate students' performance in solving problems related to the indicated practices, some resources will be necessary, such as standards, documentation, ICS components, and Industry 4.0 technologies.

For scenario a. it is important to have access to standards that include ICS protection technology requirements and recommendations. These standards serve as a basis for evaluating the insecure network topology models, provided by

the tutor, including the corporate and industrial networks. In addition, network topology and diagram design software required appropriate symbology for ICS.

For scenario b., in addition to having the control components and networks of an ICS, such as PLC, IDS, IPS, and firewalls, it is vital to have access to manuals and other documentation of cybersecurity technologies to be implemented or maintained for the protection of ICS. A vulnerable network must be set up, and the topology design must be provided to situate the student in the arrangement of the network elements.

In the scenario, c. computers need to connect to a deliberately vulnerable industrial network to assess the ability to identify assets and vulnerabilities. Computers must have virtualization software to configure the components of an ICS for pentesting, segregated from the academic network. In this way, it will be possible to assemble a vulnerable network, with ICS purposely vulnerable, to challenge students to find vulnerabilities and point out possible damages.

Scenario d. requires IIoT devices and access to code development software compatible with the practice's programming language. It can be useful to access standards used for patch management in ICS and documentation of protocols and programming languages used for the ICS integration or maintenance solutions. At last, manuals or other documentation of commercial-off-the-shelf devices and open technologies to industrial systems integration can be necessary.

Scenario e. requires access to the standard designed to carry out the cyber risk analysis of industrial processes and the documentation or standard of the defined risk analysis methodology detailing the process for performing the risk analysis. Moreover, a framework to indicate mitigations for each type of cyber-attack will be useful.

Student Performance Evaluation

The evaluation manner of problems resolution defined in each practice can consist of assessing documentation, exams, or presentations exposing what was developed to successfully solve the problem assigned in the scenario.

Conclusion

We stated that the scenarios proposed for problem-based learning, involving ICS, can be achieved based on the method proposed in this study. The method, starting from the investigation through the research of similar approaches that addressed scenarios, practices, and problems involving the learning of ICS protection technologies, enabled the analysis of information and evaluation of cybersecurity learning requirements in Industry 4.0, which brought a broad vision for future training at SENAI CIMATEC's AMP through 5 possible scenarios and 15 educational practices for PBL on ICS cybersecurity. It is crucial to clarify that the scenarios and practices set out in this study are not the first to be proposed at SENAI CIMATEC, nor the only ones possible, since ICS cybersecurity had already been carried out in the institution.

Due to paper submission limitations, the scenarios and practices proposed in this work are only those that proved to be the most important during the stages of research, analysis, and requirements evaluation. Therefore, the study established scenarios that can be used in the AMP in the future. On top of that, a collection of statistical data through satisfaction surveys submitted to the students engaged in the practices proposed here can validate the learning capacity that the scenarios and practices made possible, as well as the degree of importance of the experiences that students obtained performing the practices involved in each scenario.

References

1. Kagermann H, Wahlster W, Helbig J. Securing the future of German manufacturing industry. Recommendations for implementing the strategic initiative Industrie 4.0. Final report of the Industrie 4.0 Working Group. Acatech 2013:5-78.

2. Mahoney TC, Davis J. Cybersecurity for Manufacturers: securing the digitized and connected factory. 2017.
3. Tüv R, Ponemon Institute. The 2020 Study on the State of Industrial Security, 2020. Disponível em: https://go.tuv.com/otsurvey-2020?wt_mc=Advertising.Personalselling.no- interface.CW20_I07_FSCS.button.&cpid=CW20_I07_FSCS_PS. Acesso em: 6 de ago. 2021.
4. Sitnikova E, Foo E, Vaughn RB. IFIP AICT 406. The power of hands-on exercises in SCADA cyber security education. In IFIP AICT 2013;6(8).
5. Ribeiro MS et al. A Indústria 4.0 e a computação no Brasil. 2019.
6. ISC2. Cybersecurity Professionals Stand Up to a Pandemic, (ISC)2 Cybersecurity Workforce Study, 2020. Disponível em: https://www.isc2.org/-/media/ISC2/Research/2020/Workforce-Study/ISC2ResearchDrivenWhitepaperFINAL.as. Acesso em: 6 de ago. 2021.
7. Duch BJ, Groh SE, Allen DE. The power of problem-based learning: a practical "how to" for teaching undergraduate courses in any discipline. Stylus Publishing, LLC, 2001.
8. Willems C, Meinel C. Online assessment for hands-on cyber security training in a virtual lab. In: Proceedings of the 2012 IEEE Global Engineering Education Conference (EDUCON). IEEE 2012:1-10.
9. Figueroa A, Santiago et al. A RFID-based IoT cybersecurity lab in telecommunications engineering. In: 2018 XIII Technologies Applied to Electronics Teaching Conference (TAEE). IEEE 2018:1-8.
10. Kurt S. Problem-based learning (PBL) in educational technology. 2020;January 8. Disponível em: https://educationaltechnology.net/problem-based-learning-pbl/. Acesso em: 9 de ago. 2021.
11. Drias Z, Serhrouchni A, Vogel O. Analysis of cyber security for industrial control systems. In: 2015 International Conference on Cyber Security of Smart Cities, Industrial Control System and Communications (SSIC). IEEE 2015:1-8.
12. Futura-Automation. System-On-Chip-Engineering-Pillar. Disponível em: https://futura-automation.com/2019/07/05/the-accumulating-case-for-deterministic-control/system-on-chip-engineering-pillar-sb/. Acesso em: 11 de ago. 2021.
13. Daniel AUP, Hongmei HE, Tiwari A. Review of cybersecurity issues in industrial critical infrastructure: manufacturing in perspective. Journal of Cyber Security Technology 2017;1(1):32-74.
14. Newhouse W et al. National initiative for cybersecurity education (NICE) cybersecurity workforce framework. NIST special publication 2017;800:181.
15. Filkins B, Wylie D, Dely S. 2019 state of OT/ICS cybersecurity survey. SANS™ Institute, 2019. Disponível em: https://www.forescout.com/resources/2019-sans-state-of-ot-ics-cybersecurity-survey/. Acesso em: Acesso em: 11 de ago. 2021.
16. Stouffer K et al. Guide to industrial control systems (ICS) security. NIST special publication 2011;800(82)16.
17. DUGGAN, David et al. Penetration testing of industrial control systems. Sandia national laboratories, p. 7, 2005.
18. Futura-Automation. Understanding IEC 62443. Disponível em: https://www.iec.ch/blog/understanding-iec-62443/. Acesso em: 12 de ago. 2021.
19. Bittencourt V et al. Proposta de reformulação para aplicação de tecnologias da indústria 4.0 em uma planta de manufatura avançada. VI SAPCT, 2021.

Smart Warehouses: Logical Architecture for Logistics 4.0

Carlos César Ribeiro Santos[1*], Lucas de Freitas Gomes[1], Herman Augusto Lepikson[1], Gilana Pinheiro de Oliveira[1], Lucas Cruz da Silva[1]

[1]SENAI CIMATEC University Center; Salvador, Bahia, Brazil

This article proposes an approach based on Industry 4.0 technologies for building smart warehouses aiming to improve the performance of this logistic system operation. It is considered that the development of general and scalable logical warehouse architecture was to increase the traceability, reliability, and agility of intralogistics activities. It was observed potential gains (structuring and well-organized operations, orchestration of technological resources to improve logistical performance, reduction of human intervention in the process, increased productivity, and proof of operation errors) when modeling and simulating the proposal presented to build a testbed.

Keywords: Smart Warehouse. Enabling Technologies. Logistics 4.0.

Introduction

In recent years, logistics has acquired an essential role in organizational strategies, such as the importance and relevance of its macro processes for the objectives: supplies, production, and distribution. Logistics is responsible for managing order processing, inventories, transportation, storage combination, material handling, and packaging [1]. A challenge of logistics management is the integrated and systemic vision of all the organization's processes.

Logistics represents a significant differential in the management of the flow of materials and information of the companies when well executed in a planned manner, from the client's order to the delivery of the product to the final consumer, seeking to meet the demands with fast deliveries, with quality, and at the lowest possible cost.

Given the current scenario of intense transformations, adaptations, and reinventions in the manner of interaction with customers, partners, and suppliers, logistics in companies need to be rethought to meet a significant number of deliveries in a short period. To do that, it has become indispensable to establish different distribution channels, make the storage environment more flexible, invest in technology, and apply innovative methods that account for the growing complexity of the supply chain involved.

The development of an efficient distribution system that incorporates multichannel communication involves the application of integration technologies between the logistical links to allow process customers to contact suppliers through the most convenient channels and receive their orders in the shortest possible time. Consequently, companies tend to migrate part of their inventories to warehouses or distribution centers, which have well-structured, fast and secure internal logistics to accommodate this new demand.

Thus, this article will demonstrate the importance of warehouses as support for logistics activities. A warehouse is a physical environment where raw materials and finished or semi-finished products are allocated and destined for the next cycle of the production or distribution chain. Storage operations are complex logistics system activities that require methods and tools that ensure speed, flexibility, and accuracy to meet the requirements of the processes they serve. For Hong [2], warehouses are meaningful elements in the logistic process because their operational performance determines the efficacy of logistics. However, inefficient management of this space can lead to high operational costs caused by a poorly

Received on 16 December 2021; revised 22 February 2022.
Address for correspondence: Carlos César Ribeiro Santos. Av. Orlando Gomes, 1845 - Piatã, Salvador - BA- Brazil. Zipcode: 41650-010. E-mail: carlosrs77@hotmail.com. DOI 10.34178/jbth.v5i1.189.

J Bioeng. Tech. Health 2022;5(1):18-24.

defined layout, inadequate handling equipment, and/or excessive material handling [3].

The so-called enabling technologies of Industry 4.0 present enormous potential to make warehouses computationally intelligent and can meet the most demanding operating conditions of logistic systems with autonomous or automated storage operations. According to Pacchini [4], autonomous robots, computer simulations, systems integration, internet of things, cybersecurity, cloud computing, additive manufacturing (3D printing), augmented reality, and analytics based on big data are some of the technologies that enable the automation of traditional warehouse functions evolving them into smart warehouses.

Companies should know the steps involved in introducing smart warehouse solutions, and balance this with the risk factors which encompass this process. A careful evaluation and consideration of these specifics are required to minimize the costs and risks involved.

This paper proposes a generalizable and scalable warehouse architecture to increase the traceability, reliability, and agility of intralogistics activities based on Industry 4.0 technologies. Given the current obstacles and opportunities for implementing industry 4.0 concepts in intralogistics operations, an approach will be presented for enabling technologies into smart warehouses by building a logical architecture. The results of applying the architecture will be demonstrated on a testbed using computer modeling and simulation.

Intelligent Warehouse Approach to Logistics 4.0

In the new context of Industry 4.0, the industry aims to complete automation of its manufacturing complex, including suppliers, distributors, and customers, seeking the constant search for increased efficiency, using mainly the various enabling technologies that support it. For Hermann and colleagues [5], the main pillars of Industry 4.0 are the Internet of Things supported by Cyber-Physical Systems (CPS) and represented in manufacturing as production elements such as robots, machines, and other devices that gain connectivity and communication abilities.

These CPSs are integrated with intelligent sensors generating big data supported by artificial intelligence (AI) capable of generating more assertive decision making using a massive amount of data, having as its main benefit to analyze and draw conclusions in real-time, besides offering predictions to improve performance or predict failures of machines or processes.

On the other hand, autonomous automation contributes to robots that do not need to be precisely programmed. Because of AI, they can learn and improve their procedures without much human interference [6]. In the context that Logistics 4.0 or Intelligent Logistics is a notorious evolution of traditional logistics, in synergy with Industry 4.0, which brings in its concept of the application of information technologies with high impact power throughout the supply chain. According to Galindo [7], the logistic systems improve flexibility, adapt to market changes, and bring companies closer to customer needs, allowing them to improve the level of service and reduce storage and production costs. Szyman'ska and colleagues [8] complements the definition of Logistics 4.0 with two approaches: (1) procedural, which means increasing the efficiency and performance of supply chain members; (2) technical, which includes the cited technologies of Industry 4.0, such as digitization, automation, mobility, and IoT.

Therefore, logistics processes are considered intelligent when they can communicate and transmit information about the organization autonomously to those responsible for the process [9]. Data from all operations are closely monitored and synchronized in cyberspace, creating a network in which data can be shared in real-time [10].

The intelligent warehouse architecture proposed in this research work for a logistics 4.0 considers, as suggested by Harrison and colleagues [11] and Orellana and Torres [12], four main requirements: the devices that compose the

system, the connectivity between these devices aiming at integration, the possibility of the hardware to be digitally integrated by a regular and interoperable logical architecture extended to the communication of the systems and, finally, the 100% digitized environment.

Materials and Methods

We did a state of the art research to understand the relevant concepts about intelligent warehouses, followed by an evaluation of the needs involved in logistics operations and to define the functions that obtain a modular architecture. We followed four steps [13]: we defined the system functions, determined the connections between them, built a matrix to analyze these connections, and finally defined the modules. The modules are sets of functions with the same characteristics to meet a specific need of the system.

Figure 1 presents the proposed architecture, with an overview of the system according to its modules and the respective enabling technologies contained therein. For the development of the architecture, we examined a series of requirements to identify the technologies that most impact the intralogistics operation times related to warehouses, such as communication structure, automation of operations, integration of technologies, monitoring and tracking of products, human intervention and modularity. Each technology selected to compose the architecture was derived from an in-depth analysis of technological solutions applied in logistics operations already available in the market and to transform a traditional logistics operation into a logistics 4.0, identifying the most repetitive activities, rework, inflexibility, as well as those that required greater agility and security.

The first module (Decision Support) uses Computational Simulation with the aid of

Figure 1. The logical architecture proposed for intelligent warehouses.

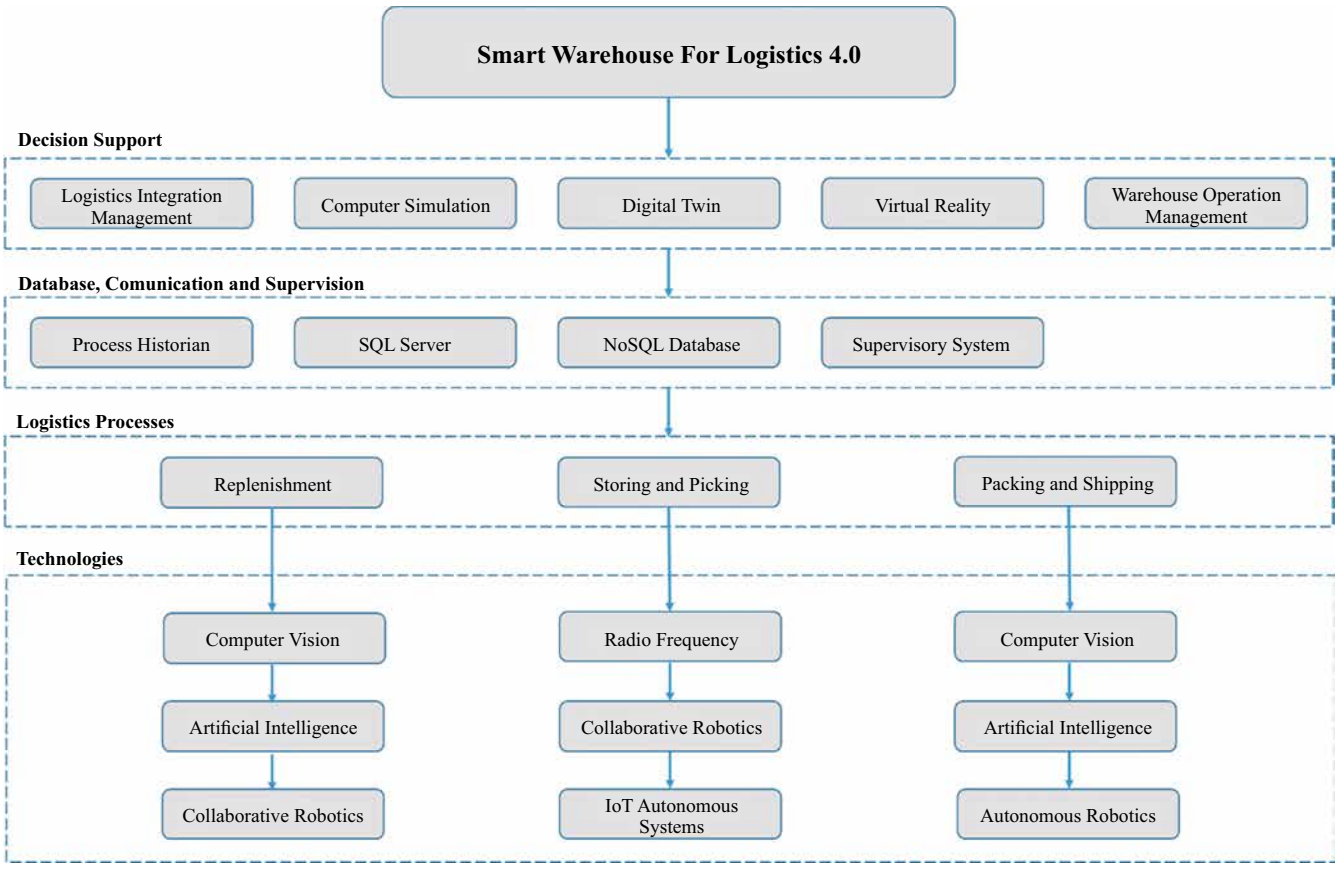

Virtual Reality as decision support tools to predict scenarios and find the best solution in an environment with minimal risks and without interrupting the real operation but feeding it back in real-time according to the digital twin paradigms. This approach allows stakeholders to interact with the virtualization of the operation in real-time and thus enable improvements in planning activities and mitigate possible errors in the operation.

The second module (Database, Communication, and Supervision) represents the communication infrastructure of the concept and the interface to the operators. The supervisory system manages a database of the system and transacts information with the controllers of the PSCs that operate the system for integrated operation. Communication between PSCs can occur via wireless or wired fieldbus networks (we adopted Modbus TCP/IP protocol for simplification). The database will store information about the items and orders to record the logistic process status. An SQL Server database is the basis of the internal system, but NoSQL databases for the supplier, customer, and market data and process historians can be added for predictive analyses. The controllers of the various equipment and processes execute the routines determined by the supervisory system or the logic established between CPSs, including the movement of collaborative and autonomous robots, as the logistics application determines.

The third module (Logistic Processes) presents the stages of the logistic process served by the system (outbound processes), which are focused on customer service, supported by the "seven rights (7Rs)" strategy, that is, to deliver the "right product", in the "right quantity", in the "right quality", in the "right place", at the "right time" for the "right customer" and the "right cost" [14, 15]. The fourth module (Technologies) presents the selected technologies of the system for its operation at the physical level. They represent the technological concepts existing in the hardware that uses these concepts to perform their functionalities in the system. The technologies are organized in the three stages of the logistic process so that it is possible to visualize at which stage each technology was implemented.

The integration of technologies and interactions between humans and machines to promote the better performance of the system, reduction of logistic waste, and time-saving encompass the construction of the system. The goal of automation and intelligence in warehouse operations is that processes become less dependent and respond adequately to the variability inherent in human work. Thus, obstacles such as lack of system integration, poor use of space, counterflows in the movement of materials, operational errors from human intervention, fatigue, excessive bureaucracy, communication failures, long delivery times, deficiencies in the traceability of processes, and products are overcome. The proposed smart warehouse approach enables, by the continuous learning that is inherent to it, to gradually eradicate these obstacles and to evolve synchronized with the best-emerging technologies for smart warehouses. To prove the method, demonstrate the potential gains, and the technical viability of the presented logical architecture, a testbed was developed using modeling software and computational simulation, based on the case of a partner company, located in Joinville-SC, Brazil. The company operates in the logistics segment, supplying the needs of its customers with solutions for moving, storing, and transporting products, the focus of the study in question. The warehouse has 740m² and 10% of this area was for the testbed (72m²) (Figure 2).

The traditional logistics operation was virtualized as a strategy to test technologies used to meet the necessity of the operation. The development of the computational model was based on some assumptions: nature of the product handled, investment restrictions, orchestration of resources, available space, mandatory process flow, flexibility, and the minimum frequency of receipt and dispatch of materials handling, and storage operation. The logic for the computational model was developed in FlexSim® software using the ProcessFlow module. ProcessFlow has a variety

Figure 2. Flowchart of the warehouse operation.

of activity blocks, and as the process flow diagram is built in the software, logic can be developed within each block and related to the 3D model. SketchUP® was used to develop the 3D components most similar to the physical components of the warehouse. Then the FlexSim® 3D model imported them. Figure 3 shows the main parameters inserted in the logic configuration.

The time parameters were calculated by observing the activities of the traditional warehouse operation and recording the time of each activity using a stopwatch, obtaining the averages and standard deviations. These values were computed into the model as a normal statistical distribution. The datasheets of the selected equipment acquired information on the operation speed of each piece of equipment.

The logic of the warehouse operation was organized into processes to facilitate the follow-up of activities during the execution of the 3D model. Figure 4 demonstrates the approximate idea of the logic construction.

This operation tends to become an intelligent operation, which occurs when solutions are pointed out, autonomously or automatically, that assist the system users in the decision-making processes, analyze the history, and allow the connection of new technologies to the existing system.

Figure 3. The main parameters collect for the simulation logic.

1	Operator loading time
2	Operator unloading time
3	Forklift loading time
4	Forklift unloading time
5	Item dimensions
6	Equipment speed

Results and Discussion

The results presented with the computational simulation allowed for more realistic analyses regarding potential gains, such as the structuring and systematization of operations, increased efficiency, accuracy, error reduction, optimization of warehouse space utilization, increased safety in operations, facilitation in the identification of bottlenecks in the logistics process, improvement in the visualization and general perception of each stage of the operation, improvement of the operator's working conditions, and reduction in the time it takes to dispatch orders.

We compared the time of the current processes with the data generated by the computational modeling, which predicts data from the testbed operation. Thus, we identified a projection of increased productivity between the traditional process and logistics 4.0 with the application of the enabling technologies mentioned (Figure 5).

Conclusion

The presented structure is a low investment option because the technology involved can be found in equipment and systems already available in the market, and its integration is done using hardware and software modules with content-oriented approaches, able to operate in heterogeneous scenarios, involving devices from different suppliers with minimal adaptation and short implementation time. It also allows automation in stages for minimal interruption of current operations and a lower volume of financial investment. A step forward for the concept

Figure 4. Example of the FlexSim® process flow and its connections.

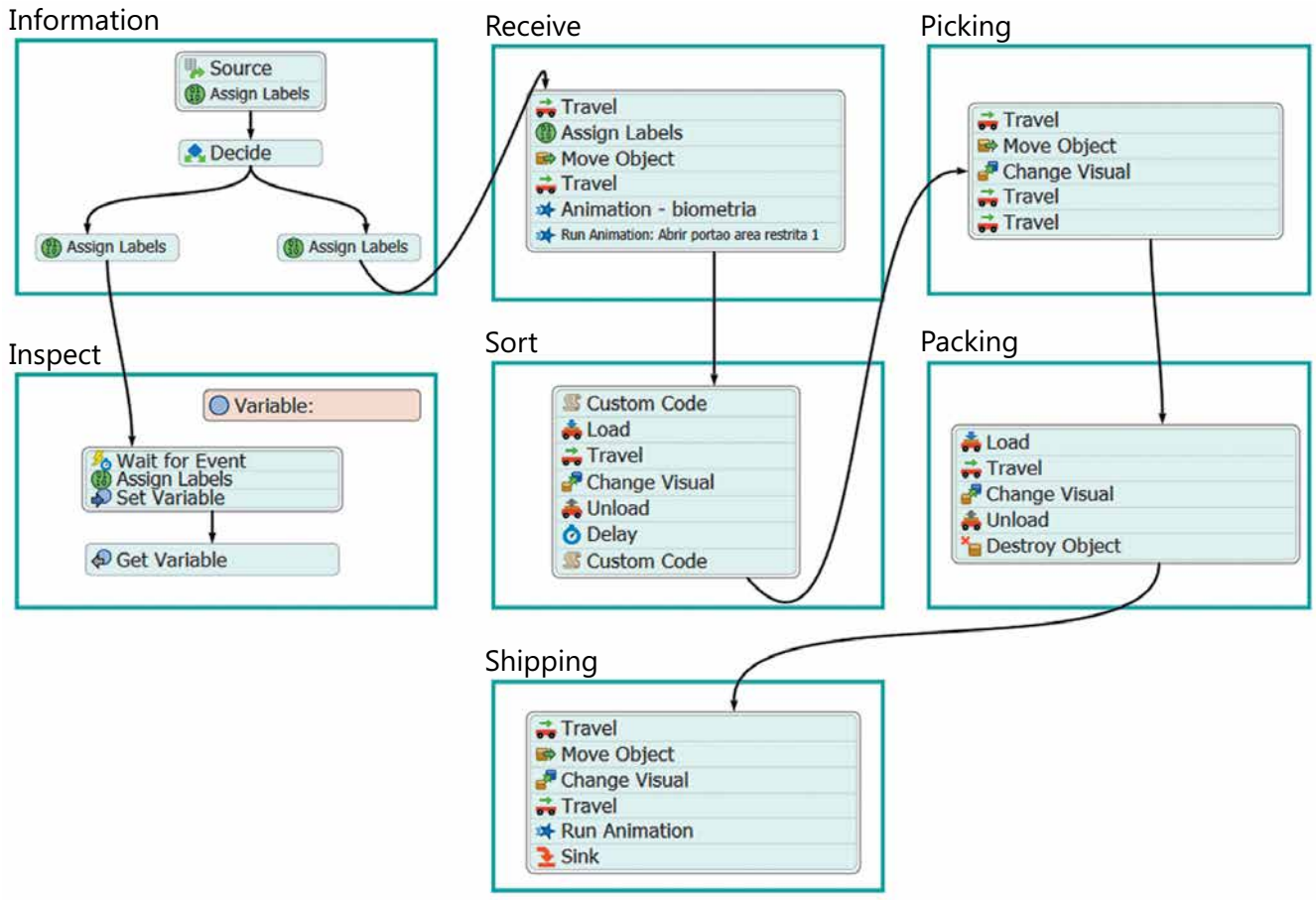

Figure 5. Comparison between traditional inbound and outbound operations with the testbed (simulated scenario).

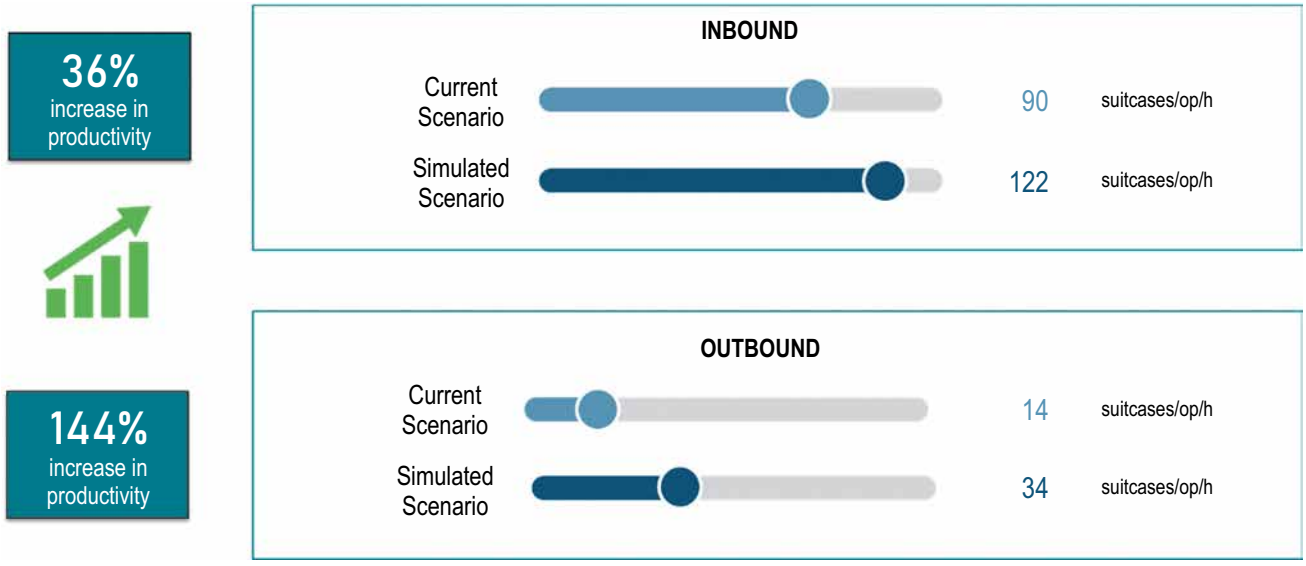

proposed here will be to seek platform-agnostic solutions independent of proprietary solutions for scalability and technological updating of the system.

The proposed architecture can be used as a strategy for other logistics operators who wish to automate their processes to make them intelligent. In the long run, successive small modernizations at shorter intervals make a more effective contribution than major upgrades at longer intervals.

Principles should be followed to build a modular architecture such as the analysis of the impact of enabling technologies on the operation through computer simulations and digital twin resources, to mitigate integration risks in advance, identify the processing capacity and the best structure for the flow of materials and information, as well as the trends and costs involved to generate the functions to be performed by the system. A relevant aspect was the determination of the database, communication network, and supervisory system to establish connectivity between the technological resources. Once well defined, they can provide the intended generalizable characteristic for customizations and implementations of technologies in intralogistics processes. Finally, promoting the integration of the set of Industry 4.0 enables technologies to promote an improvement in warehouse performance, with the reduction of logistics waste and time savings.

Therefore, companies aiming to modernize their intralogistics operations to increase their efficiency, flexibility, and connectivity, can take into consideration the suggested logical architecture with the combination of features aimed at intelligent warehouse systems, in a way that allows a planned configuration, able to interconnect through modern and secure communication networks, and a digital architecture designed to allow systems to behave in an integrated and coherent way.

A step forward in the concept proposed here will be to seek agnostic platforms, which are independent of proprietary solutions for the sake of scalability and technological updating of the system.

References

1. Bowersox DJ, Closs DJ, Copper MB, Bowersox JC. Gestão Logística da Cadeia de Suprimentos. 4ª. ed. Porto Alegre: AMGH, 2014.
2. Hong Y. The application of barcode technology in logistics and warehouse management. First International Workshop on Education Technology and Computer Science 2009:732-735.
3. Kamalli A. Smart warehouse *vs*. traditional warehouse. Int. J, 2019.
4. Pacchini P. The degree of readiness of industrial companies to implement industry 4.0: a study in the brazilian automotive sector. Nove de Julho University, 2019.
5. Hermann M, Pentek P, Otto B. Design principles for industry 4.0 scenarios. Proceedings of the Annual Hawaii International Conference on System Sciences 2016;7427673:3928-3937.
6. Jahn C, Kernsten W, Ringle C. Logistics 4.0 and sustainable supply chain management: innovative solutions for logistics and sustainable supply chain management in the context of industry 4.0. Hamburg International Conference on Logistics (HICL), 2018.
7. Galindo L. The challenges of logistics 4.0 for the supply chain management and the information technology. Master's thesis, Master of Science in Mechanical Engineering, Norwegian University of Science and Technology, Department of Production and Quality Engineering, 2016.
8. Szyman'ska O, Adamczak O, Cyplik M. Logistics 4.0- a new paradigm or set of known solutions? Logistics Production 2017;7.
9. Amodu O, Othman M. Machine-to-machine communication: An overview of opportunities. Computer Network 2018;145(9):225–276.
10. Lee J, Baghieri B, Kao H. Cyber-physical systems architecture for industry 4.0- based manufacturing systems. Manufacturing Letters 2014;3.
11. Harrison R, Vera D, Ahmad B. Engineering the smart factory. Chinese Journal of Mechanical Engineering 2019;29.
12. Orellana F, Torres R. International journal of computer integrated manufacturing. Chinese Journal of Mechanical Engineering 2019;32:441–451.
13. Lameche KM, Najid N, Castagna P, Kouiss K. Modularity in the design of reconfigurable manufacturing systems. IFAC-PapersOnLine 2017;50(1):3511–3516.
14. Teoman S. Achieving the customized "rights" of logistics by adopting novel tecnologies: a conceptual approach and literature review. UTMS Journal of Economics 2020;11:231–242.
15. Rushton A, Croucher P, Baker P. Handbook of logistics and distribution management. 6th ed. [Place of publication not identified]: Kogan Page, 2017.

Development of Experimental Bench for Wireless Power Transfer

Ítala Liz da Conceição Santana Silva[1*], Wanberton Gabriel de Souza[2]
[1]SENAI CIMATEC University Center; [2]Centro de Competência em Transferência de Energia sem Fio; Salvador, Bahia, Brazil

Wireless-power-transfer (WPT) for powering low-power devices has increased in recent years. The inductive resonant coupling method is the most used technique for this application and consists of taking advantage of the magnetic field generated in a coil so that there is current circulation in another nearby coil. In this work, using this technique, the series-series (SS) compensation topology was used to develop a test bench that should supply a load of up to 10W. Therefore, a brief explanation of the topic, calculations used, defined parameters, and we presented preliminary results of the proposed system.
Keywords: Wireless Energy Transfer. Inductive Resonant Coupling. Series-Series Compensation. Low-Power.

Introduction

Systems based on wireless energy transfer have been applied in various areas such as electronic devices, electric vehicles, autonomous underwater vehicles (AUVs), biomedical implants, and the military field. Consequently, the need to develop increasingly efficient topologies to meet the needs of these applications.

With this project, we seek to define the parameters and infrastructure of a test bench for wireless energy transfer outdoors over short distances for small loads and low power. For this, we showed the theory that supports the technology, simulations, and calculations of the system parameters. We planned to validate the efficiency of the developed system.

Theoretical Foundation

In this section, We used the theory as the basis for the development of the system will be discussed.

Received on 13 December 2021; revised 27 February 2022.
Address for correspondence: Ítala Liza da Conceição Santana Silva. Av. Orlando Gomes, 1845 - Piatã, Salvador - BA-Brazil. Zipcode: 41650-010. E-mail: italaliz.eng@gmail.com.
DOI 10.34178/jbth.v5i1.190.

J Bioeng. Tech. Health 2022;5(1):25-31.

Input Circuit

There are several ways to power a WPT system. In the literature, the most used form is using an inverter in bridge H. This circuit has the function of transforming a direct current (DC) into an alternating current (AC) for the resonant grid at the desired frequency. For this, you need a power signal that provides a sinusoidal signal on the inductive link. There are several techniques for obtaining this sinusoidal signal, both analog and digital.

Its working principle consists of the operation of two transistors at a time, responsible for generating the two half cycles of the AC network. In this context, conduction provokes the positive half-cycle, while the others are in cut. The others are cut-off, and the negative half-cycle is generated [1].

In this scenario, the LC compensation circuit works as a filter, eliminating the harmonics of the fundamental frequency, thus approximating a sinusoidal output signal.

Inductive Resonant Coupling

The inductive resonant coupling is currently the most used transmission method for WPT systems and consists of the induction of time-varying magnetic fields to transport energy. In it, operating frequencies of up to tens of MHz are used because in the inductive coupling, the transmitter and receiver are in means of very low magnetic

permeability, making the coupling weak and the transfer of energy impracticable to traditional frequencies. Furthermore, the magnetic field is easily dispersed in all directions, resulting in large losses and low efficiency. When using inductive resonant coupling, the transmitter and receiver operate at the resonant frequency, significantly reducing losses. The type of capacitor connection (series or parallel) will depend on the source and load characteristics [2]. Due to frequency, the source must be AC (to generate a varying magnetic field of adjustable frequency) and for transmission, there will be a compensation circuit. Finally, there is a rectifier circuit that will supply the load. Figure 1 shows the standard diagram of a WPT system.

LC circuits are used in the resonant loop so that the system operates at the resonant frequency, and the efficiency is improved. There is also a concern when using high frequencies because the current suffers losses resulting from the Skin effect. It is recommended the use of wire Litz, hollow or larger cross-section wires to reduce these losses.

Main System Parameters

Coupling Factor (k)

In addition to the operation at the resonance frequency, other parameters are crucial for the proper functioning of the WPT system, such as the coupling factor (k). The value of "k" is directly linked to the distance and position between the coils. Its value decreases with the distance and misalignment of the coils, making the use of inductive resonant coupling restricted to short-distance applications. The greater the number of magnetic field lines, the greater the coupling factor between them. However, the coupling is not perfect, which makes it necessary to use capacitors to compensate for inductive losses [3].

The coupling factor is calculated by expression (1):

$$k = \frac{1}{\left[1 + 2^{\frac{2}{3}}\left(\frac{d}{\sqrt{a.b}}\right)^2\right]^{\frac{3}{2}}} \quad (1)$$

Where d is the distance between the coils, and a and b are the radius of the transmitting and receiving coils, respectively.

Quality factor (Q)

The quality factor (Q) guarantees "optimal" resonance at high frequencies. It usually has a high value for work frequency. This parameter counterbalances the drop in the coupling factor with the variation in the distance. So that efficiency can be maintained [4].

Increasing the value of Q reduces stray resistances, hence system losses, and can be optimized by reducing losses due to high frequency. It is a relationship between the energy that the system stores and the energy that it dissipates [4]. It is a parameter of the coils and the compensation circuits and can be mathematically described in expression (2):

$$Q = \omega \frac{L}{R} \quad (2)$$

Where ω is the angular frequency of the system, L is the coil's self-inductance and R is its resistance.

Figure 1. Standard diagram - WPT system.

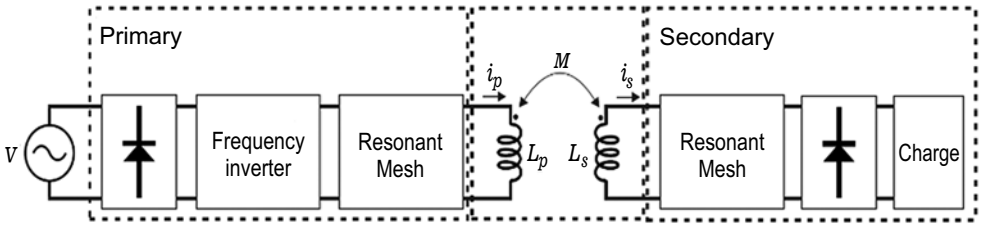

Coil Geometry

Geometry is a parameter that directly affects system efficiency. When comparing spiral-type and helix-type coils, [2] we obtained the following results: when changing the distance between the coils, the coupling coefficient between the helical coils is much smaller than that of the spiral-shaped coil. Subsequently, the spiral-type coil is significantly superior to the helix-type coil in terms of higher inductance value and, as a result, has a higher coupling coefficient [2]. Therefore, the helix-type coil topology is not feasible (Figure 2).

Thus, the flat spiral geometry was adopted in the project. In this geometry, the length of the conductor can be expressed by calculating the Archimedean spiral given by (3):

$$l = \pi . x . y^2 + \pi y \left(2 \frac{d_{int}}{2} + x \right) \quad (3)$$

Where x is the diameter of the conductor and, $y = \frac{\left(\frac{d_{ext}}{2} - \frac{d_{int}}{2}\right)}{x}$, d_{ext} and d_{int} are the inner and outer diameters of the coil, respectively.

Coil Self-Inductance

There are several approaches to coil models and geometries, as well as their respective advantages and disadvantages in the literature. Also, there are several ways to calculate the self-inductance of the coils. The self-inductance of the planar circular coil is calculated by the following approximate Equation (4):

$$L = \frac{\mu . N^2 (d_{int} + d_{ext})}{4} \left[\ln \left(\frac{2.46}{\phi} + 0.20 \phi^2 \right) \right] \quad (4)$$

Where $\phi = (d_{ext} - d_{int})/(d_{ext} + d_{int})$

Mutual Inductance

Mutual inductance (M) represents the interaction between the primary and the secondary. Faraday and Lenz's Law explains the theory that governs mutual inductance. The greater the mutual inductance, the greater the number of magnetic field lines delivered to the receiver [4]. The simplest way to get the value of *M* is to use the approximate Equation of k, making $M = k\sqrt{L_p . L_s}$, since M has a complex analytical solution.

Compensation Circuit - Series-Series (SS) Topology

The compensation circuit is used so that the system operates at the resonance frequency and reduces losses due to the influence of harmonics and electromagnetic interference [3]. Of the studied topologies, the one that best meets the project requirements, whose results are found a simple only way, is the SS topology, shown in Figure 3. Its main advantage is the independence between the values of the

Figure 2. Comparison between spiral and helix coils [2].

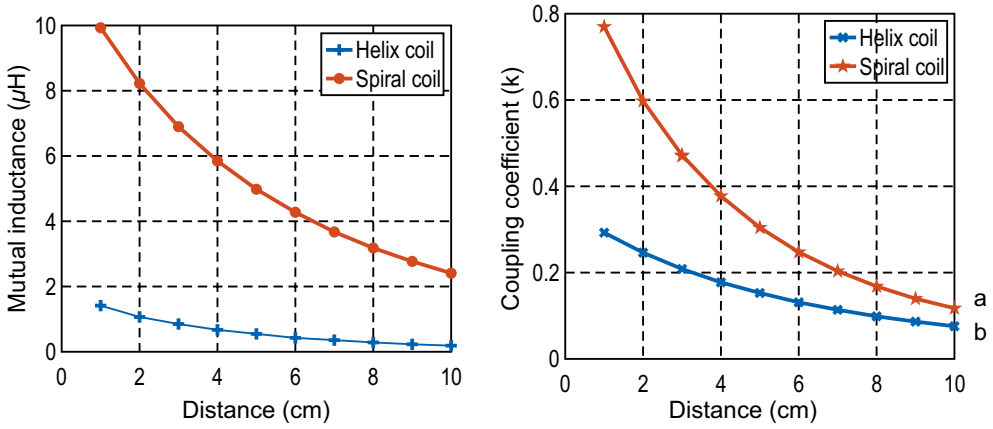

primary capacitance (C_p), the magnetic coupling coefficient (k), and the quality factor (Q) [5].

Figure 3. Compensation Circuit - Series-Series (SS) Topology.

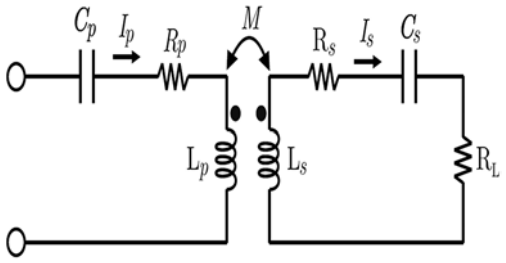

Where:
L_P and L_s are the primary and secondary auto inductances, respectively;
C_p and C_s are the primary and secondary capacitances, respectively;
R_p and R_s are the primary and secondary ohmic losses, respectively;
I_p and I_s are the currents flowing in the primary and secondary, respectively.
The resonant frequency is obtained by:

$$f_{res} = \frac{1}{2\pi\sqrt{LC}} \quad (5)$$

Physical Infrastructure

Coils are made using wires Litz. In its use, the number of intertwined conductors must be observed because it directly affects the shunt capacitance. In its structure, the material is generally used that interferes insignificantly with the quality factor and the resonance frequency, such as glass, styrofoam, and acrylic.

Materials and Methods

Based on the theory described in item 1 (Introduction), initially, the shape of the coil, the circular planar geometry, was defined. After that, combinations of the number of turns and how they influenced the efficiency of the system were tested. Thus, the geometric parameters were chosen.

With the coil geometry defined, frequency x efficiency calculations were made to define the working frequency.Then, the other parameters of the project were calculated, such as self-inductance, mutual inductance, and quality factor.

After defining the calculated parameters, the functioning of the electrical circuit was tested in the PSIM software. Two forms of input signal were tested: using a PWM signal as a carrier and a square wave signal at the resonant frequency. Then the input form was defined. The bench was assembled in acrylic and the tests began.

Results and Discussion

After tests, it was concluded that the best efficiency results are for coils whose transmitter is slightly larger than the receiver, because of this, N of 20 and 10 turns was chosen for the transmitter and receiver. Based on the studies studied, frequencies of 85 kHz, 500 kHz, and 13.56 MHz were tested. The most efficient result was for a frequency of 500 kHz. In the process of assembling the coil, the Litz AWG 12 wire conductor (2.052mm in diameter) was used and the winding was manual, as shown in Figure 4.

The self-inductance of the coils was measured using an LCR meter.

As the coils were manually wound, some specified parameters were not met, such as the spacing between the turns, central alignment, and the length, factors that directly change the value of the auto inductance L. Considering these divergences, the values of L are satisfactory. We presented a summary of the calculated and actual parameters (Table 1).

We assembled the circuit to analyze the behavior of the system (Figure 5).

For the circuit presented, an input signal of $12V$, a load of 4.1Ω, $C_P = 5nF$, and $C_s = 36nF$. The simulation results were $V_L = 6.41\,V$ and $I_L = 1{,}56A$ (Figure 6).

After the simulation, the bench assembly process was carried out. With the infrastructure

Figure 4. Transmitting and receiving coils.

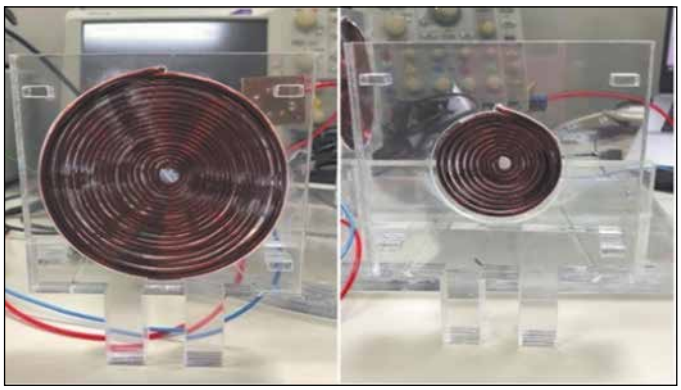

Figure 5. Assembled circuit diagram.

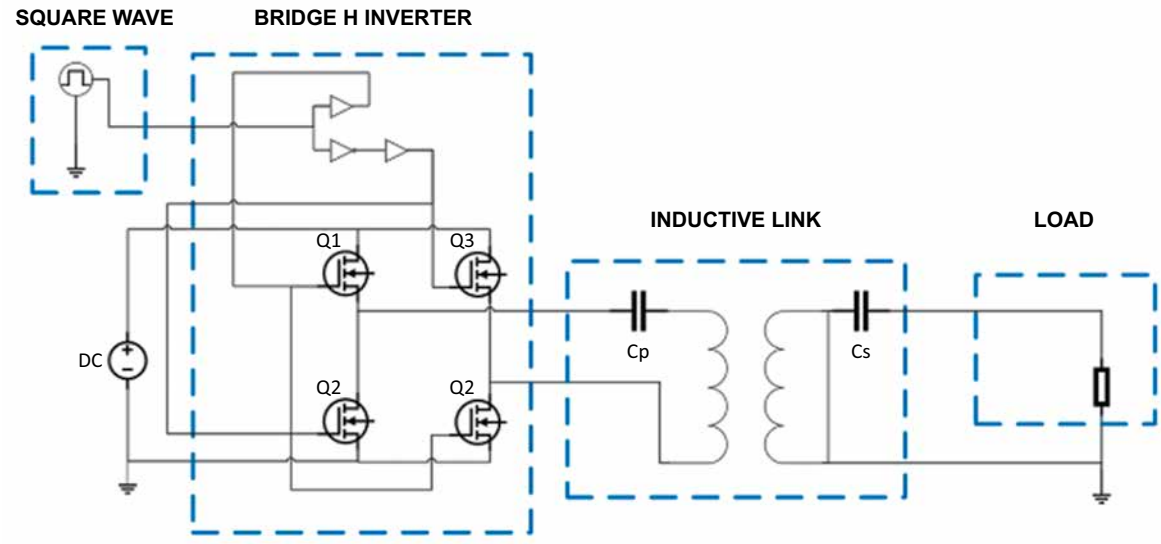

Figure 6. Voltage and current in the simulated resistive load.

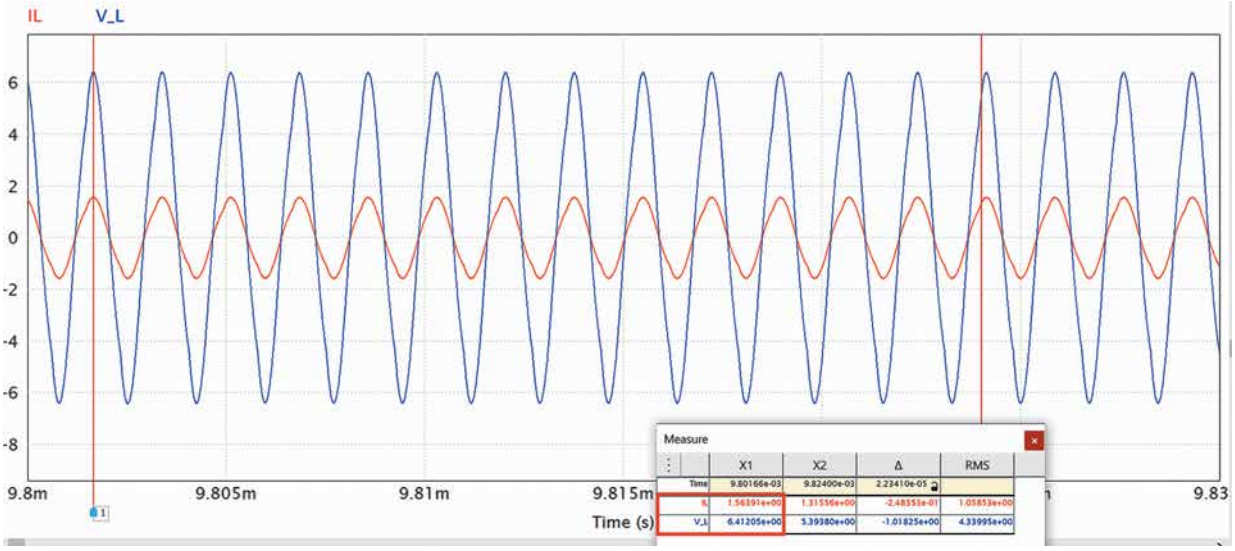

Table 1. Coil parameters.

Constructive parameter	Calculated value	Real value
Working frequency (kHz)	500	578.81
Number of turns Tx (N_1)	20	20
Number of turns Rx (N_2)	10	10
Coil inner diameter (d_{in}) (cm)	1	1
Conductor diameter (w) (mm)	2.052	2.052
Spacing between turns (s) (mm)	0.25	0.0
Coil outside diameter Tx ($d_{ext_{Tx}}$) (cm)	10.21	10.20
Coil outside diameter Rx ($d_{ext_{Rx}}$) (cm)	5.6	5.6
Coil length Tx (l_{Tx}) (m)	3.81	3.91
Coil length Rx (l_{Rx}) (m)	1.10	1.21

ready, the system components were connected for testing (Figure 7).

After validating the functioning of the system, performance tests were performed, varying the distance and alignment between the coils (Figure 8).

Analyzing the Figures, we verified that voltage and current values drop significantly with increasing distance and misalignment between the coils, as expected based on the studied theory. We compared calculated, simulated, and measured values (Figure 9).

Considering that some Equations used in the calculations are approximations found in the literature and that the simulation works with ideal conditions, the measurement results were expected and proved satisfactory.

Conclusion

The project was divided into phases. In the first phase, a survey of the state of the art was carried out to support the development of the bench. After that, studies related to the inductive link and physical structure were deepened. Subsequently, the design of the compensation circuit and the other components of the system were assembled, and the assembly and testing were carried out. Currently, more performance tests are being done and at the end of the period defined in the schedule, it is expected to obtain a functional test bench with all expected results validated.

Acknowledgments

To the FIEB SENAI CIMATEC system for its financial and structural contribution, which is

Figure 7. Test-lined and vertical misalignment between the coils.

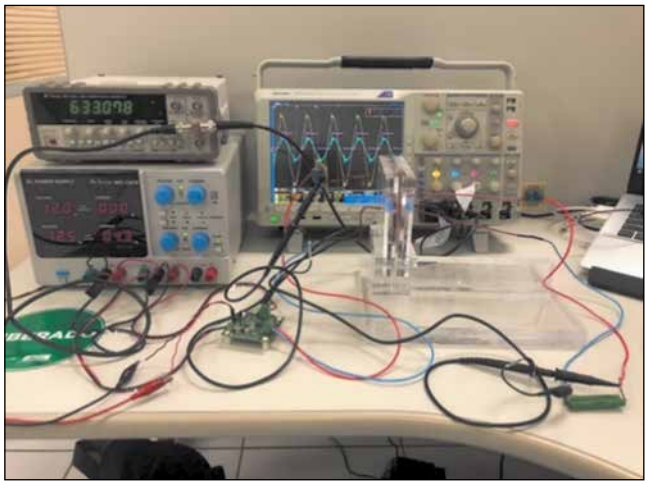

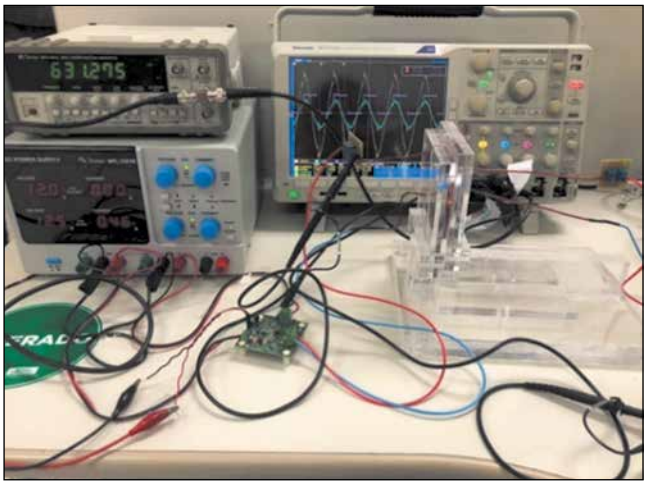

Figure 8. Vertical misalignment between the coils – Voltage and current.

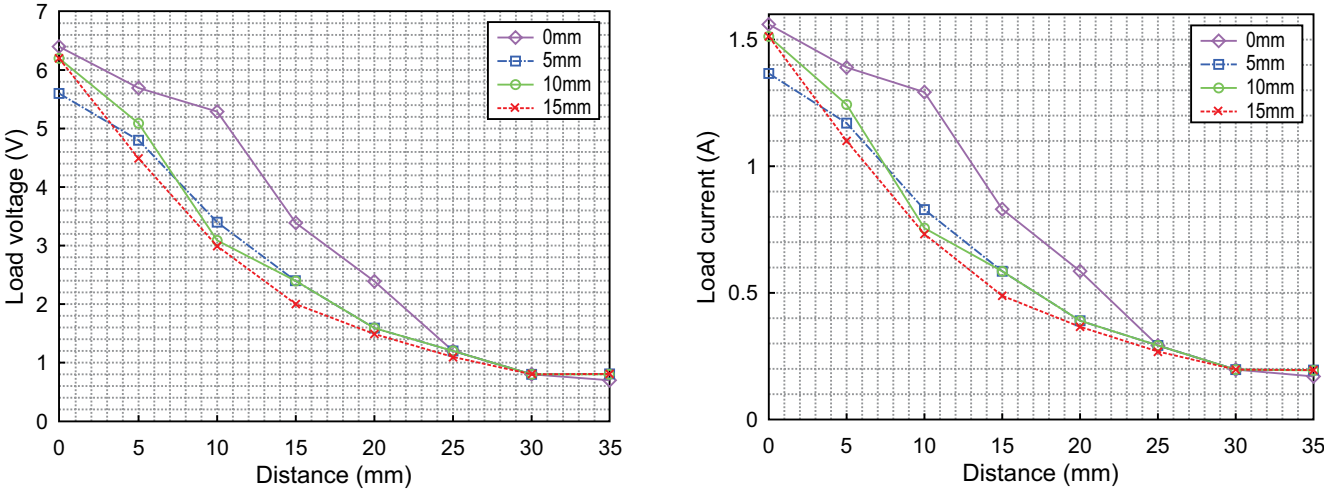

Figure 9. Results – Voltage and current.

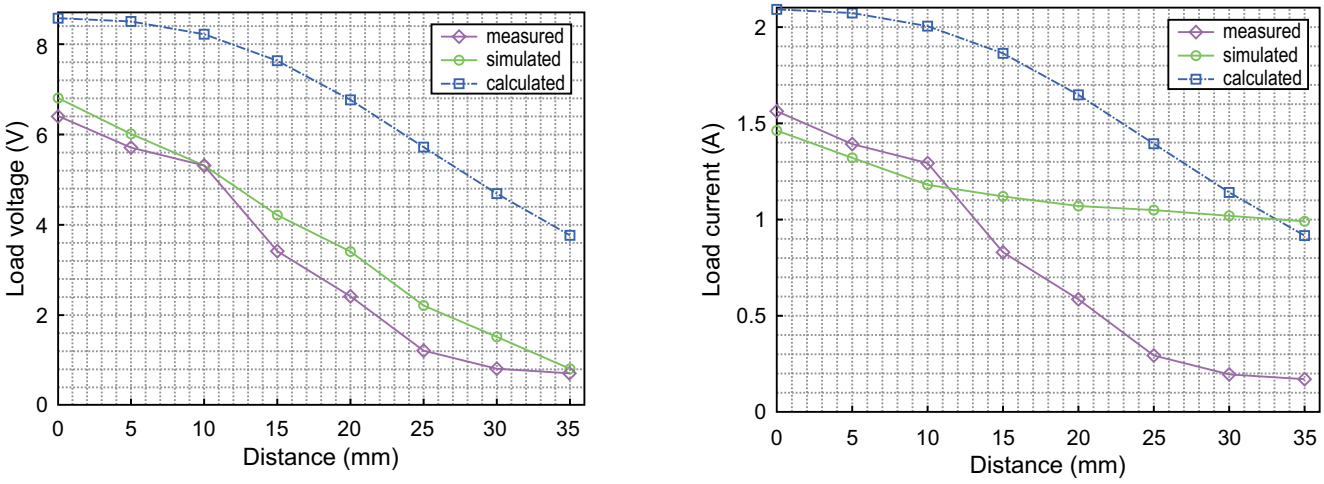

fundamental for carrying out the work. This work was carried out with the support of the coordination of the Embedded Electronics and Generation, Transmission, and Distribution sectors at SENAI CIMATEC.

References

1. Fernandes RC, Azauri AO. Tópicos selecionados sobre o estado-da-arte em transferência indutiva de potência. Eletrônica de Potência, Campo Grande 2013;19(1):58-71.
2. Bana V. Maritterization of coupled coil in seawater for wireless power transfer. (No. SPAWAR/SCP-TR-2026). Space and Naval Warfare Systems Center Pacific San Diego Ca, 2013.
3. Abreu RL. Projeto e implementação de um dispositivo para transferência de energia sem fios por modos ressonantes autossintonizáveis. Tese, Universidade Federal de Itajubá, 2017.
4. Silva ILCS, Conceição JP. Test bench design for wireless energy transfer using the resonant inductive coupling method. VI International Symposium on Innovation and Technology, 2020.
5. Orekan T, Zhang P, Shih C. Analysis, design, and maximum power-efficiency tracking for undersea wireless power transfer. IEEE Journal of Emerging and Selected Topics in Power Electronics 2017;6(2):843-854.

A Comparison of Deep Learning Architectures for the 3D Generation Data

Yasmin da Silva Bonfim[1*], Gabriel Sete Ribeiro Lago dos Santos[1], Gustavo Oliveira Ramos Cruz[1], Flávio Santos Conterato[1]

[1]SENAI CIMATEC University Center; Salvador, Bahia, Brazil

There is a need to identify the best artificial images for each use case faced with several Deep Learning architectures for generating them. Twelve models with different hyperparameters were created to compare several networks with the generative architectures Autoencoder, Variational Autoencoder, and Generative Adversarial Networks in the 3D MNIST dataset. After training, the models were compared with loss functions to assess the difference between the original and artificial data, so that greater complexity did not translate into better performance, indicating the Autoencoder models as the best cost-benefit.

Keywords: Generative Networks. 3D Data. Comparison. Machine Learning.

Introduction

Computer vision has been providing many projects developed in image generation, with deep learning technologies (DL) showing advances for the generation of data in 2D, making use of architectures already relevant in the area [1]. On the other hand, the 3D segment is often in the background, maybe because of the high complexity concerning 2D or the computational power needed to process this data [2].

The need for automated 3D data generation comes from the difficulty of creating three-dimensional representations manually, requiring too much time and research to build the items that will be portrayed [3].

The 3D MNIST dataset was used, which has 12,000 images in three dimensions [4]. The data was adapted from MNIST, which has numbers from 0 to 9 handwritten in a 2D representation [5].

The article aims to compare the Autoencoder, Variational Autoencoder (VAE), and Generative Adversarial Networks (GANs) architectures regarding several evaluation metrics to present the performance of each architecture for representing 3D data [6-8].

Received on 15 December 2021; revised 20 February 2022.
Address for correspondence: Yasmin da Silva Bonfim. Av. Orlando Gomes, 1845 - Piatã, Salvador - BA- Brazil. Zipcode: 41650-010. E-mail: yasmin.bonfim@ba.estudante.senai.br.
DOI 10.34178/jbth.v5i1.191.

J Bioeng. Tech. Health 2022;5(1):32-36.

Autoencoder

The Autoencoder (AU) architecture is composed of two smaller networks that seek to compress the input into a latent representation, a version Where only the essence of its structure remains. In the first network, the encoder, the original data is reduced to a one-dimensional vector h, where its characteristics are categorized by increasing importance, between 0 and 1, to be discarded or preserved. In the next step, the decoder network receives the vectorized structure and performs the inverse process, returning the data to its original size and aspect, but with only the essence of its structure [9].

$$Loss = -Log\ P(x|x') \quad (1)$$

To check the quality of the representation created by the network, the loss function observed in Equation 1 is used, where -log P compares the original input x with its latent representation x'. The loss in an autoencoder should be as small as possible, but it will hardly be zero. Considering that one of the main characteristics of the AU architecture is to learn the essentials and return data with reduced dimensionality, a loss of value 0 implies a faithful reproduction of the image, which in turn denotes low learning of its main components, essentially creating a network that returns your input without a concrete benefit [10].

Variational Autoencoder

The Variational Autoencoder (VAE) is an architecture composed of the union of two networks, an encoder, which maps the inputs and compresses them from the input to the latent space; and the decoder, which maps the data from the latent space to perform its decompression. The difference between VAE and Autoencoder architectures is the guarantee of properties in the latent space to allow the generation of new data. The latent space is the compressed data: its reproduction with lower dimensionality. Broadly, the VAE requires the standard Gaussian distribution anterior to the latent space. Thus, the VAE tends to maximize Equation 2 [11].

$$P(z) = N(z|0, I) \quad (2)$$

To solve it, the VAE needs to deal with defining the information that will be represented by the latent variable z and how to deal with the integral over z. The latent variable can be understood as the choice of a character to be generated by the model before assigning a value to any specific pixel, that is, the model will produce configurations for the generation of the character. The z settings tend to produce a character that resembles the initial die. Furthermore, the interpretation of dimensional samples can be extracted from a simple distribution, being it N (0, I), where I is an identity matrix [11]. That said, the model parameters are trained to minimize the reconstruction error between the reconstructed and the initial data, making use of the Loss function KL divergence, acting as a regularization term, to calculate this divergence.

Generative Adversarial Networks

Generative Adversarial Networks (GAN), are generative architectures based on Deep Learning, in which an adversarial training process takes place between two networks: A Generative model G that is based on the original distribution of data to generate a new sample, and a Discriminative model D that estimates the probability a data sample coming either from the original data distribution or from the sample generated by the Generative model G. This training occurs until the Discriminator becomes unable to discern between the original and generated data [8].

GANs are often used in the Computer Vision field to perform various tasks involving images. They can be used to generate higher resolution versions of images and create sketches, paintings, and others. During the training stage of this architecture, with the data generated by the Generator model, the Discriminator model has the role of correctly classifying between real and generated data. In consideration of the above, the final function of value V (G, D) is based on Equation 3, which involves the minimization of the Discriminator's error and the maximum precision of the Generator when creating the images [8].

$$\min_G \max_D V(D, G) = Ex \sim Pdata(x) [Log\ D(x)] + Ez \sim Pz(z) [Log\ (1 - D(G(Z)))] \quad (3)$$

Recurrent Neural Networks

The Recurrent Neural Network (RNN) is an artificial neural network, used for sequential data or time series. The RNN, unlike traditional neural networks, can remember previous information from the feedback, allowing the information to persist [12]. To decide, the network considers its current input and what it learned from the previous input. It has a "memory", which stores the information of the calculations performed, enriching the expressive power of the model by capturing causal and contextual information [13]. That said, RNN manages to reduce the complexity of parameters, in addition to adjusting the weights through backpropagation and descending gradient processes, facilitating the learning process.

As there were advances in the development of RNNs, other architectures were created from it, such as Long-Short Term Memory (LSTM) [13] and Gated Recurrent Unit (GRU) [14].

Convolutional Neural Network

The Convolutional Neural Network (CNN) is a neural network widely used in problems dealing with image data, such as pixels. Important applicability of CNN is the extraction or detection of image contents when the input propagates through deeper layers [15]. During the convolution process applied to images, weights are assigned to certain sets of pixels that can indicate lines, curves, and eventually, complex patterns, where higher weights denote greater importance of that set of pixels for the current task. In addition, there are other types of convolutional neural network architectures, such as the Fully Convolutional Network (FCN), a kind of convolutional neural network, which contains only convolutional layers, not having "Dense" layers.

Multilayer Perceptron

The Multilayer Perceptron, or MLP, is a simple artificial neural network with several interconnected neurons that present a non-linear mapping between an input vector and an output vector [16]. Efficiently, MLPs backpropagate the network's error, based on that error, the weights of previous layers are recalculated starting from the last layer up to the first.

Materials and Methods

The approach chosen for this work was the comparative between practical experiments of several generative networks with different activation functions, number of layers, and number of neurons per layer. This exploratory, empirical, quantitative, and qualitative research seeks to identify the advantages of each architecture, ranging from the network training time to the quality of the data generated at the end of the process. The work was divided into 3 stages:

(1) search,
(2) generation,
(3) evaluation and synthesis.

In stage (1), a literature review was carried out where relevant works on the AU, VAE, and GAN architectures were identified, to verify the validity of the proposed comparison. During (2) a single base model was created for each architecture, subsequently, the bases were adapted into 4 models, divided into FCN, CNN with MLP, LSTM, and GRU, amounting to 12 models. In stage (3), the results of the models were grouped in tabular form, comparing the differences between the original image and that generated through the loss metrics Binary Cross-Entropy and Mean Squared Error (MSE), described in Equations 4 and 5, generating a Table per metric, with both divided between architectures and their respective networks [17].

$$H(X) = -[\theta \log 2\, \theta + (1 - \theta) \log 2(1 - \theta)] \quad (4)$$

$$\frac{1}{N} \sum_{j=1}^{D} (\theta_j - \theta_j)^2 \quad (5)$$

Results and Discussion

The Autoencoder FCN model presented the best results for Binary Cross-Entropy, with a total loss of 0.1304 concerning the original data, followed by the Autoencoder models GRU, LSTM, and CNN with MLP, respectively, with the latter having the same loss value as the VAE model with the same architecture (Table 1).

For the MSE metric, Table 2 demonstrates a similar hierarchy, with FCN, GRU, and LSTM Autoencoder models having the smallest difference between the original and generated data, followed by the VAE CNN with MLP. Comparing the two Tables, it becomes noticeable that GANs obtained the worst performance for both metrics in all proposed architectures. To match the performance of GANs, it would be necessary to increase the time and computational power expressively, leading to the conclusion that this model should be preferentially used when there is a high processing capacity.

Table 1. Loss binary cross-entropy.

	CNN+MLP	FCN	LSTM	GRU
AU	0.2249	0.1304	0.1626	0.1495
VAE	0.2249	0.2946	0.2283	0.2272
GAN	5.5372	6.3513	12.9795	5.9794

Table 2. Metric MSE.

	CNN+MLP	FCN	LSTM	GRU
AU	0.0760	0.0110	0.0535	0.0156
VAE	0.0749	0.0888	0.0765	0.0733
GAN	0.9264	0.9139	0.8890	0.8449

Conclusion

This study aimed to evaluate the AU, VAE, and GAN architectures in their ability to reproduce three-dimensional data using the MNIST 3D dataset as a basis. Using the Mean Squared Error and Binary Cross-Entropy metrics, it was possible to observe that the AU-based models obtained representations closer to the original data, furthermore, these models required a lower tuning of hyperparameters and training time, obtaining high cost-effectiveness in comparison to other architectures. In parallel, the VAE architectures obtained results close to the original data, with the LSTM and CNN models being comparable to the quality of the AUs. As for the GAN constructions, in addition to having a longer training, the resulting images and the metrics evaluated had poor quality.

Acknowledgments

We thank the institution SENAI CIMATEC and the coordination of the Artificial Intelligence course for providing us with skills and competencies in preparation for this research. We thank professor Flávio Santos Conterato for his commitment and impassivity in guiding students for this article.

References

1. Krizhevsky A, Sutskever I, Hinton GE. Imagenet classification with deep convolutional neural networks. Advances in neural information processing systems, v. 25, p. 1097-1105, 2012. On: <https://papers.nips.cc/paper/2012/file/c399862d3b9d6b76c8436e924a68c45bPaper.pdf>. Available at: 31 de july 2021.
2. Ahmed E et al. A survey on deep learning advances on different 3D data representations. arXiv preprint arXiv:1808.01462, 2018. On:<https://arxiv.org/pdf/1808.01462.pdf>. Available at: 31 de july 2021.
3. Teo BG, Dhillon SK. An automated 3D modeling pipeline for constructing 3D models of MONOGENEAN HARDPART using machine learning techniques. Bmc Bioinformatics [S.L.] 2019;20(19):1-21. 24 dez. 2019. Springer Science and Business Media LLC. http://dx.doi.org/10.1186/s12859-019-3210-x. On: <https://bmcbioinformatics.biomedcentral.com/articles/10.1186/s12859-0193210-x#citeas>. Available at: 31 july 2021.
4. Castro DI. 3D MNIST. Kaggle, 2019. On<https://www.kaggle.com/daavoo/3d-mnist>. Available at: 30 de june 2021.
5. Lecun Y. The MNIST database of handwritten digits. http://yann. lecun.com/exdb/mnist/, 1998. On: <http://yann.lecun.com/exdb/mnist/index.html>.Available at: 31 july 2021.
6. Bank D, Koenigstein N, Giryes R. Autoencoders. arXiv preprint arXiv:2003.05991, 2020. On:<https://arxiv.org/pdf/2003.05991.pdf>. Available at: 31 july 2021.
7. Kingma DP, Wwlling M. An introduction to variational autoencoders. arXiv preprint arXiv:1906.02691, 2019. On:<https://arxiv.org/pdf/1906.02691.pdf>. Acesso em: 13 aug. 2021.

8. Goodfellow I et al. Generative adversarial nets. Advances in neural information processing systems, v. 27, 2014. On:<https://arxiv.org/pdf/1406.2661.pdf>. Available at: 1 aug. 2021.
9. Costa-Jussà MR, Nuez A, Segura C. Experimental research on encoder-decoder architectures with attention for chatbots. Computación y Sistemas 2018;22(4):1233-1239. On:<https://www.researchgate.net/publication/332549468_Experimental_Research_on_Encoder-Decoder_Architectures_with_Attention_for_Chatbots>. Available at: 22 aug. 2021.
10. Meng Q et al. Relational autoencoder for feature extraction. In: 2017 International Joint Conference on Neural Networks (IJCNN). IEEE, 2017. p. 364-371. On: <https://ieeexplore.ieee.org/abstract/document/7965877>. Available at: 20 aug. 2021.
11. Doersch C. Tutorial on variational autoencoders. arXiv preprint arXiv:1606.05908, 2016. On: <https://arxiv.org/pdf/1606.05908v3.pdf>. Available at: 1 aug. 2021.
12. Lipton ZC et al. A critical review of recurrent neural networksfor sequence learning. Arxvi, San Diego, p. 1-38, 5 june. 2015. On:<https://arxiv.org/pdf/1506.00019.pdf>. Available at: 1 aug. 2021.
13. Sherstinsky A. Fundamentals of recurrent neural network (RNN) and long short-term memory (LSTM) network. Physica D: Nonlinear Phenomena, [S.L.], v. 404, p. 132306, mar. 2020. Elsevier BV. http://dx.doi.org/10.1016/j.physd.2019.132306. On: <https://www.sciencedirect.com/science/article/abs/pii/S0167278919305974>. Available at: 1 aug. 2021.
14. Cho K et al. Learning phrase representations using RNN encoderdecoder for statistical machine translation. arXiv preprint arXiv:1406.1078, 2014. On: <https://arxiv.org/pdf/1406.1078.pdf>. Available at: 1 aug. 2021.
15. Albawi S, Mohammed TA, Al-Zawi S. Understanding of a convolutional neural network. 2017 International Conference On Engineering And Technology (Icet), [S.L.], p. 1-6, aug. 2017. IEEE. http://dx.doi.org/10.1109/icengtechnol.2017.8308186. On: <https://ieeexplore.ieee.org/abstract/document/8308186>. Available at: 14 aug. 2021.
16. Gardner MW, Doeling SR. Artificial neural networks (the multilayer perceptron)—a review of applications in the atmospheric sciences. Atmospheric Environment, [S.L.], v. 32, n. 14-15, p. 2627-2636, aug. 1998. Elsevier BV. http://dx.doi.org/10.1016/s1352-2310(97)00447-0. On:<https://www.sciencedirect.com/science/article/abs/pii/S1352231097004470>. Available at: 14 aug. 2021.
17. Murphy KP. Machine learning: a probabilistic perspective. MIT press, 2012. On:<http://noiselab.ucsd.edu/ECE228/Murphy_Machine_Learning.pdf>. Available at: 17 sep. 2021.

Comparative Between Neural Networks Generate Predictions for Global Solar Radiation and Air Temperature

Lucas Calil Barbosa Duarte[1*], Moisés Araújo da Paixão[1], Luis Felipe da Fé Bastos[1], Flávio Santos Conterato[1]
[1]SENAI CIMATEC University Center; Salvador, Bahia, Brazil

Technology is becoming an increasingly important and indispensable tool in human life, making it necessary to develop various forms of renewable energies. However, over time it became necessary to improve this technology that becomes more advanced and efficient. The purpose of the research is to compare the results of three distinct AI algorithms, forecasting in two hours, using the database available by the Instituto Nacional de Meteorologia (INMET). The results indicate that the K-Nearest Neighbors Regression network proved to be more effective for estimating Global Solar Radiation (W/m²) and Multi-LayerPerceptron for forecasting Air Temperature (ºC).
Keywords: MLP. KNN. SVR. Renewable Energy. Solar Energy.

Introduction

The neural network is an algorithm capable of extracting information from a data set, simulating the learning through mathematical calculations and complex network architectures. We chose this algorithm due to its effectiveness in regression problems with time series and low inference time concerning other mathematical models for weather forecasting, such as the Advanced Research Weather Research and Forecasting (WRF-ARW) [1].

This article focuses on comparing and analyzing the efficiency of different neural networks for solar radiation prediction and, the air temperature of the dry-bulb in two hours.

We did the research at Lençóis (Bahia, Brazil), due to the volume of data found in the same time series. We collected the database at the Instituto Nacional de Meteorologia (INMET) from 2014 to 2019. The algorithms will be called models A, B, and C. Each model was trained with the two variables, and the networks with the best estimates were retrained in a more complex scenario and called validation models.

Received on 16 December 2021; revised 26 February 2022.
Address for correspondence: Lucal Calil Barbosa Duarte. Av. Orlando Gomes, 1845 - Piatã, Salvador - BA- Brazil. Zipcode: 41650-010. E-mail: l.calilxix@gmail.com. DOI 10.34178/jbth.v5i1.192.

J Bioeng. Tech. Health 2022;5(1):37-43.

Materials and Methods

Machine Learning and Neural Networks

There is much variety of neural network architectures used to estimate values of mathematical methods probabilistic. In the studied models, costless library frameworks available by Scikit-Learn, Tensorflow, and Keras were used, with requirements to find networks that are well suited to the variable "Global Radiation (W/m²)" and "Air Temperature - Dry-Bulb (ºC)".

Model A - Multilayer-Perceptron (MLP) (Figure 1)

Through the error back-propagation algorithm, this model adjusts weights for each training period to make predictions based on the weights passed previously (in the first run, the perceptron receives the input values, the weights). The input values are multiplied by the weights and then summed, the resulting value is summed with the bias, and the "error" is the difference between the real and predicted values. This is taken into account to adjust the weights kept for the next runs.

The activation function is a mathematical model used to adjust the weights, in which case the model tries to adjust between a positive and negative value. The user-defined output (Y) must be estimated by the model. For several input values, Multi-Layer

Perceptron is used, this architecture generates more efficient processing.

Within the hyperparameters, there are several changeable parameters (which could be keys or numbers, such as the "Dense Layer" that receives the activation function and the number of neurons and the "DropOut Layer"). The metric and the loss are verified in the model compilation to evaluate the training, the optimizer, and the value of the learning rate.

Model B - K-Nearest Neighbors Regression (KNN Regression)

It is a clustering algorithm that calculates the distance of data according to the proximity of their values, in other words, according to the similarity between the data, clusters are generated. The parameter "K" is used to define the number of closest Neighbors that will form a cluster, a data group. Among the hyperparameters of the network, there are: "uniform" and "distance", which is how the weights will be calculated (Figure 2).

Model C - Support Vector Machine Regression (SVR)

The SVR model is similar to KNN, however, this model uses linear and non-linear regression techniques to estimate continuous ordered values, based on their distribution the network divides and reorganizes the data. Figure 4 shows one of the head hyperparameters of this neural network model, the kernel. Another parameter observed is the RBF model, which is defined as the default due to its greater effectiveness in complex environments.

Experiment Flow

The experiment was carried out with 3 different models and each model was trained for two variables, and the best models were selected for the validation stage when the networks were trained again with the triple of data, totaling 8 training sessions. The models selected to be retrained are A and B, because of their results. Figure 4 describes the KNN regression for global radiation and MLP for Dry-Bulb air temperature.

Results and Discussion

Due to the numerical variation of the data captured by the sensors of the station under study, it was necessary to scale the data in "Min Max Scaler" to avoid overfitting during the training of the models. Only "X" was called, which corresponded to the twenty-four columns used by the neural networks to associate the variables with other values and adjust the weights (Table 1).

Table 2 compared actual and predicted values through neural network models A, B, and C, evaluated by mean absolute error and mean square error metrics. The smallest values indicate the validation step of model A for "Air Temp." and model B for "Global Radiation".

The models selected for validation estimated values close to the actual ones, even in more complex scenarios (Figure 5).

Table 3 shows the results of the validation models using other metrics. It is observed that the greater data volume on the training resulted in a greater error rate.

Conclusion

After training the validation models, we observed bias because the accumulation of data resulted in an error rate. To avoid overfitting, a smaller data split can be used, referring to a period of approximately one year, for a new training model. The KNN Regression model has very high error values due to the large scale of data ranging from 0 to 3000. Nevertheless, the model predicted the moment when the sensors did not receive global radiation. The MLP network is efficient for predicting air temperature - dry-bulb -, the back-propagation provides a better adjustment for these values, but, depending on the data volume, it may be necessary to add more neurons in the Dense and DropOut layers.

Figure 1. MLP configuration.

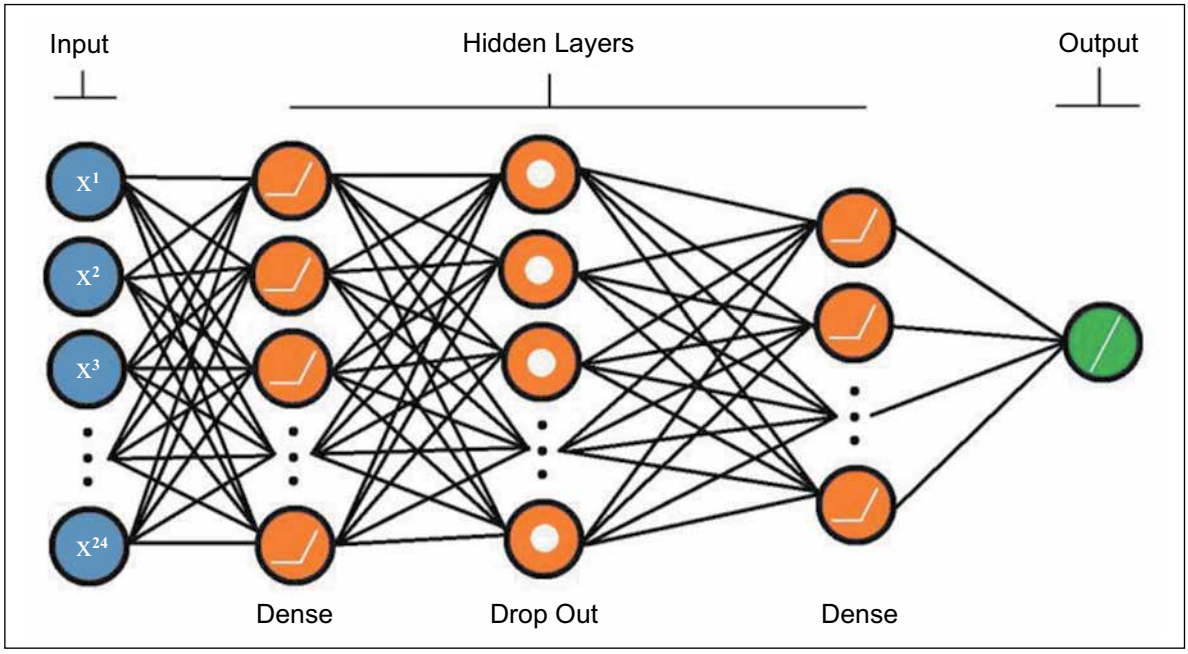

Figure 2. KNN example.

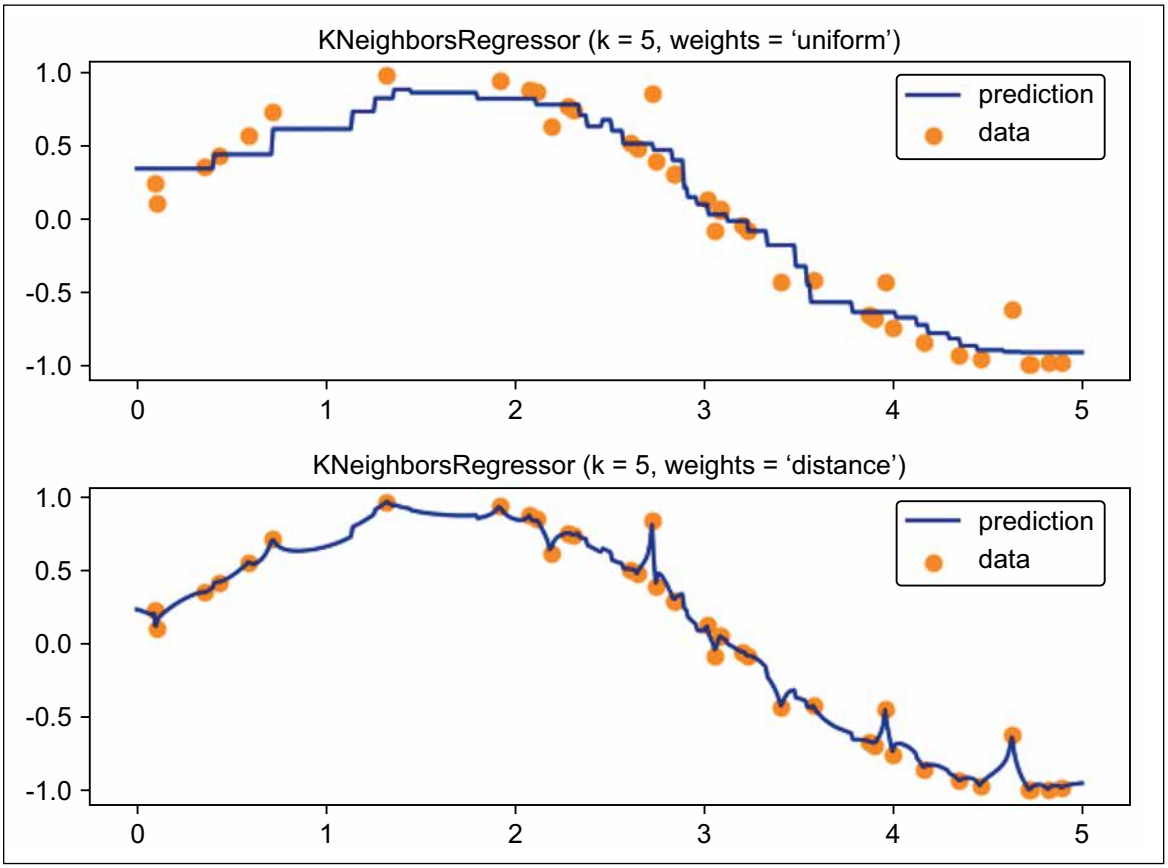

Source: scikit-learn developers.

Figure 3. SVR example.

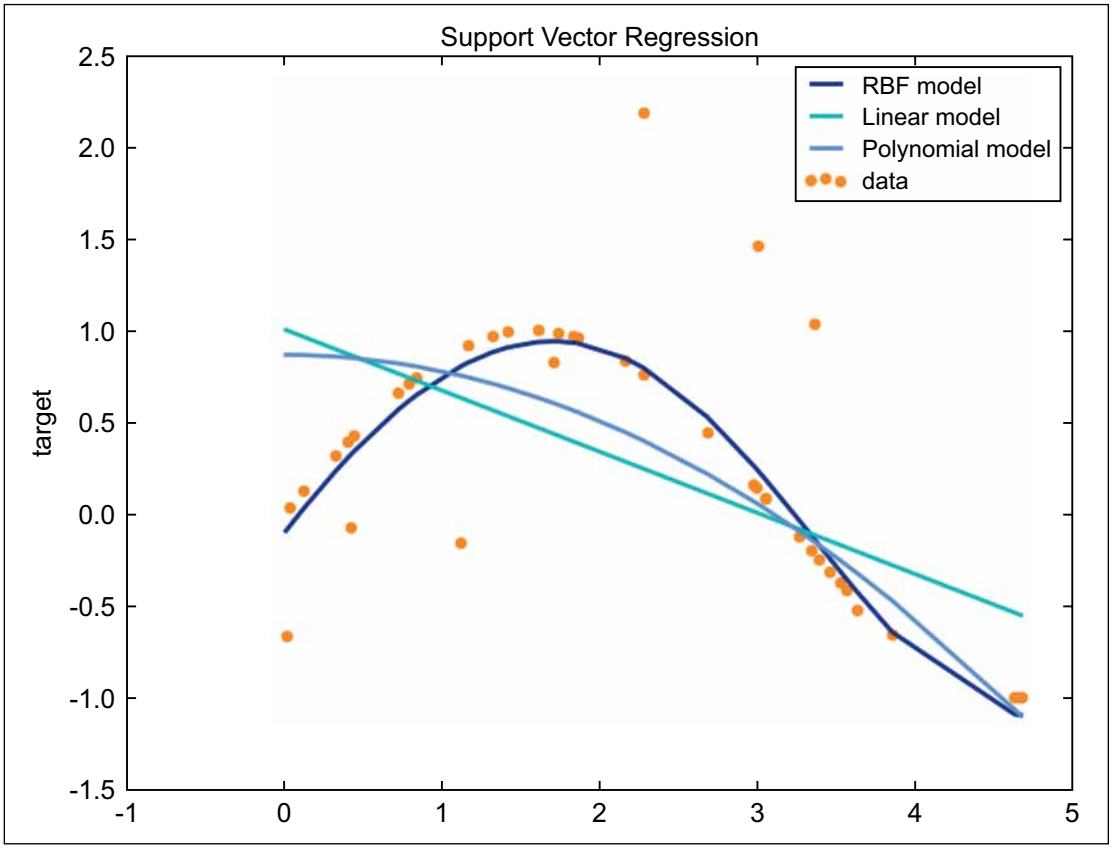

Source: scikit-learn developers.

Figure 4. Training flow.

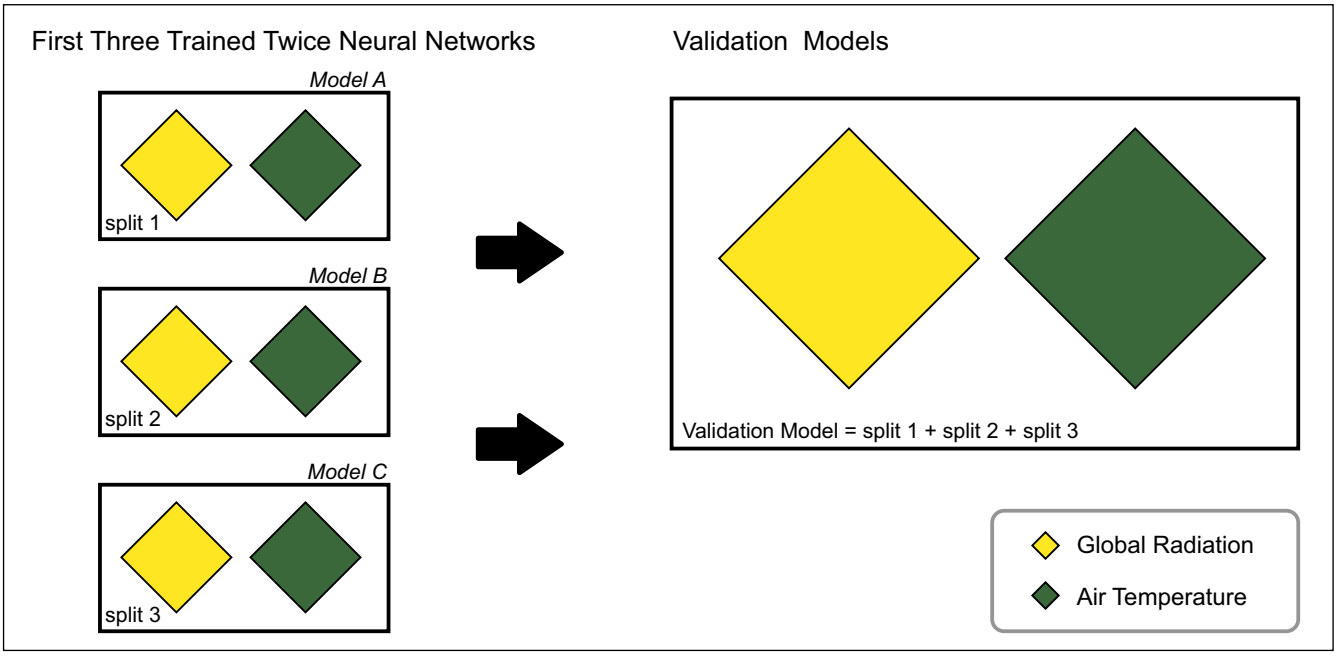

Table 1. Predicted variables in 24 hours.

Global Radiation(W/m²)	Air Temperature - Dry-Bulb (°C)
0.0	22.9
0.0	21.8
0.0	20.8
0.0	19.7
0.0	21.4
0.0	20.6
0.0	20.8
0.0	21.2
0.0	21.0
38.8	21.0
407.2	22.4
615.8	22.8
1001.6	23.9
1650.8	25.4
2716.1	27.8
3221.3	28.6
2823.1	29.5
3492.8	30.9
2879.4	31.1
2031.7	31.0
1167.4	30.7
287.2	28.9
0.0	25.9
0.0	24.3

In contrast, the SVR network, despite being promising, the predicted results were far from the actual values for the two variables, due to this, it was not retrained in the validation model. From the tests carried out in this article, it is possible to think about future studies, considering the importance of using renewable energy with the help of artificial intelligence.

Acknowledgments

Thanks to Senai Cimatec technical school that provided an excellent structure for remote learning during a COVID-19 pandemic, especially to the teachers and the Institution's Coordination.

Table 2. Models results.

Variable	Model	Mean Squared Error	Mean Absolute Error
Glob. Rad.	A	324615.68	427.40
Air Temp.	A	1.87	1.02
Glob. Rad.	B	258167.69	322.00
Air Temp.	B	11.87	3.16
Glob. Rad.	C	334593.09	428.52
Air Temp.	C	5.54	1.94

Table 3. Validation model results.

	Global Radiation (KNN)	Air Temperature (MLP)
Mean Squared Error	2014813.84	3.29
Mean Absolute Error	274.10	1.48
Mean Squared Log Error	5.23	0.00
R^2	0.77	0.76
Max Error	2126.46	7.32

Figure 5. Validation models predict.

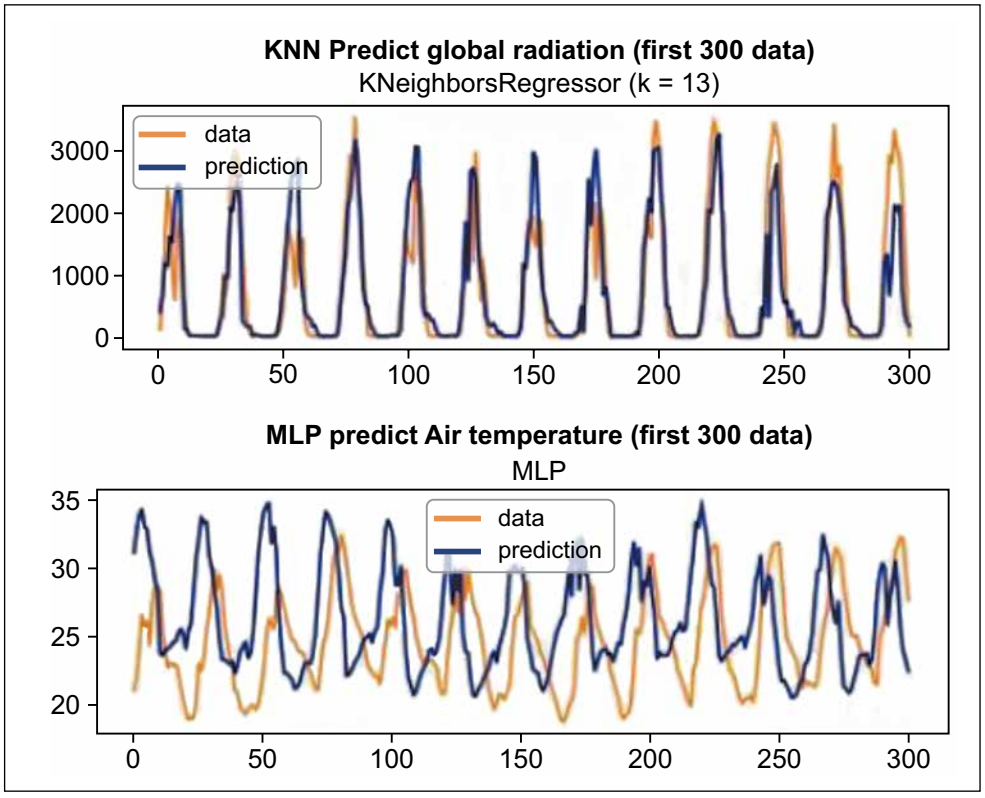

References

1. Conterato F et al. Análise do poencial de energia solar no Estado da bahia usando uma modelagem computacional. VI International Symposium on Innovation and Technology, [s. l.], 2019. Available in: http://pdf.blucher.com.br.s3-sa-east-1.amazonaws.com/engineeringproceedings/siintec2019/70.pdf. Accessed in: 2021 aug. 16.
2. Gonçalves F. Inteligência Artificial impulsiona fontes de energia renováveis. In: Gonçalves F, Frederico. Inteligência Artificial impulsiona fontes de energia renováveis. [S. l.], 1 jul. 2019. Available in: https://venturus.org.br/inteligencia-artificial-impulsiona-fontes-de-energia-renovaveis/. Accessed in: 2021 aug. 2.
3. Aplicabilidade de redes neurais artificiais para análise de geração de energia fotovoltaico conectado a rede elétrica. Revista Brasileira de Energias Renováveis, [S. l.], ano 2017, v. 6, n. 5, p. 14-15, DOI http://dx.doi.org/10.5380/rber.v6i5.48431. Accessed In: 2021 aug. 17.
4. Instituto Nacional de Meteorologia (INMET). Brasil, 2021. Available in: https://portal.inmet.gov.br. Accessed in: 2021 aug. 20.
5. Figure 1. Perceptron Example. Production: Developed by JavaTpoint. [S. l.: s. n.], 2011 - 2021. Available in: https://www.javatpoint.com/single-layer-perceptron-in-tensorflow. Accessed in: 20 aug. 2021.
6. Figure 2 KNN example. Production: scikit-learn developers (BSD License). [S. l.: s. n.], 2007 - 2020. Available in: https://scikit-learn.org/stable/auto_examples/neighbors/plot_regression.html#sphx-glr-auto-examples-neighbors-plot-regression-py. Accessed in: 20 aug. 2021.
7. Figure 3. SVR Example. Production: scikit-learn developers (BSD License). [S. l.: s. n.], 2010 - 2016. Available in: https://scikit-learn.org/0.18/auto_examples/svm/plot_svm_regression.html. Accessed in: 20 aug. 2021.

Gold Nanoparticles Synthesis with Different Reducing Agents Characterized by UV-Visible Spectroscopy and FTIR

Helena Mesquita Biz[1*], Duane da Silva Moraes[1], Tatiana Louise Avila de Campos Rocha[1]
[1]Universidade do Vale do Rio dos Sinos – UNISINOS; Vale do Rio dos Sinos, Rio Grande do Sul, Brazil

This study aims to analyze the syntheses of gold nanoparticles with different reducing agents: Sodium Citrate and Sodium Borohydride. The syntheses were characterized by Ultraviolet-visible Spectroscopy and the Fourier Transform Infrared Spectroscopy, in which we evaluated the influence of the reducing agent and the reaction agitation. The test results indicated the presence of metallic gold and confirmed the formation of gold nanoparticles. Finally, we composed a table showing the differences between the characteristics of the two reducing agents.
Keywords: Gold. Nanoparticles. Reducing. Characterization. Tests.

Introduction

Nanomaterials are classified as such if at least one of their dimensions is between 1 and 100 nm. They have unique chemical and physical properties in terms of shape, size, distribution, crystallinity, agglomeration state, and morphology [1], which make them suitable for use in various segments, including the cosmetic, chemical, food, and feed industries; in the manufacture of electronic components; in the synthesis of polymeric and pigment nanocomposites; in the design of devices for the detection of diseases, alternative mechanisms for drug and gene delivery [1,2]. For biomedical applications, one of the most explored nanomaterials is gold nanoparticles (AuNPs) as they have excellent electrical and catalytic properties, corrosion resistance, surface plasmonic resonance properties (SPR), intrinsic biocompatibility, low cytotoxicity, high stability in biological fluids, and easy functionalization with biological species of interest [2,3]. Figure 1 summarizes the characteristics of AuNPs and a simplified scheme of how biomolecules using these nanoparticles are detected.

Received on 12 December 2021; revised 20 February 2022.
Address for correspondence: Helena Mesquita Biz. Av. Unisinos, 950 - Cristo Rei, São Leopoldo - RS - Brazil Zipcode 93022-750. E-mail: helenambiz@gmail.com. DOI 10.34178/jbth.v5i1.193.

J Bioeng. Tech. Health 2022;5(1):44-51.

One of the most consolidated methodologies for gold nanoparticles synthesis is the chemical reduction of Au^{3+} ions, present in precursors such as Chloroauric Acid, in metallic gold, through reducing agents such as Sodium Citrate [4] and Sodium Borohydride [5]. The chemically synthesized gold nanoparticles are dispersed in a liquid medium, producing a colloidal solution that can have different colors depending on the size of the nanoparticles. The change in the synthesis parameters influences the shape and size of the nanoparticles, interfering, consequently, in their application. This work aimed to study the gold nanoparticles process synthesis through the chemical reduction method, in which we evaluated the influence of the reducing agent and the reaction agitation rate.

Materials and Method

To produce the gold nanoparticles, Anhydrous Sodium Citrate ($Na_3C_6H_5O_7$) from VETEC and Sodium Borohydride ($NaBH_4$) from Sigma-Aldrich were used as reducing agents; Chloroauric Acid trihydrate ($HAuCl_4.3H_2O$) purchased from Synth was used as gold precursor; Polyvinylpyrrolidone (PVP) with 10,000 g/mol from Sigma-Aldrich was used as a stabilizer; and ultrapure water, as solvent. Initially, all glassware is washed with aqua regia, prepared by a mixture of Nitric Acid (65%) and Hydrochloric Acid (37%) purchased from Química Moderna in volume ratio 1:4, for the complete cleaning and elimination of possible contaminations.

Figure 1. Properties of gold nanoparticles and schematic detection system based on AuNPs.

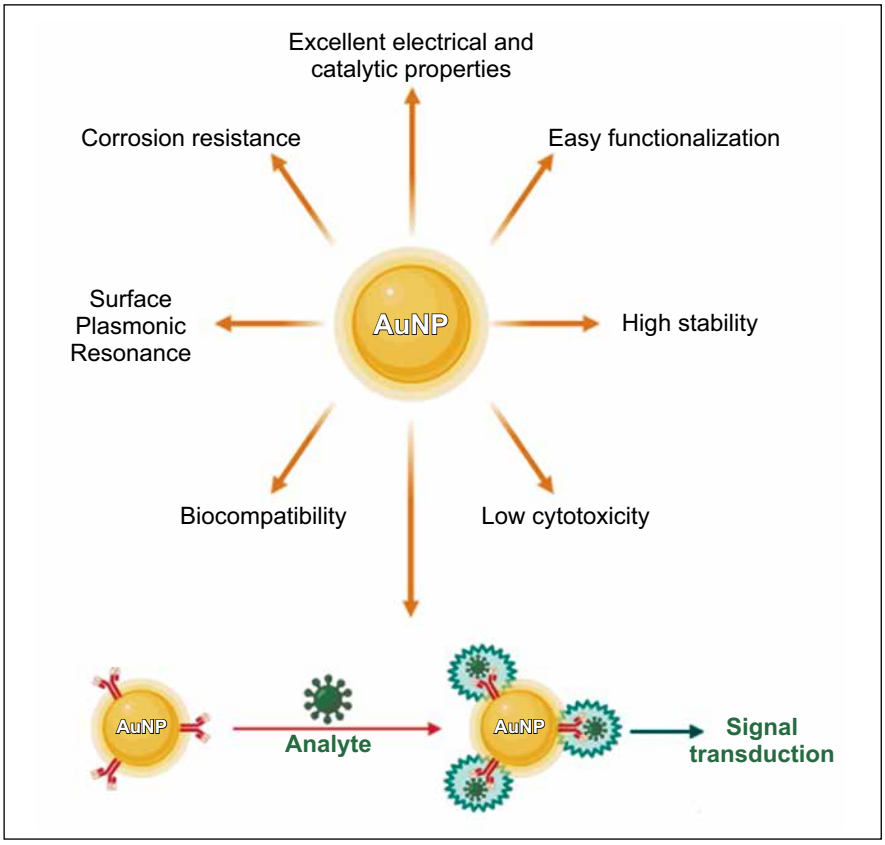

Chemical Reduction via Sodium Citrate

The experimental procedure described in this section was based on the formation of gold nanoparticles through the chemical reduction of gold ions into metallic gold using Sodium Citrate acts both as a reducing agent and as a stabilizer of AuNPs, preventing their agglomeration [4]. In 95 mL of ultrapure water, approximately 15 mg of Chloroauric Acid was added, under constant stirring and heating (90°C). Simultaneously, 5 mL of a Sodium Citrate solution (10 mg/mL) was dropped into the Chloroauric Acid solution (1 drop/s). The system remained under constant heating and stirring for another 20 minutes. Finally, the solution was kept at rest, at room temperature, for its gradual cooling and stored in a refrigerator (± 5 ºC). We analyzed the influence of the stirring speed on the characteristic of the colloidal solution. So, six samples were synthesized with the following stirring speeds: 250 rpm, 500 rpm, 750 rpm, 1,000 rpm, 1,250 rpm, and 1,500 rpm.

Chemical Reduction via Sodium Borohydride

The experimental procedure detailed the synthesis of gold nanoparticles by chemical reduction via Sodium Borohydride using Polyvinylpyrrolidone as a stabilizing reagent [6]. Approximately 25 mg of Chloroauric Acid and 60 mL of ultrapure water were added to a beaker, under constant stirring. Subsequently, 10 mg of PVP was gradually added to the solution, accompanied by another 35 mL of ultrapure water, and the system was kept under agitation for 30 min. Then, 5 mL of an aqueous solution of Sodium Borohydride, containing 1 mmol of the reducing agent, was added. The system was kept under

agitation for another 1 hour. Finally, the solution was stored in a refrigerator (± 5 ºC). Similar to the study developed with Sodium Citrate, two stirring speeds were evaluated: 750 rpm and 1,500 rpm.

Characterization

The solutions of gold nanoparticles synthesized were evaluated through the analysis of Ultraviolet-visible (UV-vis) Spectroscopy carried out in a Shimadzu UV-2600 spectrophotometer, using plastic cuvettes of 4 mL and Fourier-Transform Infrared (FTIR) Spectroscopy performed at an Agilent Technologies spectrometer, model Cary 630, with ATR accessory, Selenium, and Zinc crystals.

Results and Discussion

Chemical Reduction via Sodium Citrate

The literature shows that the synthesis of gold nanoparticles by the chemical reduction method with Sodium Citrate can be confirmed through visual changes in the color of the solution. Initially, it turns yellow because of the presence of Au^{3+} ions to colorless in the presence of the reducing agent. During the chemical reaction, it changes to a very dark blue color, and purple until it stabilizes in a reddish color (which confirms the complete reduction of gold ions into metallic gold, and the formation of gold nanoparticles) (Figure 2) [7].

UV-vis spectroscopy

Figure 3 shows the UV-visible spectra of AuNPs samples synthesized via chemical reduction with Sodium Citrate.

We can note that there is a maximum absorbance band between 500 and 550 nm in all spectra, indicating the presence of metallic gold and confirming the formation of gold nanoparticles [2]. Other studies also obtained spectra similar to Figure 3, with different maximum absorbance bands ($\lambda_{max.abs.}$), indicating distinct particle sizes (Ø), respectively: $\lambda_{max.abs.}$=519 nm and Ø≈9.0 nm [8], $\lambda_{max.abs.}$=520 – 524 nm and Ø≈10.0 nm [9], and $\lambda_{max.abs.}$=520 nm and Ø≈13.0 nm [10].

ATR-FTIR spectroscopy

All six spectra show similar behavior and the same absorption bands (Figure 4). The broad absorption band identified between 3,000 and 3,500 cm^{-1} indicates the presence of the hydroxyl functional group (-OH) in the solutions, resulting from the solvent used during the synthesis, which was ultrapure water. The peak at approximately 1,636 cm^{-1} is characteristic of the double bond between carbon and oxygen, present in carboxylic acids, such as β-Ketoglutaric acid, produced during the chemical reaction between Sodium Citrate and Chloroauric Acid (Figure 5).

Chemical Reduction via Sodium Borohydride

Figure 6 shows the photographs recorded during the synthesis of gold nanoparticles by the chemical reduction method with Sodium Borohydride, showing the visual changes in color solutions that occurred during the process. We assumed that the chemical reduction of the Chloroauric Acid gold ions to metallic gold happened since, in both syntheses, an instantaneous change in the color of the solution to dark red with the addition of Sodium Borohydride was evidenced (Figure 6) [6]. After the reaction, the solutions maintained their dark appearance, whose red/brown color was identified by placing the samples against the light.

UV-vis Spectroscopy

Figure 7 shows the spectra in the UV-visible region of AuNPs samples synthesized via chemical reduction with Sodium Borohydride.

The spectra in Figure 7 show an absorption band between 500 and 550 nm, indicating the presence of metallic gold and confirming the formation of gold nanoparticles. However, unlike samples

Figure 2. Gold colloidal solutions synthesized with Sodium Citrate.

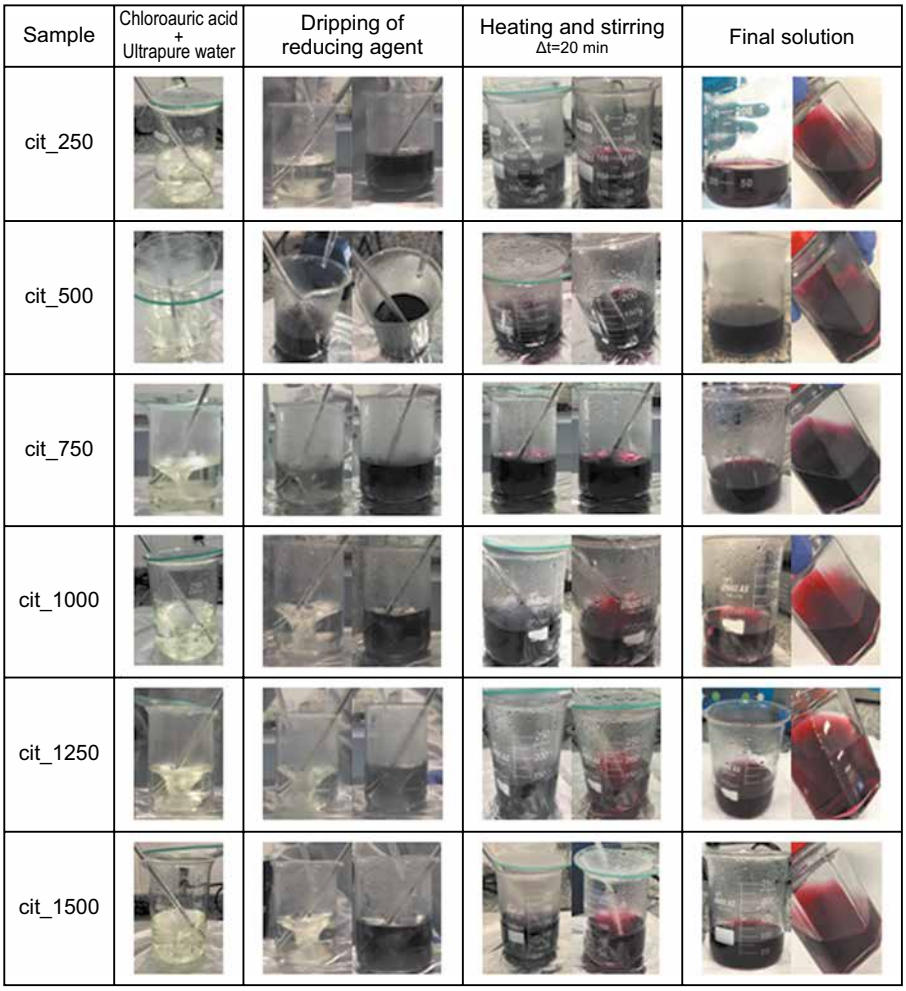

Figure 3. UV-visible spectra of Citrate-AuNPs.

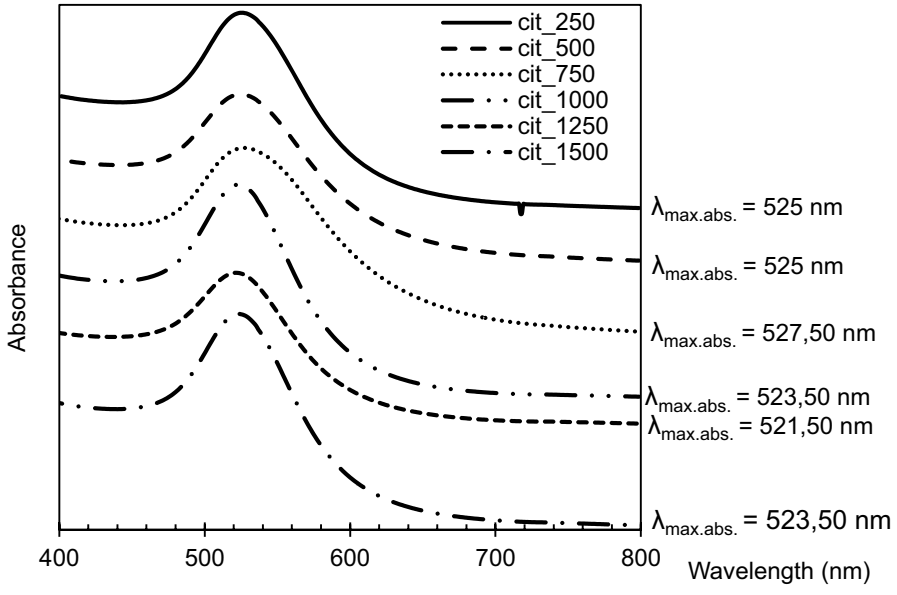

Figure 4. ATR-FTIR spectra of Citrate-AuNPs.

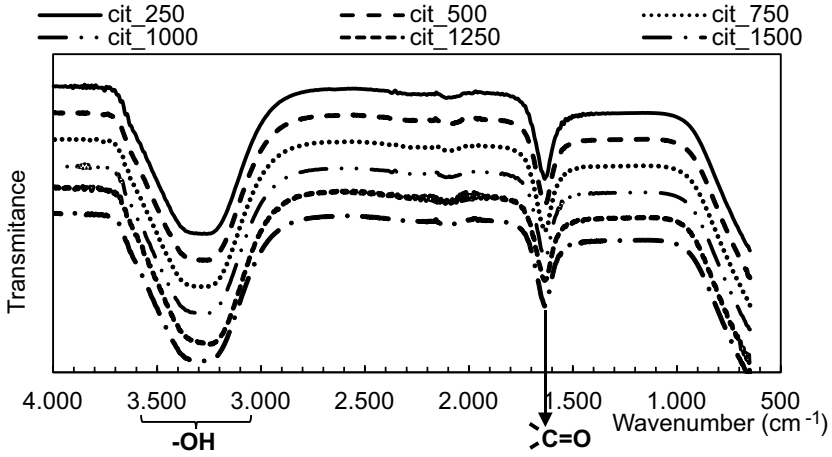

Figure 5. Reactions involved in the synthesis of Citrate-AuNPs [7].

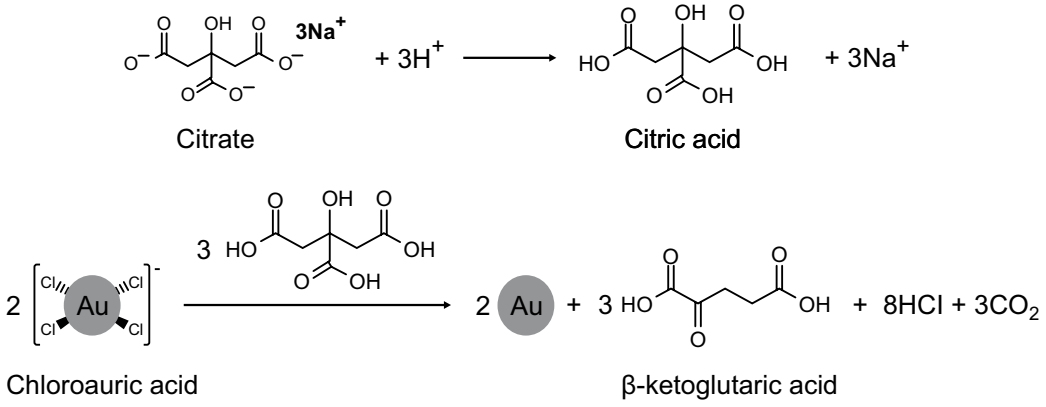

Figure 6. Record of preliminary synthesis of AuNPs with Sodium Borohydride.

Sample	Chloroauric acid + Ultrapure water	Addition of stabilizer	Stirring Δt=30 min	Addition of reducing agent	Stirring Δt=1 h	Final solution
bor_750				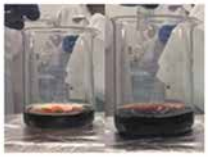		
bor_1500						

Figure 7. UV-visible spectra of Borohydride-AuNPs.

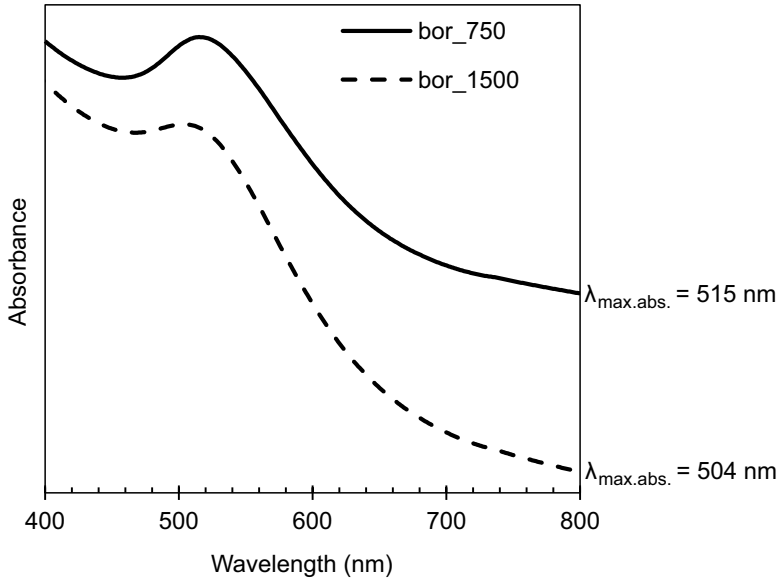

synthesized with Sodium Citrate, the plasmonic resonance band of gold in samples bor_750 and bor_1500 is less pronounced than in the others. The synthesis of gold nanoparticles with Sodium Borohydride as a reducing agent and a stabilizer used polyallylamine hydrochloride, 3-mercaptopropionic acid, and Polyvinylpyrrolidone was also observed by other authors [6,12].

ATR - FTIR spectroscopy

The broad absorption band in Figure 8, between 3,000 and 3,500 cm^{-1} is characteristic of the hydroxyl functional group (-OH), resulting from the presence of ultrapure water in the medium. The band at 1,636 cm^{-1} consists of a superposition band because of the stretches of C=O and N-H groups combinations. The absence of absorption bands around 1,285 and 1,460 cm^{-1} suggests the breakage of the pyrrolidone ring during the reaction because of the C-N bond and the CH and CH2 groups present in the chemical structure of the PVP [13].

Comparison Between Reducing Agents

Table 1 presents a comparison between the reducing agents evaluated.

Conclusion

The results showed colloidal solutions of gold nanoparticles produced with Sodium Citrate presented visual changes, which could be related to the efficiency of the synthesis, without the need to carry out the characterization. The characterization analyses contributed to confirming the visual result obtained and showing the interference of the stirring speed with the characteristics of the synthesized nanoparticles. The confirmation of whether the synthesis of gold nanoparticles with Sodium Borohydride was possible only after UV-vis analysis since the solutions obtained showed brownish and dark colors. Absorbance bands and wavenumber results followed the current literature.

Figure 8. ATR-FTIR spectra of Borohydride-AuNPs.

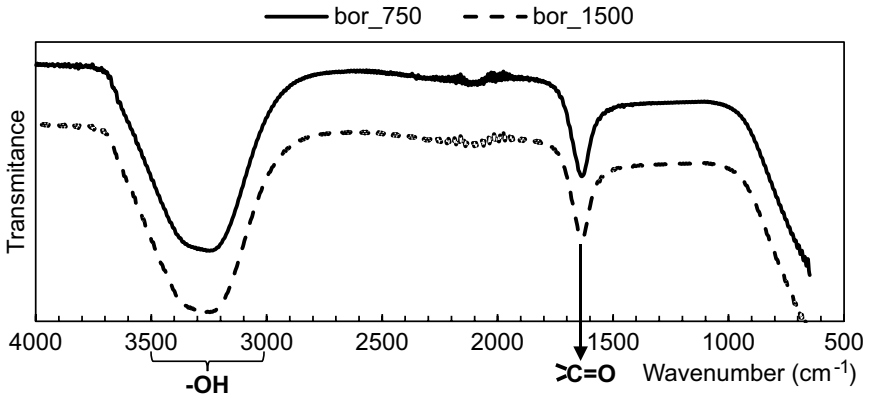

Table 1. Comparison between reducing agents.

Feature	Sodium citrate	Sodium Borohydride
Particle size	4 - 100 nm [14]	1 - 30 nm [14]
Particle size distribution	Monodispersion [15]	Polydispersion [15]
Visual appearance	Red, purple, pink and orange [16]	Brownish color
Toxicity	Non-toxic reagent	It has acute toxicity
Function	Reducing and stabilizer reagent [7]	It requires the addition of stabilizing agents
Heating	Requires heating	No heating required
Time	Quick synthesis	Longer synthesis
Synthesis effectiveness	Identified by changing the solution's color (light yellow to red)	Identified in the UV-vis analysis

Acknowledgments

The authors are grateful to itt Chip at Unisinos.

References

1. Balassoriya ER et al. Honey mediated green synthesis of nanoparticles: New era of state nanotechnology. Journal of Nanomaterials 2017:1-10.
2. Da Silva AA. Síntese e estabilização e nanopartículas de ouro para fins biotecnológicos e cosméticos. Dissertação (Mestrado em Ciências na Área de Tecnologia Nuclear-Materiais) – Universidade de São Paulo, São Paulo, 2016.
3. Das S et al. Nanomaterials for biomedical applications. Frontiers in Life Science 2013;7(3-4):90-98.
4. Turkevich J et al. A study of the nucleation and growth processes in the synthesis of colloidal gold. Discussions of the Faraday Society 1951;11:55-75.
5. Beust M et al. Synthesis of thiol-derivated gold nanoparticles in a two-phase liquid-Liquid dystem. Journal of the Chemical Society Chemical Communications 1994;(7):801-802.
6. Lin C et al. Size effect of gold nanoparticles in catalytic reduction of p-nitrophenol with $NaBH_4$. Molecules 2013;18:12609-12620.
7. Giri B. Laboratory Methods in Microfluidcs. Elsevier, 2017. p. 103-107.
8. Ojea-Jimenez I et al. Small gold nanoparticles synthesized with sodium citrate and heavy water: Insights into the reaction mechanism. The Journal of Physical Chemistry, 2010;114(4):1800-1804.

9. Hanzic N et al. The synthesis of gold nanoparticles by Citrate-radiolytical method. Radiation Physics and Chemistry 2015;106:77-82.
10. Shokouki N et al. Microfluidic chip-photothermal lens microscopy for DNA hybridization assay using gold nanoparticles. Analytical and Bioanalytical Chemistry 2018;411:6119-6128.
11. Silverstein R M. et al. Identificação Espectrométrica de Compostos Orgânicos. 8ª ed. Rio de Janeiro: LTC, 2019.
12. Casanova MCR. Síntese, caracterização e estudo da estabilidade de nanopartículas metálicas estabilizadas com polieletrólitos e tióis. Dissertação (Mestrado em Ciências) – Universidade de São Paulo, São Carlos, 2010.
13. De Amorim AM. Estudo das propriedades térmicas, espectrocópicas e eletroquímicas de complexos formados entre o polímero polivinilpirrolidona (PVP) e sais de cobre (II). Tese (Doutorado em Química) – Universidade Federal de Santa Catarina, Florianópolis, 2010.
14. De Souza CD, Nogueira BR, Rostelato MECM. Review of the methodologies used in the synthesis gold nanoparticles by chemical reduction. Journal of Alloys and Compounds 2019;798:714-740.
15. Oliveira JP et al. A helpful method for controlled synthesis of monodisperse gold nanoparticles through response surface modeling. Arabian Journal of Chemistry 2020;13:216-226.
16. Nanodays. Exploring Materials – Nano Gold. 2012. Available at: https://www.nisenet.org/sites/ default/files/ catalog/uploads/8880.pdf. Accessed on: 29 mar. 2021.

Energy and Exergetic Evaluation of Thermodynamic Systems Applied to Water Heating at Low Temperatures

Geovana Pires Araujo Lima[1,2*], Luccas Barbosa Carneiro[1], Alex Álisson Bandeira Santos[1], Josiane Dantas Viana Barbosa[1]

[1]SENAI CIMATEC Univesity Center; Salvador, Bahia; [2]Universidade Estadual De Santa Cruz (UESC) - Campus Soane Nazaré Ilhéus; Bahia, Brazil

Given the changes in human needs in the 21st century, which are increasingly dependent on different energy sources, this work aims to compare the energetic and exergetic efficiency of a shower heated by electric resistance and a solar heater. The method employed is based on the first and second principles of thermodynamics. We found that, under conditions at low heating temperature, the shower has better exergetic efficiency due to solar heating when compared to electrical energy since the destroyed exergy is lesser in the solar heater. Energy efficiency (quantitative aspect) is bigger in electrical resistance because presents better performing energy than solar energy. Therefore, for the final use, of heating at low temperatures, the solar heater is recommended from the thermodynamic perspective.

Keywords: Efficiency. Exergetic Analysis. Shower. Electric Resistance. Solar Heater.

Introduction

Electricity consumption in Brazil is based on an energy matrix mainly composed of hydropower plants. Brazilian government data from 2019 show that around 64% of the country's electric energy advances in hydropower plants, followed by thermoelectric plants (in 23%), and the remaining 13% are distributed in nuclear and renewable energy - mainly solar and wind [1]. Energy sources must be chosen according to their application to reduce losses. Thus, Deckmann and Pomilio [2] approach their work with electricity quality (QEE) that is transported in Brazil, suggesting modeling in the exergetic sphere for electricity distribution systems. It shows that the quality of energy is not only linked to its end use but also its transport.

Martins Júnior, Lopes Júnior, and Silva Júnior [3] approach in their work that solar energy is an excellent source of renewable energy with higher energy and exergetic quality in uses. However, a contribution from solar energy in 2016 generated an energy capacity of around 21 MW, which represents a negligible share of the Brazilian energy matrix. The authors point out that there is a potential field for the use of solar energy, highlighting the Northeast, which has an area of 1,558,000 km², with excellent levels of average irradiation and little interannual variability in most locations.

The growing concern with environmental issues and sustainable development shows that it is necessary to track the measures for decision-making of energy sources evaluated by their quality, which can be achieved based on the analysis of exergy [4]. In this sense, exergy expresses the energy capacity to carry out work, enabling the quality analysis of different energy sources in its final application. So it is possible to identify which alternatives and how best to use them for different contexts of use [5]. Thus, the study of exergy was highlighted in the scientific community, governments, and society [6] due to the possible changes that its analysis can promote to the environment from assertive decision-making for the development of energy supply strategies, mainly in the current scenario due to the increased release of greenhouse gases (GHG) into the atmosphere and the related increased in the average temperature of the Earth's surface observed in recent decades [7].

Received on 12 December 2021; revised 24 February 2022.
Address for correspondence: Geovana Pires Araujo Lima. Av. Orlando Gomes, 1845 - Piatã, Salvador - BA- Brazil. Zipcode: 41650-010. E-mail: gpalima@uesc.br. DOI 10.34178/jbth.v5i1.194.

J Bioeng. Tech. Health 2022;5(1):52-56.

Thus, concerns about sustainability should motivate analyzes to be made not only about energy efficiency, but also of the quality of the energy supplied, which consists of the study of exergetic efficiency [5]. The analyzes of energy efficiency are based on the first principle of thermodynamics, which deals with energy conservation. The evaluation based only on the first principle, makes it possible to quantify the energy involved, however, it does not allow this energy to be qualified, nor the intrinsic inefficiencies to be evidenced, due to irreversibilities. In this way, it is necessary to analyze from the second principle of thermodynamics, which makes it possible to qualify the various forms of energy involved, and in addition, it allows to verify the spontaneity of the processes and indicates the maximum useful work possible to be carried out, this can serve as a comparative parameter between the ideal and the real. Therefore, exergetic analysis allows quantifying, qualifying, and identifying the most impacting irreversibilities in the processes, comparing the yield with the ideal [8].

The performance is directly related to the destruction of exergy, which consists of the quantification of the irreversibility of the system, revealing the distance that it is from an ideal condition. In energy transformation processes, as the transformation occurs, more irreversibilities are generated, thereby reducing the capacity to perform work [9]. Thus, the evaluation of exergetic efficiency considers the quality of the energy taking into account its final application, seeking the least degradation of the energy.

In this sense, this work seeks to demonstrate the importance of exergetic energy analysis as a decision-making factor in the choice of energy sources, considering their end use. For this, a hypothetical case of a shower for hot baths was used. The study was based on the concepts presented by Kotas [10] and articles published in different databases [4, 5, 7, 8, 11, 12].

Materials and Method

The mathematical modeling of this study was supported by Kotas [10], which defines the exergy as a stream of matter, which can be divided into distinct components. In the absence of nuclear effects, magnetism, electricity, and surface tension, it is mathematically written according to Equation 1:

$$\dot{E} = \dot{E}_k + \dot{E}_p + \dot{E}_{ph} + \dot{E}_0 \quad (1)$$

On what:
$\dot{E}_k$: kinetic exergy;
$\dot{E}_p$: potential exergy;
$\dot{E}_{ph}$: physical exergy;
$\dot{E}_0$: chemical exergy.

It is common to work with specific properties that consist of the ratio between the property and its mass. The specific exergy, ε = E / m, can be represented according to Equation 2:

$$\varepsilon = \varepsilon_k + \varepsilon_p + \varepsilon_{ph} + \varepsilon_0 \quad (2)$$

In the present study, the portion corresponding to kinetic, potential, and chemical exergy is negligible. And the Equation can be simplified as shown in Equation 3:

$$\varepsilon_{ph} = \Delta h - T_0 \Delta s \quad (3)$$

On what:
Δh: variation of the specific enthalpy;
T_0: reference temperature;
Δs: variation of specific entropy.

The exergetic efficiency can be calculated using the formula in Equation 4:

$$\varepsilon = \dot{m} \frac{(e_{in} - e_{out})}{\dot{w}} \quad (4)$$

On what:
$\dot{m}$: mass flow;
e: specific exergy;
$\dot{w}$: power.

Initially, a search was carried out in different databases for the construction of theoretical

knowledge, and in addition, data related to the systems under study was sought. With the necessary information in place, an evaluation was made of the energy and exergetic efficiency of the water heating process from its different energy sources, one consisting of the traditional way, via electric energy, and the other from solar heating. The analysis of energy efficiency was based on the first principle of thermodynamics (Equation 5):

$$\eta = \frac{q\rho c_p(T_2 - T_1)}{\dot{w}} \quad (5)$$

On what:
q: volumetric flow;
ρ: specific mass;
c_p: specific heat;
T_1: inlet temperature;
T_2: outlet temperature;
$\dot{w}$: power.

In addition to calculating the energy efficiency for electric showers and the solar heater, their exergetic efficiency was evaluated. This efficiency is presented in Equation 6, which consists of the ratio between useful work and available work.

$$\eta = \frac{W_{useful}}{W_{avaliable}} \quad (6)$$

W_{useful}: useful work that has been tapped;
$W_{avaliable}$: available work that has been provided to the system.

It is important to note that, to validate the results, data were consulted in the literature referring to a 4.4 kW electric shower and a solar heater model Heliotek - MC Evolution, from Bosch. To carry out the analysis, it considered values of inlet temperature equal to 20°C and outlet of 40°C, and flow rate of 0.05 L / s. The studied fluid is water, which has specific heat, and a specific mass equal to 4.2 kJ / kg.K and 1000 kg / m³, respectively. For the electric shower, the average power is 4.4 kW. For the solar heater, the specifications of the model Heliotek - MC Evolution, from Bosch [13] were used. Applying the values presented in Equation (5), efficiency for the electric shower of 95% is obtained, by the values presented in the literature [4, 12]. And for the solar heater, the efficiency obtained was 54% [13].

Results and Discussion

In terms of exergetic efficiency, it is possible to define the yield based on the ratio between the useful work and the available work, according to Equation (6), performing the calculation, it is obtained that the electric shower has a yield of approximately 7% by the results of Costa and colleagues [4]. And for the solar heater, the exergetic efficiency was approximately 12%, also converging with the results presented in the literature [11]. It is noticed that for both sources, the exergetic efficiency is low, this is because the water is heated at a low temperature (from 20°C to 40°C), in this range the possibility of carrying out work is very small. Table 1 summarizes the results achieved.

Table 1. Energy and exergetic performance from different sources.

Energy Source	Energy efficiency (1st principle)	Exergetic efficiency (2nd principle)
Electrical Energy	95%	7%
Solar Energy	54%	12%

The results show that the process of heating water at low temperatures has low exergetic efficiency. In this sense, it is important to choose sources of energy supply compatible with the end-user. Therefore, electrical energy, which has high quality, should not be used to carry out a process of low exergetic yield, this causes high destruction of exergy. The use of a solar system is more appropriate concerning electrical energy, which, as can be seen in Table 1, the use of solar energy instead of electrical energy, provides a 72% increase in exergetic efficiency, even though the solar

system presents low efficiency, of approximately 12%, caused by the nature of the process. From the results obtained in Table 1, we observed that the value found with the application of the First Principle (quantity) is different from the value-added with the Second Principle (quality), showing that it is necessary to evaluate energy resources both from the perspective energy efficiency as well as exergetics, so that it is possible to select integrated resource planning. With this, it takes one to adopt environmentally correct actions, one can adopt the energy efficiency indexes together with the exergetic, as parameters of decision making on energy sources according to their end-use, contributing to reducing the exergetic destruction of the system and consequently influencing the mitigation of environmental impacts. It is worth mentioning that it is necessary to carry out complementary studies to choose the system that best suits the desired objectives [14]. From an exergetic perspective, heating using solar energy is more advantageous than using electrical energy. However, it is necessary to carry out a technical-economic analysis to verify whether it is financially attractive to invest in a solar system for heating water in the place of interest.

Conclusion

The present work had an objective to make an energetic and exergetic comparison in a water heating system carried out by electric energy and solar heating. We found that for low-temperature heating systems, relatively higher exergetic efficiency is obtained using solar heating, compared to the use of electrical energy. There is less destruction of exergy. About the energy aspects, evaluated only from the perspective of the first principle of thermodynamics (energy conservation), the source of electrical energy is more efficient, which is following the literature, as electrical energy has a better performance compared to solar. Thus, for the case addressed in this work, water heating at low temperature, the solar heater proved to be more appropriate than electrical resistance, it is worth mentioning that the study considered only thermodynamic aspects, requiring a technical-economic analysis to check the best alternative. As a suggestion for future studies, a thermoeconomic analysis of the use of water heating systems is proposed for the two conditions discussed in this work, verifying whether the financial contribution used in a solar heating system, for example, is justified because it has better efficiency.

Acknowledgments

SENAI CIMATEC for the infrastructure and Fapesb for the financial support (BOL no 3014/2019).

References

1. Brasil. Ministério de Minas e Energia. Resenha Energética Brasileira. Brasília, 2020.
2. Deckmann SM, Pomilio JA. Avaliação da qualidade da energia elétrica. Available in: <http://www. dsce. fee. unicamp. br/antenor/pdffiles/qualidade/b5. pdf>.2017.
3. Martins Jr, ACO, Lopes Jr, JC, Silva Jr, HX. Potencial de Geração de Energia Solar: O Brasil e o Mundo. In: 14ª National Environment Congress. Poços de Caldas, Brazil, 2017.
4. Costa JM, Oliveira Filho D, Silva JN, Raggi LA. Planejamento integrado dos recursos–uma análise exergética. Revista Engenharia na Agricultura-Reveng 2008;16(4).
5. Mosquim RF, Oliveira Jr, S, Mady CEK Modeling the exergy behavior of São Paulo State in Brazil. Journal of Cleaner Production 2018;197: 643-655.
6. Obama B. The irreversible momentum of clean energy. Science 2017:126-129.
7. Pachauri RK, Allen MR, Barros VR, Broome J, Cramer W, Christ R, Dubash NK. Climate change 2014: synthesis report. Contribution of Working Groups I, II, and III to the fifth assessment report of the Intergovernmental Panel on Climate Change 2014:151. IPCC.
8. Amaral FF, Santos AAB. Avaliação exergética de um ciclo de refrigeração de etileno. X CONEM. X National Congress of Mechanical Engineering Salvador, Brazil, 2018.
9. Brzustowski TA, Golem PJ. Second-law analysis of energy processes - Part I: Exergy - An introduction. Transactions of the Society for Mechanical Engineers 1977;(4)4.

10. Kotas TJ. The exergy method of thermal plant analysis. 1985
11. Silva YC. Análise exergética e termoeconômica de um sistema solar termodinâmico de aquecimento de água. Masters dissertation. UFRGS Universidade Federal do Rio Grande do Sul. Rio Grande do Sul, Brazil, 2012.
12. Pessini R. Caracterização do rendimento térmico em chuveiros e duchas de banho doméstico, 2011. UFRGS Universidade Federal do Rio Grande do Sul. Rio Grande do Sul, Brazil.
13. Bosch H. 2020 – MC Evolution. Linha de aquecimento para banhos. Especificações técnicas. Available in: <http://www.heliotek.com.br/para-casa/aquecedor-solar-para-banho/coletor-solar/mc-evolution>. Acess in: <19 de janeiro de 2020>.
14. Santos DRD. Avaliação técnico-econômica comparativa de sistemas de aquecimento de água utilizando diferentes fontes energéticas (elétrica, solar e GLP). Masters dissertation. Universidade Estadual do Oeste do Paraná. Paraná, Brazil, 2019.

Evaluation on the Ultrasonic Technique for Lekeage Detection in Onshore Oil and Gas Pipelines

João Vitor Silva Mendes[1*], Danielle Mascarenhas dos Santos[1], Adeilson de Sousa Silva[1], Amanda Bandeira Aragão Rigaud Lima[1], Herman Augusto Lepikson[1]

[1]SENAI-CIMATEC University Center; Salvador, Bahia, Brazil

Pipelines are currently considered the safest means of transporting hydrocarbons. However, accidents with leaks in pipelines are still recurrent, despite safety regulations. Therefore, there is a need to detect these leaks efficiently and adapt to the environment. This article evaluates the possibilities that the ultrasonic technique presents for leaks detection in pipelines. An algorithm was used to divide into steps of importance, concepts such as technical feasibility, suitability, and capability. The method proves to be quite versatile and promises to be very accurate, an alternative for detecting leaks in long pipelines.

Keywords: Ultrasonic. Leakage. Pipelines. Evaluation. Hydrocarbons.

Introduction

Currently, pipelines are considered the safest means of transporting fuel. Today there are about 2.5 million kilometers of these pipelines transporting hydrocarbons [1]. However, even built and operated within the maximum international safety standards of the oil and gas industry, the pipelines are subject to construction problems, deterioration processes, and third-party interference, which lead to leaks [1,2]. Pipeline leaks are one of the most common types of accidents and one of the causes of large losses and soil contamination [1,3].

Environmental Issues Caused by Oil and Gas Leaks

Due to the discovery of new oil and natural gas deposits in Tabasco in Mexico, there has been an increase in infrastructure investments at the place, due to the abundance of hydrocarbons, reaching around 1,388 barrels per day [4]. So, the exploration and extraction of hydrocarbons have caused major damage to the environment due to the organic compounds generated by the oil spill at the site, generating several social impacts for residents of regions close to the deposits [4,5]. In 2018, around 1,600 hectares of soil contaminated by oil spills were recorded, where one of the causes is leakage in pipelines [4].

Ultrasonic Method

The ultrasonic method is characterized by a hardware-based, non-invasive acoustic method [3]. A common way to use this method is to use a pulsar, a transducer, and a device to display the captured signals. The pulsar is responsible for generating ultrasonic waves that travel along the walls of the ducts. Part of the energy of these waves will be reflected, and these signals will be captured by the receiving transducer [5]. If a leak occurs, the fluid into the pipe will be disturbed. Therefore, these waves will cause a significant variation in the voltage picked up by the transducer. The method has high sensitivity, characteristic of the acoustic method, and because of that, it can produce a higher rate of false alarms [3]. Also called lamb wave, the wave generated by the pulsar in steel pipes can be redirected and can propagate over a distance of 1km. Because of this, the ultrasonic technique presents itself as an ideal alternative for monitoring long ducts [6].

This article aims to analyze the ultrasonic technique for detecting leaks in oil and gas pipelines, using a method that allows the reader to understand in which situations the method is applicable.

Received on 20 December 2021; revised 21 February 2022.
Address for correspondence: João Vitor Silva Mendes. Av. Orlando Gomes, 1845 - Piatã, Salvador - BA- Brazil. Zipcode: 41650-010. E-mail: vitor.mendes@ieee.org. DOI 10.34178/jbth.v5i1.195.

J Bioeng. Tech. Health 2022;5(1):57-59.

Materials and Method

To evaluate the ultrasonic leak detection technique for oil and gas pipelines, we used the algorithm shown in Figure 1. The algorithm allows separating the evaluation criteria in stages and order of importance.

Results and Discussion

Technical Feasibility

To insert a method into an environment, it is first necessary to know if it can adapt to the characteristics of the location [7]. Table 1 shows some of the possibilities offered by the ultrasonic method.

The ultrasonic method has no restrictions to any material, location or type of duct [3]. However, it behaves better in pipelines made of steel. Because in steel pipes the lamb waves can be redirected and can propagate over a distance of 1km [6].

Table 1. Technical feasibility criteria [3].

Criteria	For Ultrasonic Method
Pipeline type	Without restriction
Material type	Without restriction
Location type	Without restriction
Access requirement	Power energy
Pipeline conditions	No data
Pipeline sizes	Evaluate according the equipment
On-line inspection/ Off-line inspection	Evaluate according the equipment

Pipeline size and types of inspection will vary according to the type of equipment. In addition, no restrictions on the conditions of the pipeline for the use of this technique are reported in previous research.

Technical Suitability

At this point, it is evaluated whether the method can meet the specific needs, using the criteria in Table 2. The measured parameters are the frequencies of waves that are reflected as they travel through the pipeline [6]. The purpose of the method is to detect leaks and identify the place of rupture, which can be detected to an accuracy of inches. Furthermore, it is a sensitive technique (Table 3), because the method can identify micro leaks (previously research, the method has detected leaks of 0.02L/min) [8].

Technical capability

In this step, it is necessary to evaluate what the technique requires for the place where it will be inserted. The analog signal received by the receiving transducer needs to be converted to be

Table 2. Technical suitability criteria [3].

Criteria	For Ultrasonic Method
Measured parameters	Ultrasound requency
Detection purpose	Leakage detection
Cooperate with other techniques	Not necessary
Detection efficiency	It may vary depending on the equipment used

Figure 1. Algorithm to evaluate a technique [7].

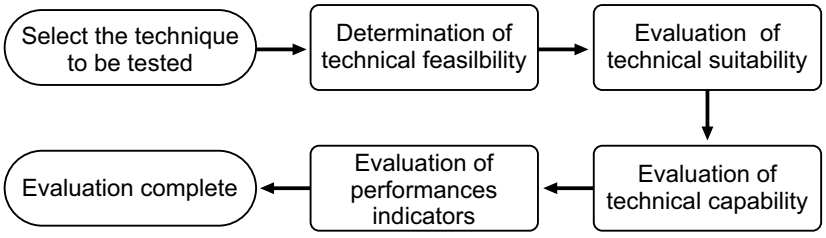

analyzed. For this, a DSP module is used, which is equipped with a large number of flash RAMs, so it demands a structure that has high processing power, to result in a fully digital signal to be analyzed, and this can be an important restriction for the operation in remote sites [8].

Evaluation of Performances Indicators

Table 3. Performances indicators of ultrasonic technique [3].

Indicators	Classification
Adaptive ability	Can
Positioning accuracy	General
Response time	Fast
Sensitivity	High
Continuous monitoring	Can
False alarm rate	General
Maintenance requirement	General
Cost	Low

Conclusion

The ultrasonic technique is an excellent alternative for detecting leaks in oil and gas pipelines, due to its ability to adapt to different environments, in states of matter, and can detect micro leaks. Especially when the ducts are made of steel since in these cases the pulses can be redirected and propagate about 1km, which makes it a choice for detecting leaks in long-distance ducts. However, the technique has negative points depending on the equipment used, there will be a need to process at least part of these signals on the edge, if it is not possible to have equipment for processing the signals, it may be that the ultrasonic method is not the ideal, as it would require high bandwidth, depending on a more detailed cost assessment, between the cost of processing and sending data. The ultrasonic leak detection technique in oil and gas pipelines has shown potential for the hydrocarbon transport sector, mainly due to its ability to detect micro leaks and monitor pipelines over long distances.Despite the high processing power that the technique requires to process your data, with technological advances this technology may become a viable alternative for the market in the coming years. However, the lack of studies and the limitations of them that prove the efficiency and safety of the technique is an impasse for the adhesion to this technology. Following studies are recommended for future research on this subject.

Acknowledgments

To FAPESB, CNPq, ANP PRH Program for the grants, to the Competence Center in Advanced Technologies, and Competence Center in Onshore Solutions for the support.

References

1. Aba EN et al. Petroleum pipeline monitoring using internet of things(IoT) platform. SN Applied Sciences, Springer 2021;3(2):1–12.
2. Glisic B. Sensing solutions for assessing and monitoring pipeline systems. In: Sensor technologies for civil infrastructures. [S.l.]: Elsevier 2014:422–460.
3 Lu H et al. Leakage detection techniques for oil and gas pipelines: State-of-the-art. Tunnelling and Underground Space Technology Elsevier 2020;98:103249.
4. Quijano JC, Torres-López K, Martínez-Rabelo F. Soil contamination by petroleum in Tabasco, Mexico, and its environmental repercussions. Gaia Scientia 2020;14:75–91.
5. Razvarz S, Jafari R, Gegov A. A review of different pipeline defect detection techniques. In: Flow modelling and Control in Pipeline Systems [S.l.]: Springer 2021:25–57.
6. Wang ML, Lynch JP, Sohn H. Sensor technologies for civil infrastructures, volume 2: Applications in structural health monitoring. [S.l.]: Elsevier 2014.
7. Marlow D.. et al. Condition assessment strategies and protocols for water and wastewater utility assets. CSIRO, 2007.
8 Farooqui MA, Al-Reyahi AS, Nasr K. Application of ultrasonic technology for well leak detection. In: ONEPETRO. International Petroleum Technology Conference. [S.l.], 2007.
9. Siqueira MHS et al. The use of ultrasonic guided waves and wavelets analysis in pipe inspection. Ultrasonics 2004;41(10):785-797.

Use of Hydrogen as Energy Source: A Literature Review

Luiz Sampaio Athayde Neto[1]*, Leonardo Reis de Souza[2], Pedro Bancillon Ventin Muniz[3], Júlio César Chaves Câmara[4]

[1]Undergraduate in Automotive Engineering, SENAI CIMATEC University Center; [2]Undergraduate in Automotive Engineering, SENAI CIMATEC University Center; [3]Master in Industry Engineering, UFBA/ SENAI CIMATEC University Center; [4]Doctor in Computational Modeling, SENAI CIMATEC University Center; Salvador, Bahia, Brazil

Hydrogen is a promising alternative to meet the world's energy demand, presenting many uses. Fuel cells are the most well-known use in automobiles. But Synthetic fuels is also an promissing alternative. Studies have shown the use of hydrogen as a fuel additive in internal combustion engines. This article aims to present a review of how hydrogen is used as a fuel source, as a replacement option for fossil fuels, reducing the environmental impact and CO_2 emissions. Finally, in this review, some advantages and disadvantages will be preseted.
Keywords: Hydrogen. Fuel Cell. Synthetic Fuel. Additive. Energy.

Introduction

Reducing the environmental impacts caused by global warming, acid rain, and the degradation of the ozone layer from the burning of fossil fuels. There are researches on courses to find alternatives according to each process [1].

Hydrogen is one of the most common elements on our planet. To several studies, Hydrogen is promised to be the energy source of the future, presenting itself as a potential substitute for fossil fuels in transportation [2]. When used as an energy source, it has the potential to reduce CO_2 emissions. H_2 is used in fuel cells to produce electricity [3]. When it comes to environmental benefits, it can drastically reduce CO_2 emissions because of its main product, which is water.

This research review presents the advantages and disadvantages of using hydrogen as an energy source, considering the differences between hydrogen-powered engines and engines powered with other fuels. Considering positive aspects of the use of hydrogen, such as low environmental impact; energy potential; the need to develop renewable and clean energy sources.

Received on 17 December 2021; revised 26 February 2022.
Address for correspondence: Luiz Sampaio Athayde Neto. Av. Orlando Gomes, 1845 - Piatã, Salvador - BA- Brazil. Zipcode: 41650-010. E-mail: luizsampaioathaydeneto@outlook.com.
DOI 10.34178/jbth.v5i1.196.

J Bioeng. Tech. Health 2022;5(1):60-64.

Hydrogen as Energy Source

Hydrogen Fuel Cell

Hydrogen is considered one of the cleanest energy sources if it comes from renewable sources [4]. It is one of the few renewable sources with commercial application and can be obtained from many sources [2]. In fuel cell applications, hydrogen can reach an efficiency of up to 60%. Condensation of Hydrogen happens at -252.77°C, specific weight of 71 g/L. The result is one of the highest energy densities per unit of mass, compared to other fuels. But there are some disadvantages, such as the difficulty of obtaining liquid hydrogen and its high cost of processing [4]. Figure 1 shows the diagram in which it is possible to identify the differences between disadvantages and advantages.

Fuel cells started to be studied in the 19th century. However, its first application happened with NASA between 1960 and 1970 in spacecraft [4]. In recent years there has been an increase in the use of fuel cells, in several areas in the search for efficiency, sustainable energy, and emission reduction [2]. Fuel cells differ from batteries because they work while being powered by fuel. Hydrogen is converted into a product based on hydrogen and energy that can be electricity or heat. Manoharan and colleagues (2019) explained that pressurized tanks are needed to store hydrogen in a fuel cell vehicle. It needs to be resistant because

Figure 1. Advantages and disadvantages of hydrogen.

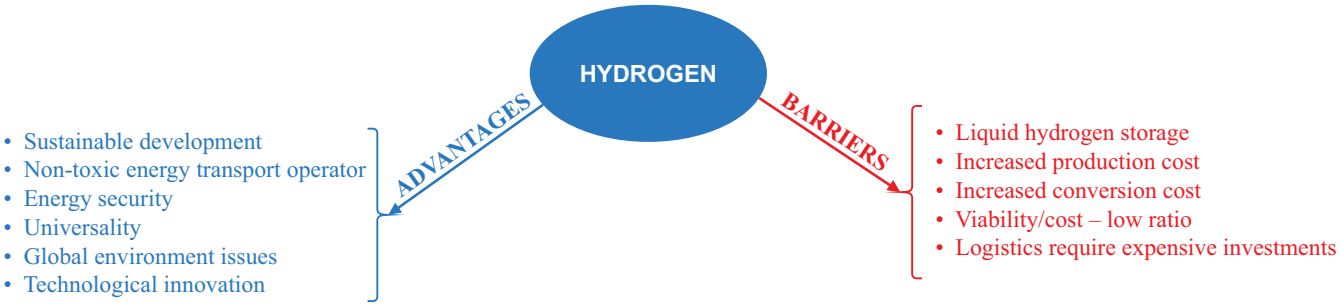

Source: Felseghi and colleagues(2019) [4].

of safety reasons. Compressed hydrogen is under a pressure of 34 MPa, with a mass of 32.5 kg at a volume of 186 L. this condition is suitable for a 500 km range. It is also possible to liquify hydrogen in a cryogenic liquid state. It happens at a temperature of -259.2 °C. its density is not that high, 1 L of hydrogen weighs $71.37*10^{-3}$ kg. However, maintaining hydrogen in a liquid state is extremely difficult. Also, liquid Hydrogen is explosive in contact with some gases.

Use of Hydrogen in Internal Combustion Engines

Hydrogen, diesel, and biodiesel mixtures have been studied by several researchers. The results showed many advantages like the absence of carbon in its molecules, calorific power compared to pure diesel, and the reduction in the emission of unfriendly gases to the environment when used in compression ignition engines). Kanth and colleagues (2021) evaluated the use of hydrogen in a mixture of rice biodiesel and biodiesel of Millettia pinnata (Karanja). The experiment (Figure 2) shows the supply of hydrogen through a pressure cylinder, which was regulated to enter the diesel engine at a pressure of 2 bar and a flow rate of 7 lpm (liters per minute). A 5.2 kW CI engine was maintained in constant rotation and variable load. The experiment results demonstrated a reduction in the specific consumption of fuel, CO and HC exhausted by the engine due to better combustion from the propagation of flame caused by hydrogen [5]. However, due to higher pressure and temperatures in combustion, the indices of NOx were slightly increased.

Mohamed and colleagues (2013) conducted an experiment involving the use of hydrogen-fueled as an additive in a CI engine. Their results showed that there was an increase in thermal efficiency and a reduction in NO rates, but there was an increase in smoke emission [6]. Karagöz and colleagues (2015) evaluated the use of hydrogen intake through the air intake system pipe of a CI engine. Hydrogen was stored in a high-pressure gas cylinder (200 bar) and was injected into the engine through a pressure regulator valve (4 bar). The system also had a flame-cutting valve for safety reasons and a flow meter. Hydrogen injection occurred through an electronically controlled valve. The details of instrumentation in the hydrogen cylinder are represented in Figure 3.

During the experiment, the engine rotation was kept constant at 1100 RPM while the load was varied (40%, 60%, 75%, and 100%). Hydrogen was injected by 30% of the total energy of the diesel and hydrogen mixture. The addition of hydrogen provided a reduction in CO emissions for all tested loads. The lower ignition delay of the H_2 is responsible for improving burning and increasing the pressure in the cylinder, providing more complete combustion of the mixture [7]. Other justification for the reduction of CO is the greater homogeneity caused by H_2. For all loads tested, there was an increase in HC. This phenomenon was associated with a higher amount of unburned fuel because of hydrogen injection into the engine. The

Figure 2. Experiment scheme for hydrogen and biofuels.

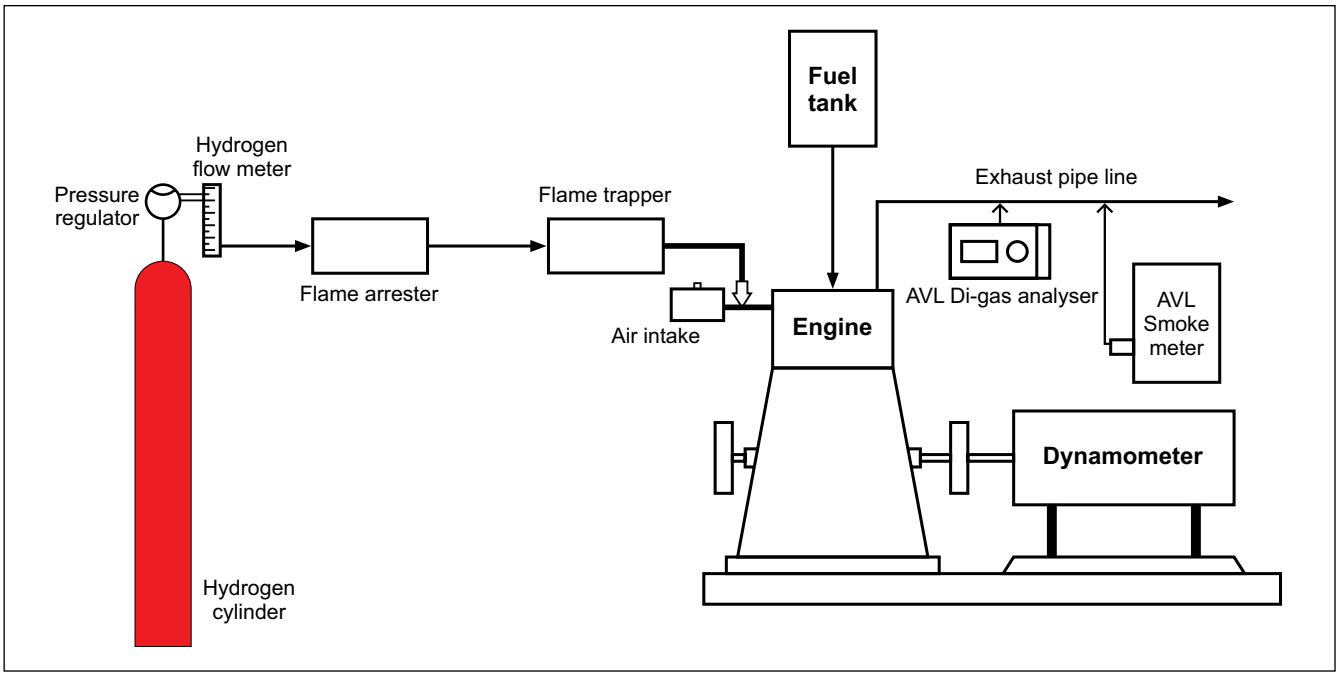

Source: Adapted from Kanth and colleagues 2021 [5].

Figure 3. Systematic display of the hydrogen.

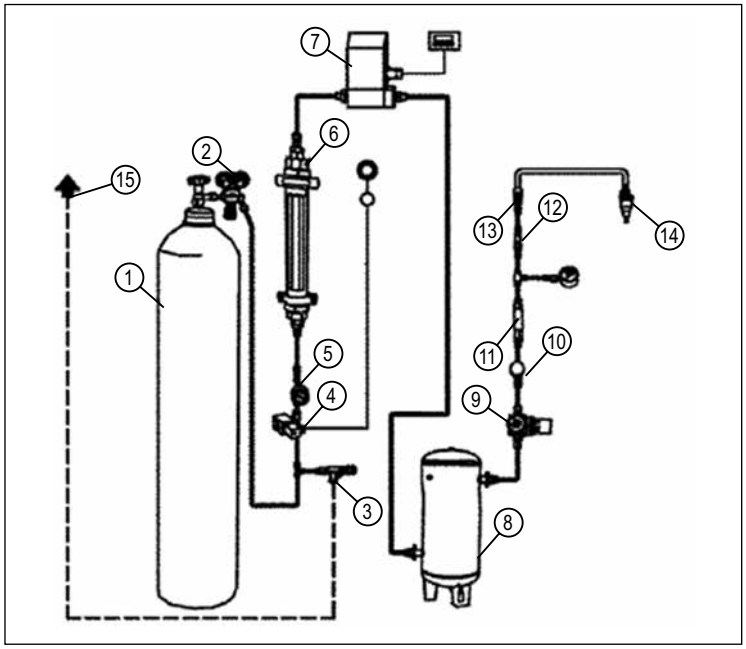

Line: 1 - Hydrogen Cylinder; 2 - Pressure regulator; 3 - Exhaust valve; 4 - Shut-off valve; 5 - Needle valve; 6 - Hydrogen Rotation; 7 - Hydrogen mass flow meter; 8 - Tank; 9 - Pressure line regulator; 10 - Ball valve; 11 - Tailing valve; 12 - Flame suppressor; 13 - Quick connection; 14 - Hydrogen Injector; 15 - Discharge line.
Source: Karagöz and colleagues (2015) [7].

results of NOx emission varied according to the load testing. For all tested loads, the NOx values were reduced compared to pure diesel, except for the 100% load. The justification pointed out by Karagöz and colleagues (2015) is reported that in varied loads (40%, 60%, and 75%) the effect of H_2 dilution causes the reduction of the emitted. For the load of 100%, the increase in the peak temperature in the cylinder results in the higher formation of NOx. Pressure analysis in the cylinder indicated an increase for all tested loads due to the rapid flammability of H_2 and reduced ignition delay.

Synthetic Fuels

The goal of synthetic fuels is to create a fuel that is sustainable for heavy transport such as ships, large trucks, and some passenger cars [8]. Synthetic fuels are less efficient than electricity, which means that electric batteries are preferred in vehicles, but it is a way to reduce carbon emissions in aeronautics and the naval industry [9]. The generation of synthetic fuels begins in the same way as hydrogen is obtained for a fuel cell application. However, there is an introduction of atmospheric CO_2 used to create a larger carbon chain, such as Alcohol, Gasoline, Diesel, or other larger hydrocarbons. Figure 4 shows the process of introducing CO_2.

Conclusion

Hydrogen is one of the best alternatives for the future due to its abundance in the universe and its high specific energy. Despite its storage problems and transport difficulties, this does not invalidate it as an alternative for the future of transport. Fuel cells appear to be the most efficient method of generating energy, as the redox process is more efficient than burning hydrogen. However, both methods are being studied by several researchers with advantages and disadvantages. Another method of using hydrogen is to be used as an additive in CI engines. In this configuration, hydrogen is injected into the inlet pipe along with atmospheric air. This configuration presents reduction results for CO, HC, and other harmful

Figure 4. Principle behind a synthetic fuel.

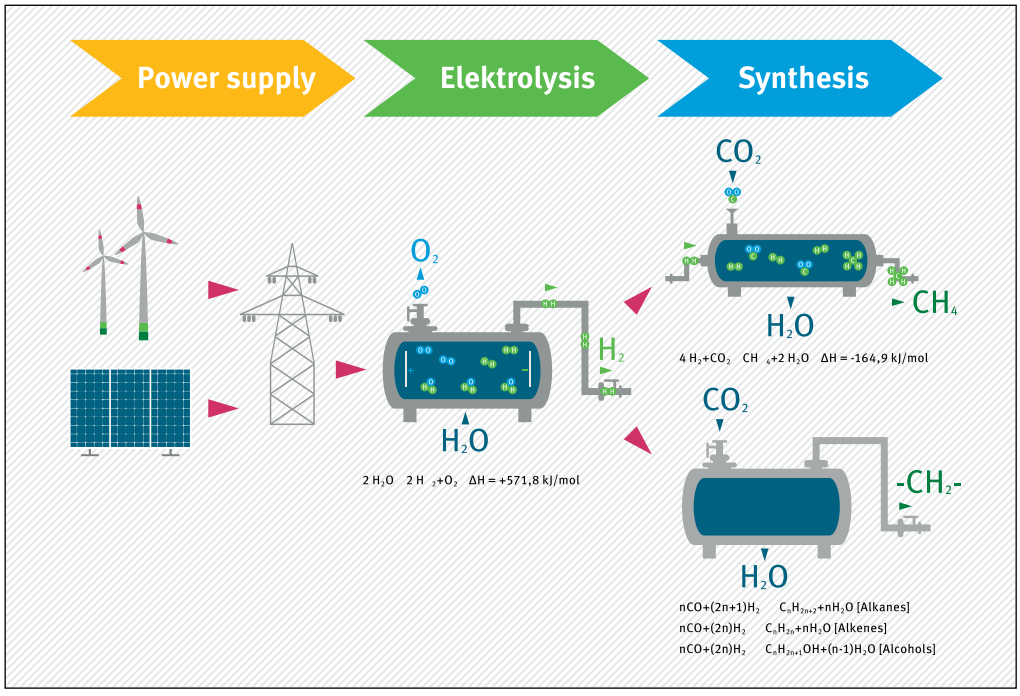

Source: Adapted from Bracker (2017) [9].

gases, but there are still NOx emissions being produced that have variable behavior. The use of synthetic fuels is a promising alternative for the transport sector, despite its high cost.

References

1. Silva IA. Hidrogênio: combustível do futuro. Ensaios e ciência: ciências biológicas, agrárias e da saúde 2016;20(2):122-126.
2. Manoharan Y, Hosseini E, Butler B, Alzharani H, Fou S, Ashuri T, Krohn J. Hydrogen fuel cell vehicles: Current status and future prospect. Applied Sciences. 2019;9:2296; doi:10.3390/app9112296.
3. Paladno PA. Uso do hidrogênio no transporte público da cidade de São Paulo. Tese (Doutorado em Tecnologia Nuclear - Reatores) - Instituto de Pesquisas Energéticas e Nucleares, Universidade de São Paulo, São Paulo, 2013. doi:10.11606/T.85.2013.tde-24102013-112007.
4. Felsegui RA, Carcadea E, Raboaca MS, Trufin CN, Filote C. Hydrogen fuel cell technology for the sustainable future of stationary applications. Energies 2019;12:4593. doi:10.3390/en12234593.
5. Kanth S, Debbarma S. Comparative performance analysis of diesel engine fuelled with hydrogen-enriched edible and nonedible biodiesel. International Journal of Hydrogen Energy 2021;46:10478–10493. https://doi.org/10.1016/j.ijhydene.2020.10.173.
6. Mohamed IM, Ramesh A. Experimental investigations on a hydrogen diesel homogeneous charge compression ignition engine with exhaust gas recirculation. International Journal of Hydrogen Energy 2013;38:10116–10125. http://dx.doi.org/10.1016/j.ijhydene.2013.05.092.
7. Karagöz Y, Sandalci T, Yüksek L, Dalkiliç AS. Engine performance and emission effects of diesel burn enriched by hydrogen on different engine loads. International Journal of Hydrogen Energy 2015:1– 12.http://dx.doi.org/10.1016/j.ijhydene.2015.03.141.
8. Hänggi S, Elbert P, Bütler T, Cabalzar U, Teske S, Bach C, Onder C. A review of synthetic fuels for passenger vehicles. Energy Reports 2019;5:555-569. https://doi.org/10.1016/j.egyr.2019.04.007.
9. Bracker J. An outline of sustainability criteria for synthetic fuels used in transport. Oko-Institut e.V. Freiburg 2017;11.

Biobutanol as an Alternative and Sustainable Fuel: A Literature Review

Ana Carolina Araújo dos Santos[1*], Ana Caroline Sobral Loureiro[1], Ana Lúcia Barbosa de Souza[1], Natália Barbosa da Silva[1], Reinaldo Coelho Mirre[1], Fernando Luiz Pellegrini Pessoa[1]
[1]SENAI CIMATEC University Center; Salvador, Bahia, Brazil

We need investiments in cleaner, renewable and sustainable energy sources to meet global fuel demand. Biobutanol is produced by the biotechnological route, by the ABE fermentation process. Biobutanol as a biofuel has gasoline-like properties, and its energy efficiency is 25% higher than ethanol. The objective of this work was to conduct a literature review on the production of biobutanol and to collect data on the market of this biofuel to understand the challenges involved in the production of biobutanol. We did the systematic review using the inclusion method. We analyzed the biobutanol world scenario and its applicability in Brazil as a solvent in industries.
Keywords: Biofuel. Biobutanol. ABE Fermentation. n-Butanol. Literature Review.

Introduction

The growing environmental need is to turn to cleaner, renewable and sustainable energy sources to meet the ever-increasing demand for fuel. Renewable energy will be the world's fastest-growing energy source, expected to double from 2015 to 2030. [1] Biofuel, produced through a biological process, has drawn scientists' attention due to its environment-friendly feature [2].

Biobutanol is butanol production from natural or organic or biodegradable or renewable biomass [3]. Butanol is higher alcohol whose chemical formula is $C_4H_{10}O$ and which has four structural isomers: n-butanol, isobutanol, tert-butanol, and sec-butanol [4].

n-Butanol is a chemical compound that falls within the alcohol reagent family. Due to their increasing use as additives, solvents, and fuels, alcohols have found their position in the market. Biobutanol as a fuel derived from biomass feedstock produced using ABE fermentation turns out to be an extremely clean and sustainable fuel with a high energy density comparable to gasoline [3].

Biobutanol is considered the gasoline of the future. It will be a good substitute for gasoline due to its physical properties such as high boiling point, economy, and safety [4, 5]. From the United States (USA) perspective, ASTM D7862 - 21 standard allows butanol intended to be blended with gasoline at 1% to 12.5% by volume for use as automotive spark-ignition engine fuel [6], while ASTM D787533 provides a method for determining the butanol and acetone content in butanol by gas chromatography technique, intended for blending with gasoline [4,7].

Brazil has a large availability of fermentable raw materials, especially sugarcane and corn, and well-established industrial facilities for alcoholic fermentation, so it has the potential to become a reference for the export of biobutanol [8].

Industrial initiatives in the n-butanol field are aimed at the biofuels market because of n-butanol's better properties compared to ethanol, as it has 25% more energy than ethanol, lower water miscibility, and less corrosive properties. Butanol can be blended with gasoline and diesel in higher proportions, it can replace gasoline use, while ethanol can only be used as an additive [5,9].

Therefore, the objective of this work was to conduct an integrative review of the production of biobutanol, collect data on the foreign and internal markets of this biofuel, and understand the challenges involved in the production of biobutanol.

Received on 18 December 2021; revised 20 February 2022.
Address for correspondence: Ana Carolina Araujo dos Santos. Av. Orlando Gomes, 1845 - Piatã, Salvador - BA- Brazil. Zipcode: 41650-010. E-mail: ana.santos@aln.senaicimatec.edu.br. DOI 10.34178/jbth.v5i1.197.

Materials and Methods

The present work sought the literature review to show the main points related to the production of the biobutanol process and commercial prospection in the Brazilian scenario. The databases that provide scientific articles were consulted, such as SciELO, ScienceDirect, and Google Academic.

The search was for articles written between 2013 and 2021, preferably considering articles available in their full version. Inclusion and exclusion criteria were also used in which more than 60 articles were found throughout the research. We evaluated 10 sources, considering some themes: Renewable energies; Production of Biobutanol, and economic and market analysis. After the sources selection, according to the inclusion criteria, we divided the review into five phases (Figure 1), according to a previously established protocol [10].

Literature Review

Phase 1: Preparation of a Guide Question

In this phase, we defined the questions that will guide the research. For the elaboration of this work, we used the following questions:

1. What are the applications of Biobutanol?
2. Is there a possibility that biobutanol is a biofuel used in Brazil?
3. What is the market forecast for biobutanol by 2030?

Phase 2: Research or Sampling in Literature

In this step, the strings used to search the literature and the databases to be searched are defined. The data were obtained using the following platforms: SciELO, Google Scholar, and Science Direct. Figure 2 shows the steps followed for the literature survey.

Steps 1 and 2 were performed to obtain information regarding the amount of research conducted on biofuels and biobutanol specifically. In step 3, we were raised on the biobutanol production processes and their production prospects. Step 4, reflects the crossover between biobutanol production and its market prospects. At this phase, we applied the inclusion and exclusion criteria. The inclusion criteria were articles, dissertations, and technical reports published in English or Portuguese. The exclusion criteria were duplicate articles and non-eligibility for the proposed theme.

Phase 3: Data Collection

In the third phase, the articles were resumed and organized according to the reference to the theme addressed. Figure 3 shows the number of publications found in the integrative review steps.

Research on biofuels has great relevance in the market. A total of 60 articles addressing the theme of biobutanol were selected. Ten articles were evaluated, considering some themes: Renewable

Figure 1. Literature review phases.

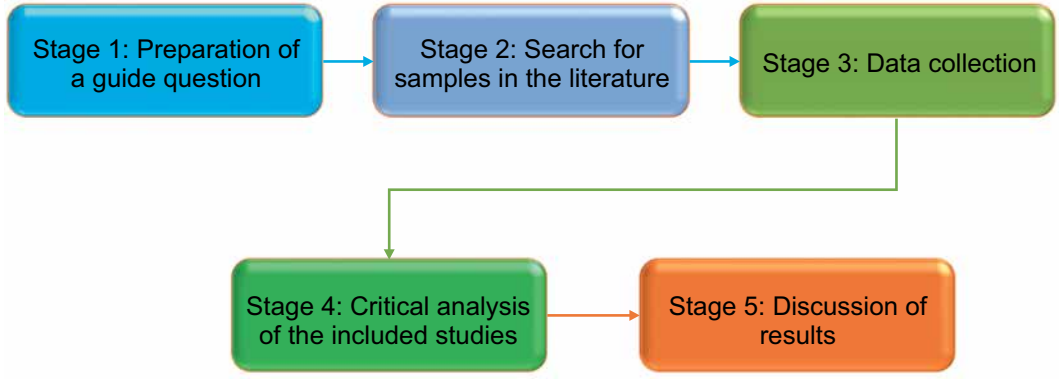

Figure 2. Steps for the literature survey.

Figure 3. Number of searches found at each phase.

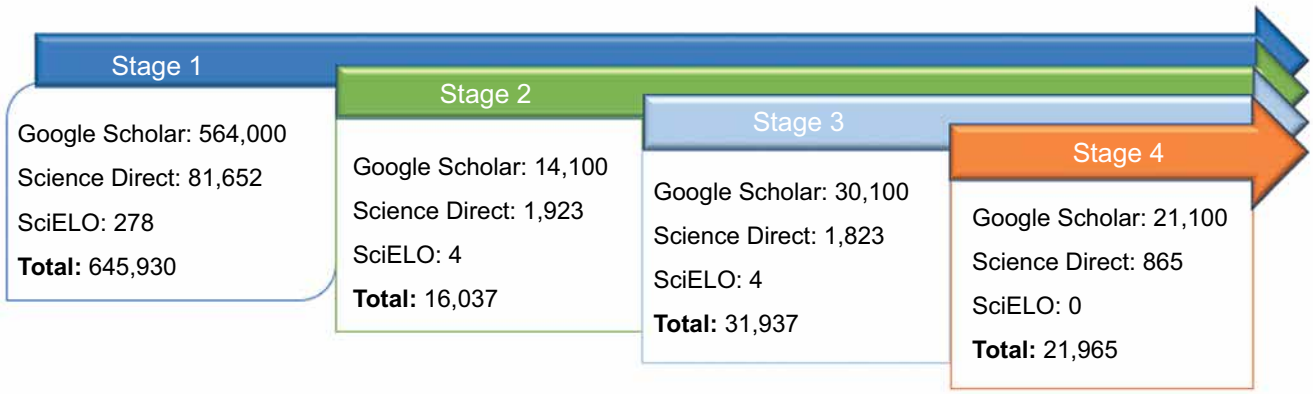

energies; Production of Biobutanol, economic and market analysis. Besides, 2 international standards and 6 technical reports without full access were consulted to understand the projection of the biobutanol market by 2030.

Phase 4: Critical Analysis of Studies Included

In this stage, we did a critical analysis of the selected literature after the inclusion and exclusion criteria of papers. Figure 4 shows the quantity of the literature survey corresponding to 67% of articles, 22% of technical reports, and 11% of international standards.

The studies address the scope of the insertion of biofuels in the energy matrix as a relevant factor to combat global warming. We focused on the applications of biobutanol as a solvent in the chemical, petrochemical, and biofuel industries. They specifically present the production of n-butanol by the biochemical route through ABE fermentation using clostridium bacteria as the main microorganism for the process.

The solvent separation technologies obtained by ABE fermentation are presented in most articles as impact agents in the economy of biochemical processes because the separation processes directly influence the production price of biobutanol.

The prospect of biobutanol by 2030 was optimistic according to the technical reports prepared between 2019 and 2021[1,11,12]. It also points out that countries such as China, India, and the United States have great interest in investing in biobutanol as fuel due [11], mainly the ability of biobutanol to be mixed and have squealing gasoline properties and have greater efficiency than ethanol. In the United States, the mixture of biobutanol in gasoline is regulated by ASTM D7862 [6] and ASTM D7875 [7]. The Brazilian market is promising for biofuels since the second largest consumer in the domestic energy matrix is the transportation sector, responsible for 31.2% of domestic energy consumption in 2020 (BEN, 2020) [13,14]. In Brazil, biobutanol is a biofuel since there is an investment in the ethanol production market adapting cars to this biofuel

Figure 4. Quantitative literature articles.

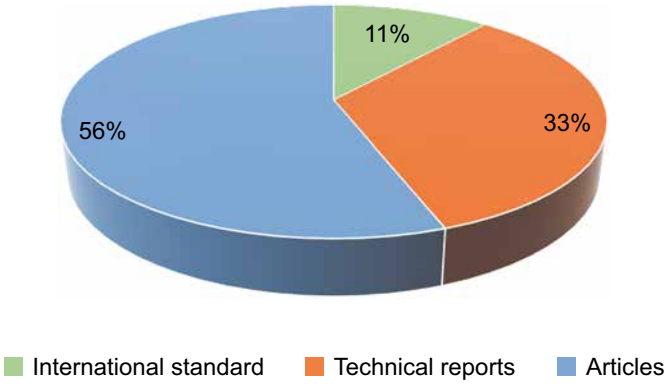

[4]. At this moment, the largest market in Brazil for biobutanol to be used is as a solvent in the paint and varnish producers' industry.

Discussion

In the phase 5, the interpretation and synthesis of the information obtained from the results of the research on the theme of biobutanol are made. The research covered the bibliography from 2011 to 2021. it is possible to observe in Figure 5 the distribution of material used in this work per year.

According to The Energy, Information Administration (EIA), the increase in world energy consumption would be around 56% in 2040 compared to 2010 [15, 16]. Shenbagamuthuraman (2021) showed that gasoline and other liquid fuels are the dominant energy sources for the transportation sector, although there is a slight decline in total transport energy consumption from 96% in 2012 to 88% in 2040. [17] US, China, and Brazil should achieve 15-27% of biofuel mixture with conventional fuel by 2020-2022 [1]. The biobutanol market is expected to register a CAGR (Compound Annual Growth Rate) of over 7%, during the forecast period. The major factors driving the market studied are carbon emission reduction and gaining prominence as a foundation for chemical manufacturing. [11] In 2020, the worldwide n-butanol market volume was more than 5.1 million metric tons. The market volume of this organic compound is forecast to grow to around 6.2 million metric tons worldwide by the year 2026 [18]. In Figure 6, we can analyze the n-butanol market by 2026.

Figure 5. Distribution of publications on the theme of research by year.

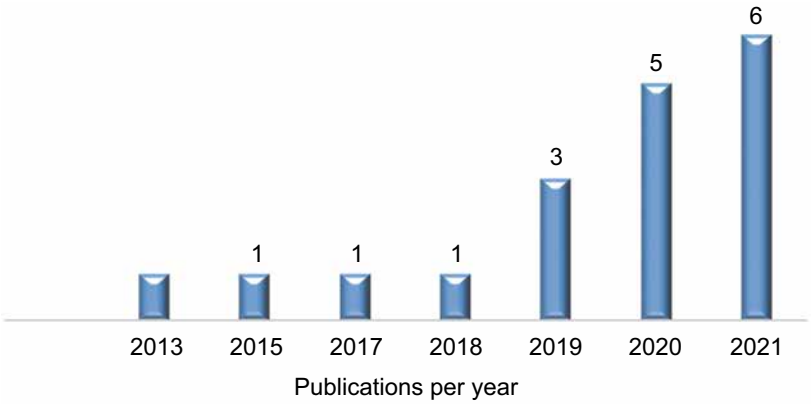

Figure 6. Global n-butanol market volume from 2015 to 2020, with a forecast from 2021 to 2026 (million metric tons).

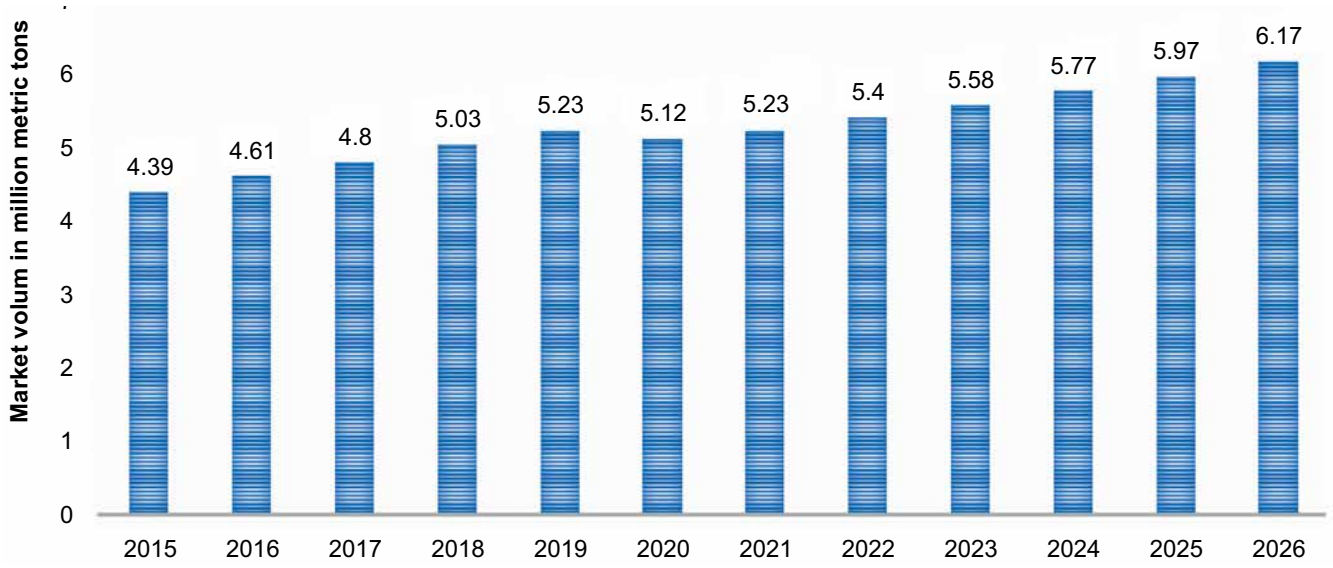

The biobutanol market is in an incipient and consolidated phase. The main biobutanol producing industries are Cathay Industrial Biotech, Gevo inc, Butamax Advanced Biofuels, and Cobalt Technologies [11]. Cobalt Technologies has developed several technological innovations to produce biobutanol to reduce production costs by 30% to 60% and radically reduce the impact of carbon compared to petroleum-derived butanol, which finds applications in various chemicals and fuels, including 1-butylene, butadiene, lubricating oil, and poly-alpha-olefins. [12] Brazil, according to the Brazilian Chemical Industry Association (ABIQUIM), Oxiteno and Elekeiroz are currently producing butanol isomers.

Conclusion

In this work, 60 more articles related to the theme were collected using the databases of the Academic, Science Direct, and SciELO. Six technical reports and 2 international standards were considered to complement the information. This review demonstrated that biobutanol holds a promise as a renewable biofuel, given its ability to be a substitute for fossil fuels and its property of being blended with gasoline and diesel. In addition, the world market is open to the possibility of inserting biobutanol as biofuels in its energy matrix, mainly in countries such as China and the US. For Brazil, biobutanol may be a great possibility for insertion as a biofuel due to the large supply of raw material from sugarcane close to the areas where the plants will be implemented. However, to date, greater use of n-butanol is as a solvent applied in the production of paints and coatings. In addition, another obstacle to the inclusion of biobutanol as biofuel in the energy matrix is the regulatory agencies, since this biofuel is an experimental fuel by the Brazilian National Agency of Petroleum, Natural Gas, and Biofuels (ANP). At present, Brazil does not have technical standards to designate the use of a mixture of this biofuel with gasoline or diesel. It was also possible to highlight the scarcity of publications about the biobutanol market in Brazil, although the country has great potential to be a producer of this biofuel.

Acknowledgments

To the ANP Human Resources Program, through PRH 27.1 ANP/FINEP/SENAI CIMATEC, for the scholarship granted and financial support for this work.

References

1. Mordor Intelligence. Biofuels Market. Available at: < Biofuels Market | 2021 - 26 | Industry Share, Size, Growth - Mordor Intelligence >. Accessed on: 18 Aug. 2021.
2. Li Y et al. Potential of acetone-butanol-ethanol (ABE) as a biofuel, 242 (2019), pp. 673 – 686. Available at: <https://doi.org/10.1016/j.fuel.2019.01.063>. Accessed on: 30 Mar. 2021.
3. Industryarc. n-Butanol Market- Forecast (2020-2025). Available at:<https://www.industryarc.com/Report/15518/n-butanol-market.html>. Accessed on: 18 Aug. 2021.
4. Brandão LFP. Estudo do 1-butanol e 2-metil-1-propanol em misturas com a gasolina e o diesel: uma análise sob a perspectiva da especificação brasileira. 2017. Tese (Doutorado em Química) - Instituto de Química, Universidade de Brasília, Brasília, Distrito Federal, 2017.
5. Pugazhendhi et al. Bio-butanol as a promising liquid fuel for the future-recent updates and perspectives. Fuel 2019;253:637-646.
6. Norma ASTM D7862 – Standard Specification for Butanol for Blending with Gasoline for Use as Automotive Spark-Ignition Engine Fuel.< https://www.abntcatalogo.com.br/norma.aspx?ID=466168 >. Accessed on: 27 Apr. 2021.
7. Norma ASTM D7875 - Standard Test Method for Determination of Butanol and Acetone Content of Butanol for Blending with Gasoline by Gas Chromatography.
8. Natalese J, Zouain D. Technology road mapping for renewable fuels: Case of biobutanol in Brazil. Journal of Technology Management and Innovation 2013;8(4):143–152.
9. Maturana MGV. Dilemas estratégicos na difusão de inovações em bioprodutos. 2019. Dissertação (Mestre em Ciências) - Escola de Química, Universidade Federal do Rio de Janeiro, Rio de Janeiro, 2019.
10. Evangelista AT et al. Princípios da química verde e a produção de ferro-gusa: uma revisão integrativa. In: V Simpósio Internacional de Inovação e Tecnologia, Anais do V SIINTEC, 1-9, 2019.
11. Mordor Intelligence. Bio-butanol Market. Available at: <https://www.mordorintelligence.com/industry-reports/bio-butanol-market>. Accessed on: 18 Aug. 2021.
12. Grang View Research. n-Butanol Market Size, Share & Trends Analysis Report By Application, Regional Outlook, Competitive Strategies, And Segment Forecasts, 2019 To 2025. Available at:< https://www.grandviewresearch.com/industry-analysis/n-butanol-market>. Accessed on: 18 Aug. 2021.
13. BEN. Balanço Energético Nacional 2021. Disponível em:<https://www.epe.gov.br/pt/publicacoes-dados-abertos/publicacoes/balanco-energetico-nacional-2021>. Accessed on: 15 Aug. 2021.
14. Ferreira ML. Importância dos biocombustíveis na bioeconomia. PPV 688 – Culturas Energéticas, 2020. Available at:< http://site.ufvjm.edu.br/ica/files/2020/07/1-Import%C3%A2ncia-dos-biocombust%C3%ADveis-na-bioeconomia.pdf>. Accessed on: 27 Apr. 2021.
15. EIA. International energy outlook. U.S.: Energy Information Administration; 2015.
16. Awad OI et.al. Overview of the oxygenated fuels in spark ignition engine: Environmental and performance. Renovar. Sustentar. Rev. Energia 2018;91:394–408. Available at: https://doi.org/10.1016/j.rser.2018.03.107. Accessed on: 27 Apr. 2021.
17 Shenbagamuthuraman V. et al. State of the art of valorizing of diverse potential feedstocks for the production of alcohols and ethers: Current changes and perspectives. Chemosphere 2022;286. Available at: https://doi.org/10.1016/j.chemosphere.2021.131587. Accessed on:15 Jun.2021.
18 Statista. Market volume of n-Butanol worldwide from 2015 to 2020. Available at: <https://www.statista.com/statistics/1245211/n-butanol-market-volume-worldwide/>. Accessed on: 18 Aug. 2021.
19. Ribeiro LCP. Produção de butanol por Clostridium beijerinckii NRRLB 598 a partir de matérias primas agroindustriais. 2019. Dissertação (Mestre em Ciências) - Escola de Química, Universidade Federal do Rio de Janeiro, Rio de Janeiro, 2019.

Risk Analysis and Indentification of Environmental Impacts Associated with Hydraulic Fracturing in Shale Gas Production

Caio Tadeu Veloso Gargur[1*], Gabriel de Veiga Cabral Malgaresi[1], Lilian Lefol Nani Guarieiro[1], Reinaldo Coelho Mirre[1]

[1]SENAI CIMATEC University Center; Salvador, Bahia, Brazil

The production of shale gas in Brazil has great potential to meet the country's energy needs. This process uses hydraulic fracturing, which is a good stimulation method, that induces fractures in the reservoir rock by injecting a fracturing fluid into it. Therefore, it permits increasing the permeability around the well, and the well's productivity index. It is crucial to understand the operation and the factors influencing the process to mitigate the risks involved in hydraulic fracturing. This work aims to identify and analyze the possible failure modes and their risks through risk analysis methods [Failure Modes and Effects Analysis (FMEA), and Fault-Tree Analysis (FTA)], in addition to connecting them to environmental impacts. We expected that this integrated method would support the safe monitoring of the technique in the future. **Keywords: Fracking. Shale Gas. FMEA. FTA. Environmental Impacts.**

Introduction

With the increase in global energy demand, the search for alternative resources has become an increasingly necessary reality. In Brazil, with the reheating of onshore field activities, there is potential for the exploration and production of unconventional gas in onshore basins, such as those in the Recôncavo Baiano, São Francisco, Sergipe-Alagoas, Parnaíba, Parecis, Paraná, Potiguar, Amazonas and Solimões [1,2].

Located in low permeability reservoirs, shale gas is exploited using the hydraulic fracturing technique, which consists of creating fractures through the reservoir rock by injecting a fracturing fluid under high pressure, leading to increased permeability in the rock and, consequently, increasing the productivity rate of the well [3,4].

The method's objective is to increase the permeability and porosity of the rock by fractures, which propagate through the rock formation, to facilitate the extraction of oil or gas. Before fracturing occurs, vertical drilling takes place to a depth of approximately 1.2 km to 3.6 km; reaching the kick-off-point (KOP), horizontal drilling begins, up to 1.2 km in length [5], to reach a larger area to extract as much oil or gas as possible. After the drilling phase, the horizontal section is fractured with the injection of chemical fluids and a high amount of water at a pressure that is higher than the fracturing pressure (5,000 psi), together with thickeners that act as support agents (sand, polymeric gums, and silica) that create a preferential path of high conductivity, facilitating the fluid flow [4].

Considered high risk, the technique is not well regarded by a part of society as it is associated with the possibility of environmental and social impacts, such as aquifer contamination, and geological risks, among other negative impacts, depending on the conditions in which it is practiced [6,7]. However, the Brazilian potential with its reserves makes an intensified effort and studies the efficiency of hydraulic fracturing for the exploration and production of shale gas and the control of its impacts favorable for the country [8,9]. In addition, the country could double its gas reserves if only 10% of the gas were commercially viable.

The use of hydraulic fracturing in Brazil requires greater knowledge about the real risks and impacts present depending on the characteristics

Received on 15 December 2021; revised 21 February 2022.
Address for correspondence: Caio Tadeu Velsoso Gargur. Av. Orlando Gomes, 1845 - Piatã, Salvador - BA- Brazil. Zipcode: 41650-010. E-mail: caio.gargur23@hotmail.com.
DOI 10.34178/jbth.v5i1.199.

J Bioeng. Tech. Health 2022;5(1):71-77.

of the reservoir, seeking to minimize failures and mitigate the environmental and social impacts arising from this practice [10]. Lima and Gonçalves [11] emphasize the need for technical knowledge about the method, to improve it, better monitor the fracture process, and minimize damage to the environment in the recovery of gas in shale gas type reservoirs. Thus, environmental studies on the impacts of hydraulic fracturing are important as they allow for the subsidizing of eventual licenses concessions by environmental agencies. Therefore, it is necessary to know the characteristics of the Brazilian aquifers and the petrophysics and geomechanics of shales [6].

The risk analysis of the shale gas production process through Hydraulic Fracture will be performed using the FMEA (Failure Modes and Effects Analysis) and FTA (Fault-Tree Analysis) methods [12]. The FMEA method is used essentially for preliminary evaluations to increase the knowledge about the functioning and performance of the studied systems by identifying the main issue in the process. Consequently, after identifying and solving the problem, there is a reduction or even cancellation of failures. The FTA Analysis method, on the other hand, is applied to carry out a systematic approach that allows identifying the root of a problem through a diagram. One of the differences that have become a complement to the FMEA method is having the ability to map a series of events until the possible causes that originated the failure are reached, that is, a correlation between failures and subsystems.

In this way, it is possible to identify failures and their severity, frequency of occurrence, probability of detection, priority problem, and their causes from the combination of methods. Therefore, they are methods that seek to improve the quality and assertiveness of the process, making it safer and more reliable.

The production of shale gas can lead to operational failures due to the extreme conditions of the process, compromising operational safety due to risks related to environmental impacts. Therefore, there is a need to understand how the fracturing mechanism occurs and what are the environmental impacts involved during this type of operation.

The objective of this work is to carry out a preliminary survey of the failure modes of hydraulic fracturing, which can occur during the fracturing stages of reservoir rock and gas production. It will be possible to identify and analyze possible risks of the interaction of hydraulic fracturing mechanics with the geological environment of the unconventional reservoir through the use of risk analysis methods FMEA and FTA, in addition to correlating the risks to their possible environmental impacts.

Materials and Methods

This study has a predominantly exploratory character, with its development based on data and information obtained from bibliographic references. Google Scholar and Science Direct databases were used on a query basis, from 2017 to 2021. Through strings such as fracking, shale gas, risk analysis, and environmental analysis, we searched for papers that associate the mechanism of hydraulic fracturing with environmental risks and impacts arising from its activity. Understanding the environmental aspect (cause) arising from the interaction of an element with the environment brings as a consequence the impact of this activity. A methodological proposal for this work involves the following steps: (i) study the hydraulic fracturing technique; (ii) identify the variables that influence the process; (iii) identify and associate environmental risks and impacts; and (iv) verify the potential application of FMEA and FTA risk analysis techniques.

Failure Modes and Effects Analysis - FMEA

The FMEA methodology was used to analyze the risks involved in the Hydraulic Fracture process to show the problem to be solved that is a priority. This priority problem is found through a Risk Matrix that contains the Risk Priority

Number - RPN, in which the higher the number, the more critical the failure in question and the faster a measure or action should be taken to avoid it. The RPN is calculated using Equation 1.

$$RPN = G\ x\ O\ x\ D \quad (1)$$

Where:
G - Severity; O - Probability of Occurrence;
D - Probability of Detection.

The "G" and "O" elements are scored from 1 to 10 following the logic of 1 for very low and 10 for very high severity or probability of occurrence, whereas in "D" 1 is for high detection probability and 10 for low probability.

Fault-Tree Analysis - FTA

Another risk analysis method is the FTA, which aims to identify the root of the problem/ fault with the highest risk score (RPN), i.e., the priority problem analyzed in the FMEA method. The analysis occurs through the assumption of causes for that failure. So, it is possible to exclude reasons for the occurrence of the problem, which facilitates its identification and subsequent remediation, and consequently, the occurrence of failure can be canceled. The method analyzes the failure modes with the highest RPN of each risk matrix, following the FMEA technique.

Results and Discussion

From the databases consulted, the interactions between the key terms fracking shale gas risk analysis and environmental analysis were tested. From the set of researched works, we noticed a lack of studies that associate risks and environmental impacts arising from the use of the hydraulic fracturing technique in the production of shale gas. Thus, the need for this type of approach stems from the importance of establishing the relationship between cause (failure mode) and effect (environmental impact) with the use of the technique. Although preliminary, the results that will be presented in this work contribute to adapting the proposed methodology to identify and assess the environmental risks and impacts of the production of shale gas.

In the course of hydraulic fracturing, problems can occur that affect the integrity of the activity and, consequently, cause environmental and social impacts. Initially, a preliminary assessment of the operational characteristics of hydraulic fracturing was carried out under the conditions of the reservoir, which allowed the identification of possible failure modes of the process and their risks, which are capable of causing potential environmental impacts (Table 1).

From Table 1, it was possible to identify the main risks associated with the hydraulic fracturing technique, which are the cause of unwanted fractures and the occurrence of fracturing fluid or gas leaks. Therefore, as proposed in the method, the risk analysis technique (FMEA) was used to analyze these main risks presented in Table 1, so that from this analysis it is possible to identify the failure mode with the highest RPN value, which demonstrates the problem that is a priority to be solved.

First, there is the risk analysis of the cause of unwanted fractures (Table 2). Unwanted fractures are those caused accidentally, which occur with the loss of control over the pressure that the fluid exerts on rock formations, only in the situation where the upper capping rock has lower minimum stress than that of the lower capping rock, there is a possibility of environmental impact since the flow of the fracturing fluid would go towards the surface, reaching existing groundwater and contaminating it.

The failure modes analyzed were: I) Exceeding the fracture pressure continuously; II) Deviation in the geomechanical study of the reservoir; III) Uncontrolled spread of the fracturing fluid.

The fracture pressure (Pf) is calculated through a geometric correlation that proportionally relates to the pressure gradients of the depth that will be fractured. Thus the reference value of Pf is obtained, and so a Pa greater than Pf is applied

Table 1. Failure modes x risks x environmental impacts.

Failure Modes	Risks	Environmental Impacts
Continuously exceed fracture pressure	Cause unwanted fractures to groundwater	Contamination of groundwater and subsoil
Deviation in the geomechanical study of the reservoir	Cause unwanted fractures to groundwater	Contamination of groundwater and subsoil
Uncontrolled spread of fracturing fluid	Cause unwanted fractures to groundwater	Contamination of groundwater and subsoil
Well cementing failure	Occurrence of fracture fluid or gas leaks	Increased concentration of toxic gases in the atmosphere Contamination of groundwater and subsoil
Piping corrosion	Occurrence of fracture fluid or gas leaks	Increased concentration of toxic gases in the atmosphere Contamination of groundwater and subsoil

Table 2. Risk matrix cause of unwanted fractures.

	Cause of unwanted fractures				
	Fail Mode	G	O	D	RPN
1	Continuosly exceed fracture pressure	8	4	3	96
2	Deviation in the geomechanical study of the reservoir	7	5	6	210
3	Uncontrolled spread of fracturing fluid	9	4	5	180

to open the fractures. However, once the fractures are opened, Pa is gradually reduced and an irregular fracture doesn't occur. On the other hand, the geomechanical study of the reservoir aims to provide prior knowledge of the rock's properties, especially its permeability, porosity, temperature, and compressibility. All this data and the proximity to some groundwater are extremely important, since, as they are estimated, an error in the calculations or the studies can cause serious environmental impacts. Lack of control in the propagation of the fracturing fluid is another failure mode, which can occur due to the existence of natural fractures in the reservoir. There is the possibility of an involuntary connection of a fracture caused by the process with a natural fracture to happen and so, with the application of the fluid of fracturing in these unforeseen sites, it is possible that new fractures would be opened, which is unwanted.

Subsequently, the risk analysis of the occurrence of fracturing fluid or gas leaks was carried out, Table 3, of which the failure modes analyzed were: I) Failure in cementing the well; II) Piping Corrosion.

In the same way as the fracturing fluid, the gases present in the reservoir rock or those from the production itself can also migrate to the surface due to a difference in density, causing the contamination of groundwater and an increase in the concentration of toxic gases in the atmosphere.

The irregular cementation of a well is one of the biggest concerns regarding the integrity of the well. This failure can be described as a poorly done zonal isolation, which if not identified or controlled, can give rise to accidents that cause personal, material, environmental and financial damage. Due to the practice of operations to avoid failures in cementing the well, its probability of

Table 3. Risk matrix occurrence of fracture fluid or gas leaks.

	Occurrence of fracture fluid or gas leaks				
	Fail Mode	G	O	D	RPN
1	Well cementing failure	9	4	5	180
2	Piping corrosion	7	5	4	140

occurrence is minimized, however, it still exists. Unlike cementing failure, piping corrosion, a process of deterioration of the internal surface of the well, is more likely to occur. In addition to harming the process, it delays the production operational schedule, generates high maintenance costs, and can also generate health risks and the environment.

After performing the risk analysis using the FMEA method, it is possible to identify the failure modes with the highest RPN. The results showed that "Deviation in the geomechanical study of the reservoir" and "Failure in cementing the well" are the problems to be solved as a priority, concerning the risk matrices in Table 2 and Table 3, respectively. Thus, it appears that the steps with the greatest possibility of causing environmental impacts are those linked to the characteristics of the reservoir, the good profile, and the injection of fracturing fluid.

After identifying the priority failures, another risk analysis was carried out, FTA, which should present the possible causes for the occurrence of the failure that will be analyzed. Thus, it was possible to build the fault tree for each problem mentioned, as can be seen in Figure 1. Through this analysis, it is possible to identify the causes of a deviation in the geomechanical study of the reservoir. One of the main reasons is the inadequate choice of the fracture model, which can occur due to an error when estimating the reservoir properties since they are performed through computational tests, which means that they are not exact. Just as the reservoir properties are not accurate, the two-dimensional and three-dimensional fracture models are not either. Therefore, due to the imprecision of the fracture models and the estimation of reservoir properties, there is a possibility of a deviation in the geomechanical study of the reservoir, which may cause unwanted fractures that can cause serious environmental impacts.

The FTA for "Cementation Failure" was also constructed (Figure 2).

From the analysis carried out, it can be seen that "Cementing Failure" has several causes to be analyzed, which may explain its greater severity and higher difficulty of detection of "Piping corrosion". The main cause of this failure can be contamination of the cement slurry, so the cement properties are altered due to interaction with the drilling fluid, which impairs the cementation of the well. There is also the possibility that the volume of the cement paste was insufficient, due to loss of circulation, which would be the invasion of fluid for formation through natural or induced fractures or in depleted formations. This can also occur due to some break-in in the well, which would lead to an unexpected increase in the diameter of the well. Furthermore, choosing a cement of a quality that meets the requirement of high shear strength is extremely important, as the cement's adherence to the good wall is crucial for efficient cementation.

Conclusion

After the risk analysis is performed on the possible failure modes arising from the fracturing and gas production steps, it is concluded that the integrated methods of FMEA and FTA, when used together, are able of providing sufficient data on the possible risks of using the Hydraulic Fracture technique in shale gas exploration and production. Even though a preliminary study, it is possible to identify the presence of environmental impacts such as groundwater contamination and increased concentration of toxic gases in the atmosphere.

Figure 1. FTA of the Deviation in the geomechanical study of the reservoir.

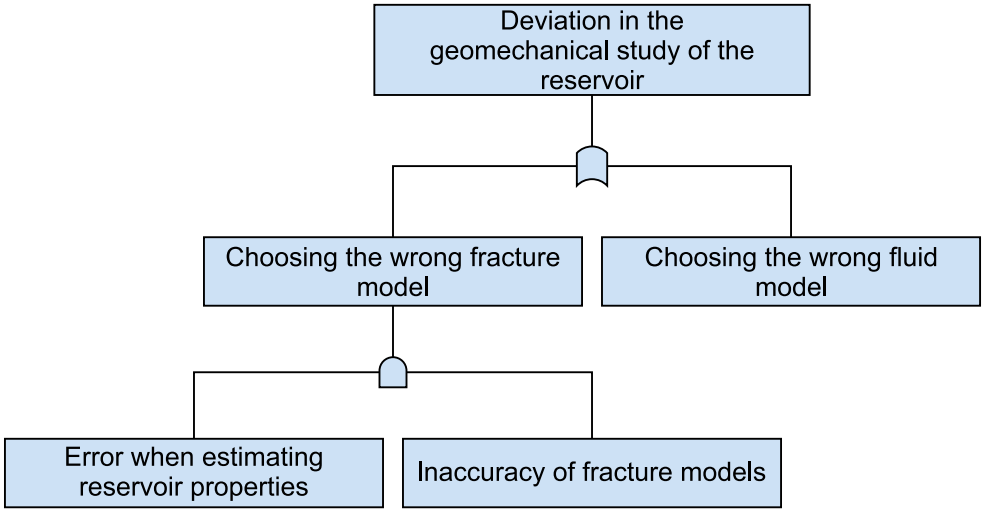

Figure 2. FTA of Failure to cement.

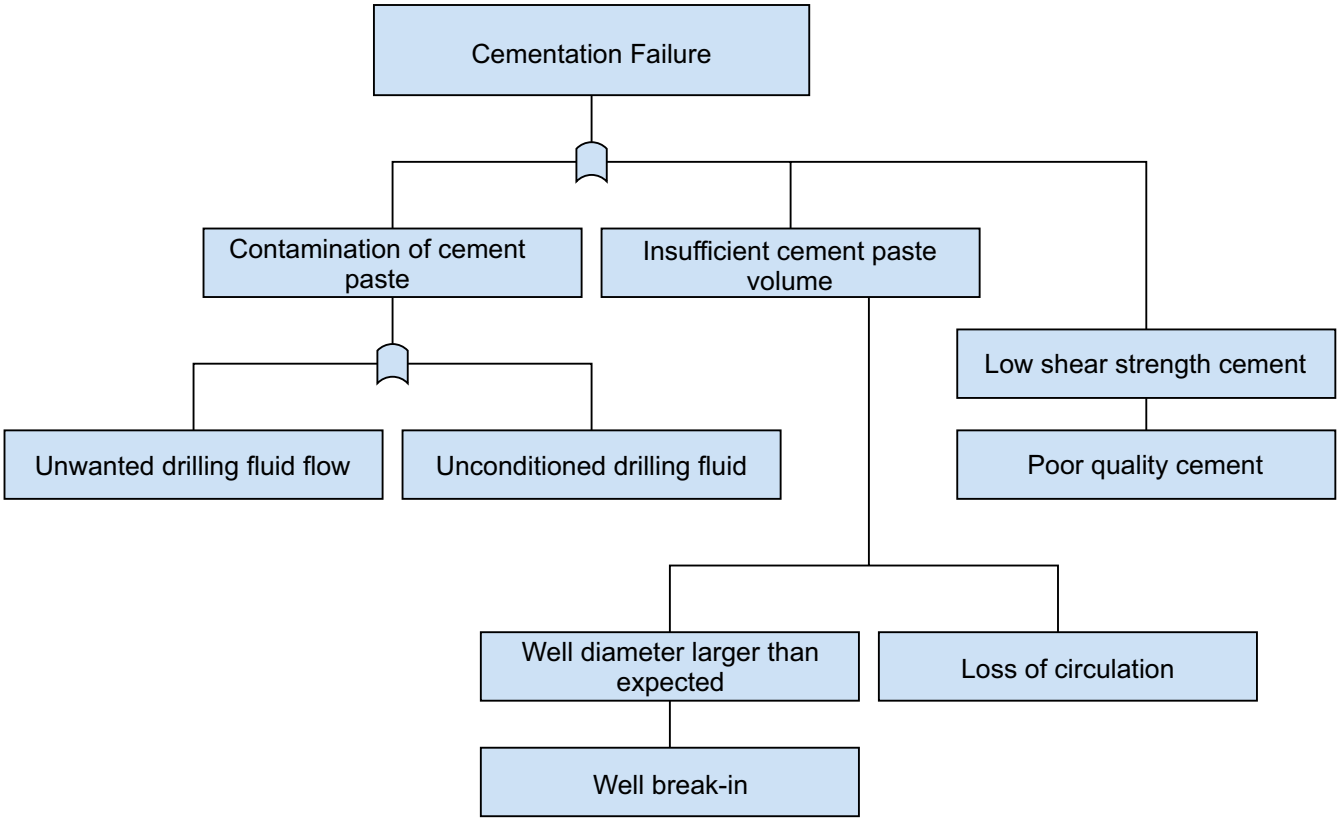

However, it is expected that with more studies in the future, based on more detailed risk analysis, it will be possible to reduce possible risks, through fracture monitoring or the application of more accurate fracture modeling software. From this, the probability of the occurrence of environmental impacts would decrease, so that the applicability of the technique would become safer and more reliable, so that, in the future, such a proposal will be able to offer greater incentive to the exploration and production of oil and gas in unconventional reservoirs, to take advantage of the energy potential available in the country.

Acknowledgments

To the Human Resources Program of the National Agency for Petroleum, Natural Gas and Biofuels, PRH 27.1 ANP/FINEP, for financing the study and the Centro de Competências Integradas Onshore.

References

1. Brasil. Aproveitamento de hidrocarbonetos em reservatórios não convencionais no Brasil. Programa de Mobilização da Indústria Nacional de Petróleo e Gás Natural, Comitê Temático de Meio Ambiente, Brasília: PROMINP/CTMA - Projeto MA 09, 2016.
2. Ordoñez R. ANP publica resolução com regras para explorar óleo e gás não convencional no Brasil. O Globo, 2014.
3. Tavares LS. Estado da arte da operação de fraturamento hidráulico. Trabalho de Conclusão de Curso (Graduação em Engenharia de Petróleo), UFF, Niterói, RJ, 2010.
4. Thomas JE. (Org.). Fundamentos de engenharia de petróleo. 2ª. Edição, Rio de Janeiro: Interciência, 2004.
5. Yew CH. Mecânica do fraturamento hidráulico. Rio de Janeiro: e-papers, 2008.
6. Lima AC, Anjos JASA. Shale gas: riscos ambientais de sua produção para o Brasil. Revista Gestão & Sustentabilidade Ambiental. Florianópolis 2015:167-180.
7. Ramos KN, Petry PM, Costa HKM. Atualizações da exploração de gás não convencional no Brasil, Revista Gestão & Sustentabilidade Ambiental. Florianópolis, 2020;9:237-258.
8. Badaró KL. Estudo do caso do shale gas: uma possibilidade energética no Brasil contemporâneo. Dissertação (Mestrado em Engenharia Industrial). UFBA, Salvador, BA, 2019.
9. Gomes I. Brazil: Country of the future or has its time come for natural gas? Oxford Institute for Energy Studies. 2014.
10. Sanberg E, Göcks N, Augustin S, Vedana L, Silva C. Abordagem técnica e legal acerca do fraturamento hidráulico no Brasil. Anais do XVIII Congresso Brasileiro de Águas Subterrâneas, UCS, Caxias do Sul, RS, 2015.
11. Lima M, Gonçalves T. Análise da recuperação de gás em reservatórios do tipo shale gas com o uso de fraturamento hidráulico. Trabalho de Conclusão de Curso (Graduação em Engenharia de Petróleo), UFRJ, Rio de Janeiro, RJ, 2020.
12. Catdoso R, Barros C, Tammela I, Rodrigues V. Análise de riscos para reduzir a ocorrência de blowouts no processo de perfuração de poços de petróleo offshore: integrando o conceito de CBM associado ao método Bow Tie. Anais do IV Congresso ABRISCO, Rio de Janeiro, RJ, 2019.

Treatment of Oily Effluents Through the Combination of Flotation and Wetland in Thermal Plants Under the Focus of Patent Documents: A Prospective Study

Barbara Lima Borges[1*], Edna dos Santos Almeida[1], Valdemir Alexandre dos Santos[2]
[1]SENAI CIMATEC University Center; Salvador, Bahia;
[2]Instituto Avançado de Tecnologia e Inovação; Recife, Pernambuco; Brazil

This study aimed to present a technological search for technologies in the processing of oily effluents through the physical-chemical flotation and biological wetland process generated in thermoelectric plants in the patent database of the Derwent World Patents Index (DWPI) using keywords. We found few studies for thermal power plant-effluent processing technologies and combined technologies for flotation and wetland effluent treatment. Patents indicated high efficiency in the combination of the processes. We did not find studies in Brazil for treatment technologies of effluents in thermoelectric plants. However, due to the country's energy scenario, investments in research in this area are recommended.
Keywords: Thermoelectric Plants. Oily Effluents. Flotation. Wetland.

Introduction

Thermoelectric power plants play a fundamental role in the operation of energy supply, as they operate as a complement to the Brazilian hydrothermal system in times of low levels of these reservoirs [1].

Thermoelectric power plants produce electrical energy from thermal energy released by chemical or nuclear reactions [2]. This production currently occurs from the combustion reaction. These plants can be classified according to different criteria: main product, type of fuel, type of thermal engine, and load character, among others. The most widespread thermal machines used in non-nuclear thermal power plants are the thermal power plants with a steam cycle, gas turbine power plants operating in simple cycles (combined-cycle plants), combustion engine plant internal, and thermoelectric cogeneration plants [3].

Depending on the technology adopted, the thermal power plant's cooling system can constitute a significant source of social and environmental problems, given the volume of water collected, evaporation losses, and the generation of effluents [4].

The generation of effluents is an environmental aspect that has great potential for environmental degradation, as they can cause changes in the quality of receiving bodies and consequently their pollution, causing damage to human health, soil and water contamination, thus it should be treated before the release to the receiving body [5].

Thus, the washing systems for equipment, lines, and rainwater drainage in thermoelectric plants, which will produce water with oily residues, must direct their effluents directly to a water treatment system. This system will treat the water to meet the quality parameters established in environmental legislation [6]. The removal of pollutants is the objective of effluent treatment. However, due to its diversity, there is no ready-made formula suitable for use in any situation. To achieve the objective, there are several treatment processes based on physical, chemical, or biological phenomena or principles, or even on their combinations [7].

In general, the combined treatment processes have greater efficiency, and for effluents with high oil content, the separation process by water-oil density difference is necessary, with flotation being one of the promising techniques. Flotation is widely used to treat effluents with high concentrations of suspended solids, oils, and greases. Among the benefits of flotation, there

Received on 12 December 2021; revised 20 February 2022.
Address for correspondence: Barbara Lima Borges. Av. Orlando Gomes, 1845 - Piatã, Salvador - BA- Brazil. Zipcode: 41650-010. E-mail: barbara.ifba@gmail.com. DOI 10.34178/jbth.v5i1.201.

J Bioeng. Tech. Health 2022;5(1):78-83.

is a reduction in odorous gases, raising the level of dissolved oxygen, which results in a better-quality effluent [8]. However, it is still necessary to polish the treated effluent, which can be done by a biological process, with wetland being one of the relatively low-cost alternatives. The wetland system represents a natural ecological solution for wastewater treatment. Natural systems are improvements in processes that occur in nature, but their differential is a small need for mechanical equipment, reduced electricity costs, and little or no need to use chemical inputs [9].

In this context, the objective of this work was to carry out a technological mapping in the patent base of the Derwent World Patents Index (DWPI), to assess the global panorama of the use of combined technologies for treating oily effluents generated by thermoelectric plants through the physical process -chemical flotation and biological wetland.

Materials and Methods

This technological prospection was carried out between May and July 2021, using the Text-Fields option in the Derwent World Patents Index (DWPI) database, with a license to use from the Centro Universitário SENAI CIMATEC - Salvador, Bahia, Brazil. The focus of the research was to collect data on the use of combined technologies in the treatment of effluents from thermal power plants through flotation and constructed wetlands.

To obtain the data, we searched using the association of keywords between 2000 and 2020. Four searches were performed in the patent database of the Derwent (Table 1). The surveys were based on the search for technologies with a focus on combinations of the techniques in this study.

The patents selected for data processing were those most associated with the proposed theme of combined technologies for the treatment of oily effluents through the flotation and wetland process in thermoelectric power plants.

Based on data collection in Derwent, 11 documents were identified related to the research interest area of this study. From the research, it was possible to identify the countries having the technology of interest, demonstrate the annual evolution of publications, as well as carry out an assessment of the area of analysis of the international patent classification codes (IPC) contained in the documents.

In addition, the patents found were read to identify and list the technical and environmental aspects and advantages contained in the documents.

Results and Discussion

Patent analysis is a robust approach that has been widely used to identify competition, design

Table 1. Patent Search for keywords from the Derwent World Patents Index (DWPI).

Search	Keyword	Number of Patent Documents
1	[(effluent or wastewater) near treatment] and (oil or oily) and (thermoelectric)	7
2	[(effluent or wastewater) near treatment] and (oil or oily) and (flotation) and (wetland)	4
3	[(effluent or wastewater) near treatment] and (oil or oily) and (flotation) and (thermoelectric)	0
4	[(effluent or wastewater) near treatment] and (oil or oily) and (wetland) and (thermoelectric)	0

strategies for the future, support the development of new processes and products in a given target technology field, and especially gain competitive sustainability advantages. Thus, the analysis of the evolution of a specific technology is of great importance to assess the impacts and potential market interest in a new or better technological demand [10].

Annual Evolution of Patents

Figure 1 shows the results for the filing of patents for the technologies studied from 2009, the year in which the first registration in China took place, CN101462816A. This record features equipment characterized by a modularized structure and high treatment efficiency [11].

From the analysis of the annual evolution (Figure 1) between 2015 and 2019, the largest number of publications was identified, representing 82% (9) of the total number of documents. In 2015, the largest number of inventions in technology was carried out, representing 45% (5) of the total number of documents identified. The annual evolution data of the patents studied in this prospect, found in the period from 2000 to 2020, shows that the technology is in a stage of knowledge accumulation, where the number of patents filed is still reduced, with a total of 7 patents filed in the area. Treatment of oily effluents from thermoelectric power plants and four patents filed in the area of effluent treatment by combining flotation and wetland techniques over a period of 21 years. During this period, no patents were found filed in the study area with a combination of flotation and wetland techniques for the treatment of oily effluents from thermoelectric power plants.

International Patent Classification (IPC)

The International Patent Classification – IPC was put into effect in 1971 to establish a current categorization for registered patents. This classification helps in the search for patents, making access to technological information in documents [12]. The most common IPC was C02F 9/14, which refers to the multi-stage treatment of water, wastewater, or sewage with, at least, one step being a biological treatment (Figure 2). The IPC codes B63J 4/00, B63B 35/00, C02F 1/00, and C02F 1/44 were found in three patent

Figure 1. Annual evolution of patent document publications on oily effluent treatments through the flotation and wetland process in thermoelectric plants deposited between 2000 and 2020.

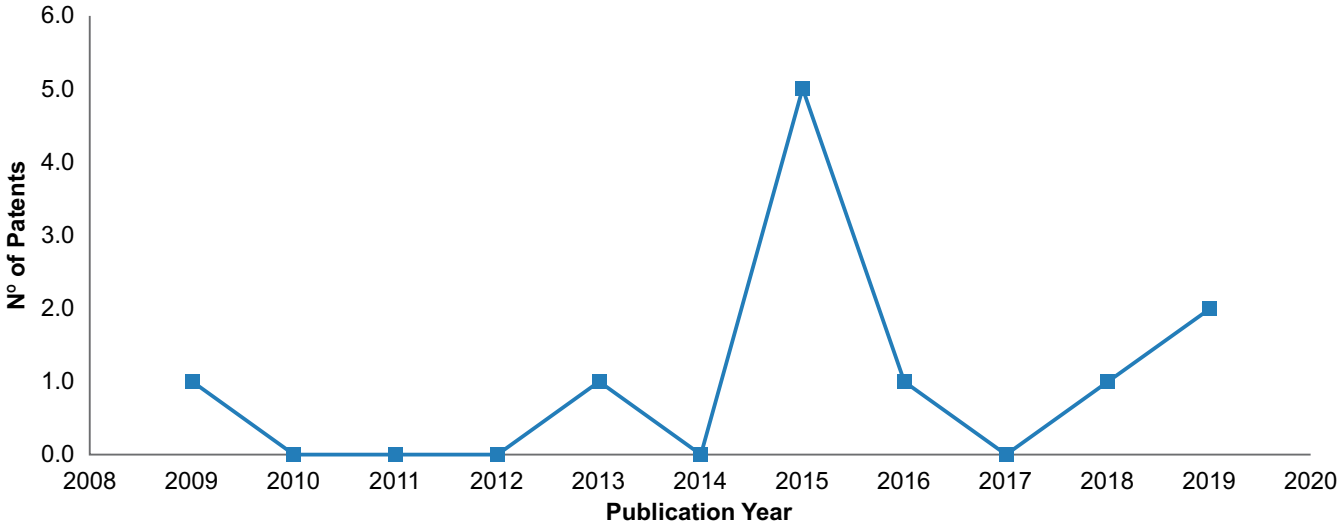

documents (Table 2). These patent codes are present in subsection B63, which refers to processing, transport, separation, and mixing operations in ships or other vessels; related equipment, and in subsection C02, which refers to the treatment of water, wastewater, sewage, or sludge and sludge.

Two documents present technologies for combined effluent treatments. Patent CN101462816A claims an integrated water treatment through an industrial pond with chemical treatment and aeration device in a thermoelectric power station. The equipment is characterized by high treatment efficiency, with a wide range of applications and little investment [11]. Patent CN207047070U claims a turbidity treatment system for organic wastewater belonging to environmental protection facilities. The system uses effluent treatment through flotation associated with a wetland pool. The model is presented as a kind of organic wastewater treatment plant that has a simple structure and high oil yield [13].

Countries Holding the Technologies

Concerning technology holders, of the 11 patent documents found for this study, China was the country with the highest number of patents filed (55% of the total), as seen in Figure 3. This result is since China has an electrical matrix in which coal-fired thermoelectric plants predominate, holding about 65% of the installed capacity, followed by hydroelectric plants, with 20% [14].

Conclusion

From this technological prospection, it is possible to conclude that, in the twenty years evaluated, few studies were found for

Figure 2. Distribution of the most used International Patent Classification codes in patent documents.

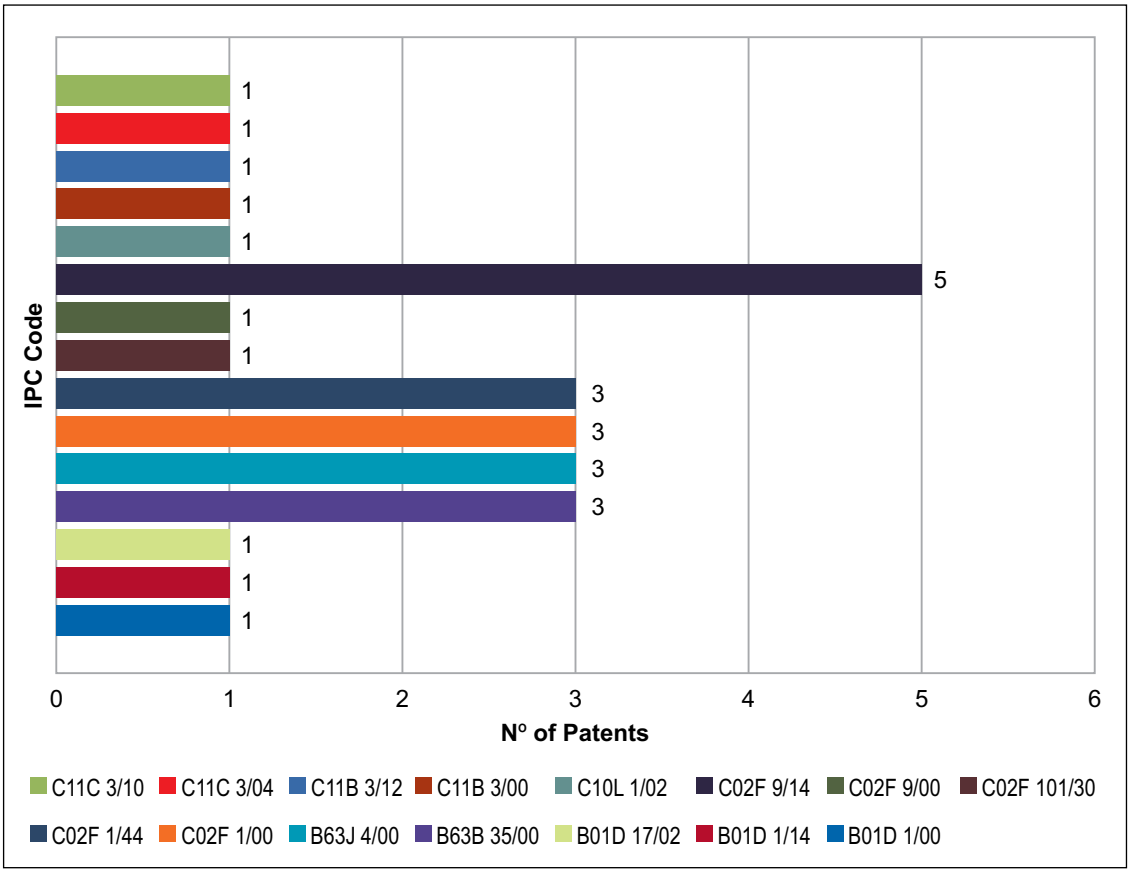

Table 2. Description of International Patent Classification codes in patent documents.

IPC Code	Code Description
B63B 35/00	Vessels or similar floating structures are specially adapted for special purposes and not included elsewhere.
B63J 4/00	Facilities for the treatment of wastewater or sewage.
C02F 1/00	Treatment of water, wastewater, or sewage.
C02F 1/44	Treatment of water, wastewater, or sewage by dialysis, osmosis or reverse osmosis.

Figure 3. Main depositor countries of the study technology between 2009 and 2020.

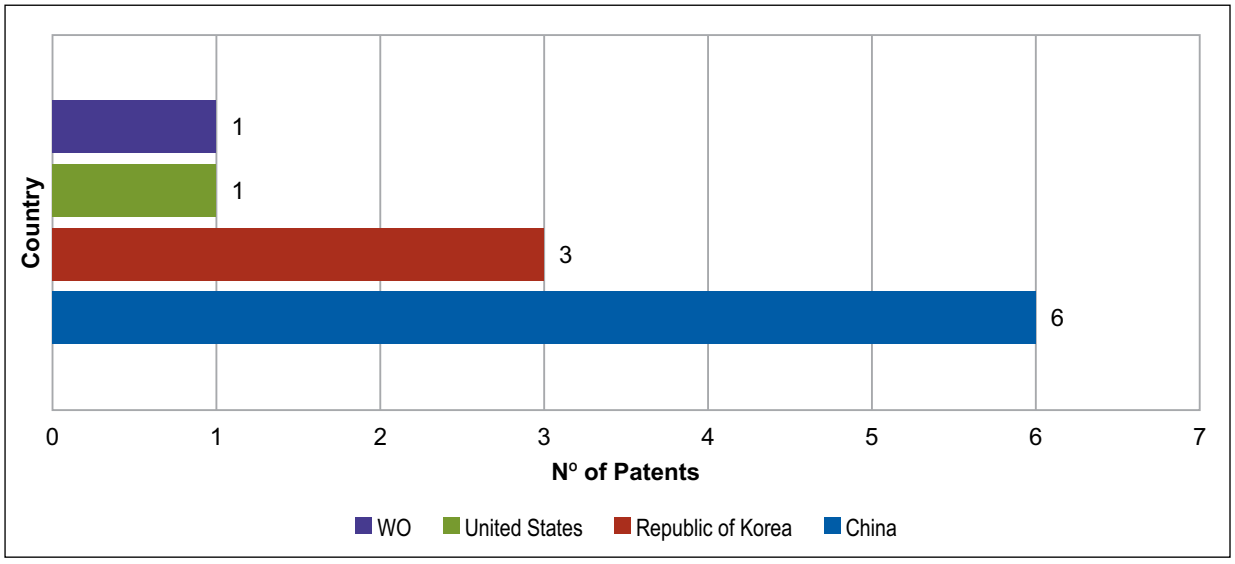

technologies in the treatment of effluents from thermal power plants and combined technologies for the treatment of effluents through flotation and wetland. China stands out in research on these issues, probably due to its electrical matrix. The two patents found that the use of combined physical and biological wastewater treatment processes is indicated as processes that require low financial investment and high yield. Thus, for the oily effluent condition generated in thermoelectric power plants, this combination is promising.

No studies were found in Brazil for the development of technologies for the treatment of effluents in thermoelectric plants, however with the vulnerable generation pattern in the country during the dry periods of the year, when the effective energy supply is lower than the installed hydropower capacity investment in research in this area is recommended.

References

1. Gomes LS. Avaliação do potencial energético aplicado a uma usina termelétrica de fontes renováveis. Available on https://fga.unb.br/articles/0001/2466/TCC1__Layane_VF4.pdf (Acessed on Oct 20, 2020).
2. Yoshimi AA. Estudo dos impactos ambientais de uma usina termoelétrica na cidade de Canas. Available on https://sistemas.eel.usp.br/bibliotecas/monografias/2014/MEQ14001.pdf (Acessed on Jan 01, 2021).

3. Tolmasquim MT. Energia termelétrica Gás Natural, Biomassa, Carvão, Nuclear. Available on https://www.epe.gov.br/sites-pt/publicacoes-dados-abertos/publicacoes/PublicacoesArquivos/publicacao-173/Energia%20Termel%C3%A9trica%20-%20Online%2013maio2016.pdf (Acessed on Mar 06, 2021).
4. IEMA – Instituto de Energia e Meio Ambiente. Regulação ambiental da termeletricidade no Brasil – gestão de recursos hídricos. Available on https://energiaeambiente.org.br/wp-content/uploads/2015/01/RegulacCCA7aCC83o-agua-2015-07-18_versaCC83o_site.pdf (Acessed on Apr 15, 2021).
5. Soares SJC. et al. Análise do efluente final gerado em uma usina termoelétrica no distrito industrial do município de São Luís – MA. Available on https://www.brazilianjournals.com/index.php/BRJD/article/view/9791/8207 (Acessed on Feb 03, 2021).
6. CEPEMAR. Descrição do empreendimento. Available on https://iema.es.gov.br/Media/iema/CQAI/EIA/2007/Termel%C3%A9trica%20de%20Viana/2%20-%20Descri%C3%A7%C3%A3o%20do%20empreendimento.pdf (Acessed on Jul 19, 2021).
7. Jerônimo CEM. Estudo de técnicas para o tratamento alternativo de efluentes oleosos oriundos da industrialização da castanha de caju. Available on https://repositorio.ufrn.br/jspui/bitstream/123456789/15901/1/CarlosEMJ_TESE.pdf (Acessed on Jun 21, 2021).
8. Andrade GC. Eficiência dos processos de flotação e filtração com uso de coagulante natural e químico no tratamento de efluente de laticínio. Available on: http://repositorio.roca.utfpr.edu.br/jspui/bitstream/1/5316/1/LD_COEAM_2015_1_07.pdf (Acessed on: Aug 04, 2021).
9. Zinato TMC, Guimarães MM. Estudo sobre a utilização de “wetlands” construídas para tratamento de águas residuárias no brasil. Available on: https://www.ibeas.org.br/congresso/Trabalhos2017/IX-001.pdf (Acessed on: Aug 04, 2021).
10. Valente CG. Technological Potential of Avocado Oil: Prospective Study Based on Patent Documents. Available on: https://pubmed.ncbi.nlm.nih.gov/31113349/ (Accessed on Jul 30, 2021).
11. Zhao W-R, Yanh Y, Bao J-Z, Rui H. et al. Apparatus for integrated treatment and comprehensive utilization of wastewater and use thereof. CN101462816A, 2009.
12. INPI. Classificação de Patentes. Available on: http://antigo.inpi.gov.br/menu-servicos/patente/classificacao-de-patentes. (Acessed on Feb 10, 2021).
13. Yang J, Mao HB. High turbidity organic wastewater system. CN207047070U, 2018.
14. Castro N. et al. O Setor Elétrico Chinês e o papel das Usinas Hidrelétricas Reversíveis. Available on: http://www.gesel.ie.ufrj.br/app/webroot/files/publications/07_castro_27_06_2018.pdf (Acessed on: Mar 22, 2021).

A Brief Overview of Ammonia and Urea Production and Their Simulations Strategies

Artur Santos Bispo[1*], Fernando Luiz Pellegrini Pessoa[1], Ana Lucia Barbosa de Souza[1]
[1]SENAI CIMATEC University Center; Salvador, Bahia, Brazil

To engender a simulation of the integrated Ammonia - Urea process, a literature review was carried out about these industrial processes, focusing on extracting information from the literature, such as the types of processes and their description, thermo-physical-chemical properties, and thermodynamic and kinetic models related to the process. Furthermore, research was carried out on thermodynamic models for NH_3-CO_2-H_2O systems, capable of describing an integrated Ammonia-Urea plant.
Keywords: Ammonia. Urea. Simulation. Literature Review.

Introduction

The high relevance of studies involving ammonia and urea can be verified when discussing the market importance and the various applications of these two products.

Therefore, it is almost essential to develop simulation strategies for their production, serving as a basis for more in-depth studies of intensification and optimization, to enhance the production and commercialization of products and their derivatives.

Thus, for more specific studies to be carried out, it is necessary to have a general knowledge about the synthesis and applications of both ammonia and urea.

Ammonia

The production of ammonia, in general, and summarized, is carried out from the reaction between N_2 and H_2 (Equation 1) (Haber-Bosch reaction) [1].

$$N_{2(g)}+3H_{2(g)} \rightarrow 2NH_{3(g)} \quad (1)$$

Received on 12 December 2021; revised 20 February 2022.
Address for correspondence: Artur Santos Bispo. Av. Orlando Gomes, 1845 - Piatã, Salvador - BA- Brazil. Zipcode: 41650-010. E-mail: artur.bispo@outlook.com.br. DOI 10.34178/jbth.v5i1.202.

J Bioeng. Tech. Health 2022;5(1):84-90.

The enthalpy of formation of this reaction ($\Delta_f H^{\theta}$), at a temperature of 298.15 K, corresponds to -45.898 kJ/mol (exothermic reaction) [2]. As for its applications, ammonia serves as raw material for different types of products. Among the areas of activity of ammonia, we have [3]:

- Fertilizer production – Ammonium sulfate, ammonium phosphate, ammonium nitrate, and urea (the focus of this study).
- Explosives – Nitric Acid
- Polymers – Nylon, fibers, and other types of plastics.

On an industrial scale, in short, ammonia is produced from water, air, and energy - generally, hydrocarbons, which, in turn, also provide hydrogen. In this scenario, the hydrocarbons are converted into methane (NH_4), which, subsequently, by hydrolysis, are converted into H_2 (which will be used in the synthesis, together with the N_2 feed), CO, and CO_2 (removed during the process) [1,2].

Urea

In general, urea is produced, on an industrial scale, through the reaction between ammonia (NH_3) and carbon dioxide (CO_2) which normally occurs under high pressure and temperature conditions (13 - 30 MPa and 170 – 300 °C), being represented by the following stoichiometric Equation 2 [4,5].

$$2NH_3+CO_2 \leftrightarrow NH_2CONH_2+H_20 \quad (2)$$

However, the generation of $CO(NH_2)_2$ does not occur directly, instead, the process is divided into two steps. At first, ammonium carbamate is formed at the expense of the direct reaction between NH_3 and CO_2 (Equation 3) [5].

$$2NH_3+CO_2 \leftrightarrow NH_2CO_2NH_4 \quad (3)$$

Then, the process of dehydration of $NH_2CO_2NH_4$ can be observed, causing the formation of the product of interest (urea) and water (Equation 4) [5].

$$NH_2CO_2NH_4 \leftrightarrow NH_2CONH_2+H_2O \quad (4)$$

In addition to the previous reactions, another process that occurs in parallel and that is often not considered in the formation of biuret ($NH_2CONHCONH_2$) (Equation 5) [5].

$$2NH_2CONH_2 \rightarrow NH_2CONHCONH_2+NH_3 \quad (5)$$

As for urea's market applications, the compound is despicable in its performance as a fertilizer, being the most used nitrogen fertilizer in Brazil. All this highlight is mainly due to its high concentration of nitrogen (about 46% of its composition), which is an extremely important compound for the vitality and growth of plants [4].

Bearing in mind the importance of the market of both products, mainly for economic sectors that involve agribusiness (since ammonia is used to produce urea, which is a widely used fertilizer), this work aims to carry out a bibliographical review of the production processes of both and their simulation strategies and about thermodynamic models for NH_3-CO_2-H_2O systems, capable of describing an integrated Ammonia-Urea plant.

Materials and Methods

We did a literature review on ammonia and urea production and simulation processing. Data were collected from open-source platforms like Google Scholar, SciELO, and CAPES, also portals/ websites such as UreaKnowHow and the Aspen Plus simulation files. The keywords used for the state-of-the-art search were: urea, ammonia, simulation, synthesis, Aspen Plus, industrial production, and thermodynamic models.

The research included data about the different technologies used to produce ammonia and urea and the differences between them, thermo-physical-chemical properties; product formation kinetics, and thermodynamic models appropriate for NH_3-CO_2-H_2O systems.

Results and Discussion

This section will approach the review results. Initially, the research focused on obtaining data and information about ammonia production. For this, the main references used were Pattabathula (2016), Sunny (2016), Christensen (2001), Garcês (2021), and the files and reports of the Aspen Plus software.

Ammonia

Process Description

As mentioned in the previous sections, ammonia is produced from the Haber-Bosch reaction (Equation 1), which consists of reacting H_2 and N_2 to form NH_3. However, on an industrial scale, some steps precede and follow this synthesis [1].

To understand these steps, it is necessary to define the type of technology used to produce ammonia. Among the various types of technologies found in the literature, - such as BASF (1910), Kellogg (1960), KBR (Kellogg modified by Braun) - the research focus was given to the Haldor Topsoe's plant (as it is the plant used as a base by Aspen Plus to simulate the ammonia production process) [6].

The process itself can be separated into 8 steps, namely: Natural gas desulfurization, Reforming, CO Conversion, CO_2 Removal, Methanation, Synthesis, Tailgas Scrubbing, and Refrigeration [2].

*Natural Gas Desulfurizatio*n

The natural gas fed to the plant is supplied dry and contains a maximum of 40 ppm - by weight - of sulfur (a poison for the catalyst in the subsequent step) [2,7].

Thus, this step has the function - as the name suggests - to reduce the concentration of sulfur. This reduction is separated into two parts called PDS (Pre-Desulfurization) and FDS (Final Desulfurization). At first, the organic compounds containing sulfur are removed through a catalytic conversion process into H2S, and then catalytic hydrogenation is carried out to remove the residual sulfur [2,7].

Reforming

This stage of the process, like the previous one, is also divided into two parts: primary and secondary reform [1,2].

Here, the hydrocarbons in the feed - now sulfur-free - are converted into hydrogen and carbon oxides (CO and CO_2), so at the end of the process, the reformed gas contains about 0.3% - by volume - of CH_4 [2].

The two main reactions that occur at this stage are as follows (Equations 6 and 7):

$$CH_4+H_2O \rightarrow CO+3H_2 \quad (6)$$

$$CO+H_2O \rightarrow CO_2+H_2 \quad (7)$$

CO Conversion / CO_2 Removal

In these two steps, the objective is to remove all carbon oxides from the mixture to generate Syngas. At first, most of the CO present in the reformed gas is converted into CO_2 in two catalytic stages, the first is high and the second at low temperature, considering the following stoichiometry (Equation 8) [2,7]:

$$CO+H_20 \rightarrow CO_2+H_2 \quad (8)$$

Then, almost all the CO_2 contained in the mixture is removed through absorption in a solution with a concentration of 0.31% methyl-diethanolamine (MDEA). At the end of this process, syngas is obtained - with about 0.1% vol. of CO_2 in the mixture [2].

Methanation

Even in small amounts, carbon oxides are poisonous to the catalyst of the ammonia synthesis step. Thus, these are converted to CH_4 with the aid of a nickel catalyst (Equations 9 and 10). In the end, the remaining carbon oxides do not exceed 10 ppm [2].

$$CO+3H_2 \rightarrow CH_4+H_2O \quad (9)$$

$$CO_2+4H_2 \rightarrow CH_4+2H_20 \quad (10)$$

Synthesis

The syngas, in this step, goes through a centrifugal compressor that raises its pressure to approximately 300 bar and the hydrogen and nitrogen react and are catalytically converted into ammonia by the Haber-Bosch Equation (Equation 1) [2].

In the plant simulated in the aspen plus files, this step uses Haldor Topsoe's S-200 ammonia conversion strategy (Figure 1), which consists of a two-bed radial flow converter with indirect heat exchange between the two beds. In this way, efficient use of the converter volume, low-pressure drops, and high conversion occur - due to indirect cooling [2].

Tailgas Scrubbing/Refrigeration

In tailgas scrubbing, the ammonia present in the purge gas is recovered and fed into the refrigeration unit and the rest of the gas is used as fuel in the reform stage - more specifically in the primary reformer [2].

Finally, the ammonia fed into the refrigeration unit is liquefied and directed to its intended

Figure 1. Ammonia synthesis step – Aspen Plus (hereda 2021).

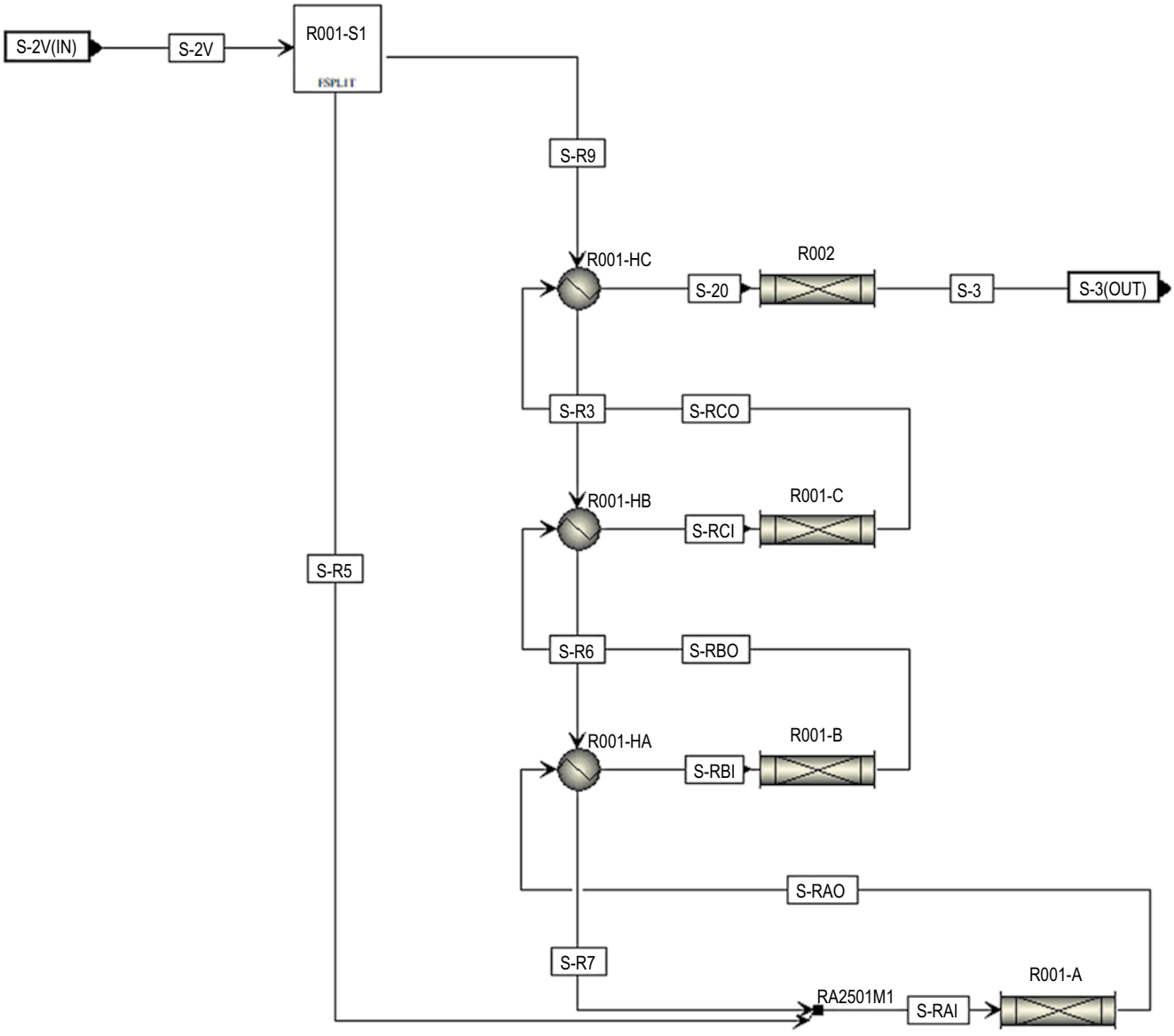

purpose, whether it is feeding the urea plant or for storage. Figure 2 shows an ammonia synthesis plant, which uses the Haldor Topsoe technology, by Profertil [2,7].

Urea

Process Description

Knowing the production of ammonia, the research was able to progress and deepen the urea production process. For this, the main bibliographical references were used for Chinda (2015) and Bispo (2021).

As previously done, first the main urea synthesis technologies were searched and, according to the research, the two most used are those of the companies Stamicarbon and Toyo Engineering - other technologies were also found, such as that of the Snamprogetti company, however, will not be considered in this review [4].

The difference between these two technologies can be seen in the ammonia feed. In the Stamicarbon process, NH_3 is fed into the Carbamate Condenser/

Figure 2. Haldor Topsoe ammonia plant example - Profertil [2,7].

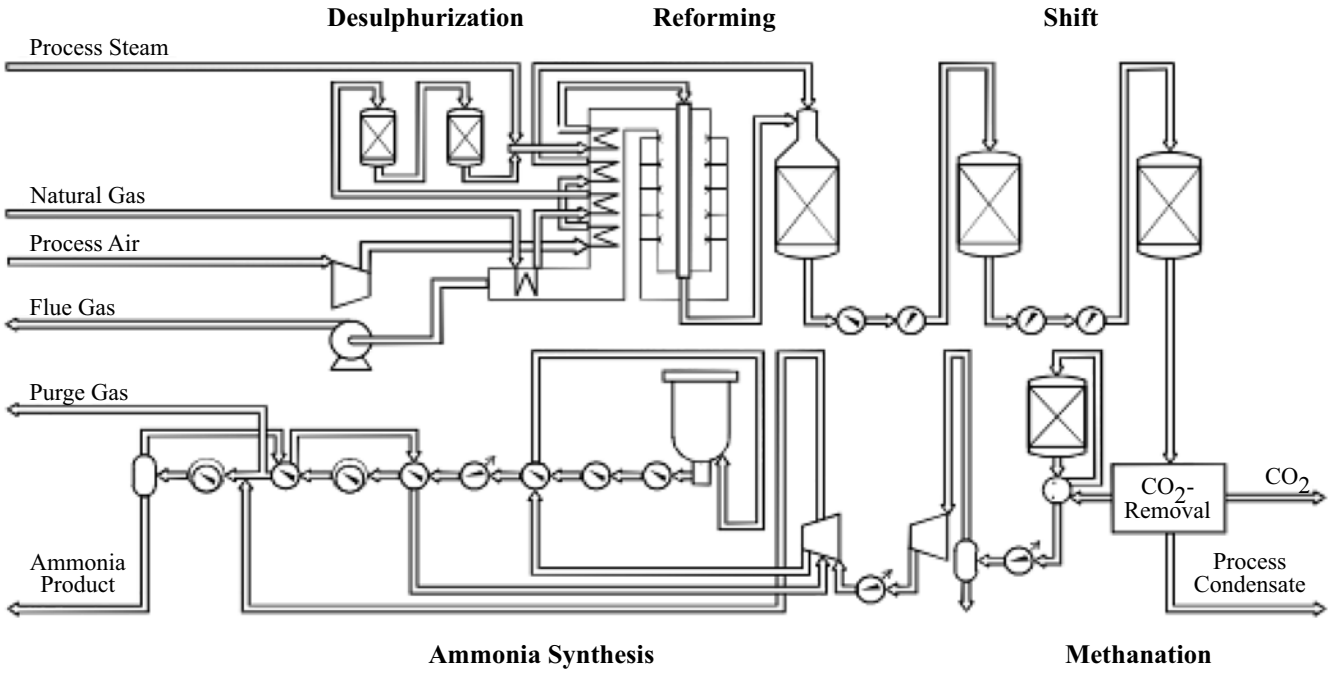

Pool Condenser, while in the ACES21 (Toyo) process, the feed occurs directly into the reactor. This distinction between plants may reverberate in the formation of biuret, since the direct insertion of ammonia into the reactor will increase its concentration in the equipment, disfavoring the reaction to form $NH_2CONHCONH_2$. The research focus was given to the Stamicarbon plant (as it is the plant used as a base by Aspen Plus to simulate the urea production process) (Figure 3) [4,8].

Fugure 3 presents the synthesis section works using CO_2 stripping technology and is composed of four steps/equipment: Stripper, Pool Condenser/ Carbamate Condenser, Reactor, and Scrubber [4,9,10].

Stripper

In the stripper, the decomposition of ammonium carbamate into NH_3 and CO_2 occurs due to the countercurrent contact between the pure CO_2 feed stream and the stream containing the reactor bottom product (composed of ammonium carbamate, urea, water, and biuret). Thus, a gaseous output stream is generated at the top of the equipment, containing ammonia and carbon dioxide, directed to the Pool Condenser, and an underflow containing urea, water, and biuret [4].

Pool Condenser

Feeding NH_3, CO_2, and ammonium carbamate, the Pool Condenser is responsible both for forming the liquid $NH_2CO_2NH_4$ that will dehydrate in the Reactor, forming urea and for synthesizing part of the urea resulting from the process. Then, two outputs are generated and directed to the Reactor, one in the liquid state (urea, ammonium carbamate, and water) and the other in the gaseous state (remaining NH_3 and CO_2) [4].

Reactor

Being fed with urea, carbamate, water, ammonia, and carbon dioxide, the reactor is responsible for providing the three main reactions of the process (Equations 3, 4, and 5). Thus, the equipment has two outlets, the bottom one – composed of ammonium carbamate, urea, H_2O,

Figure 3. Urea synthesis – Stamicarbon x ACES21 (Toyo) [4].

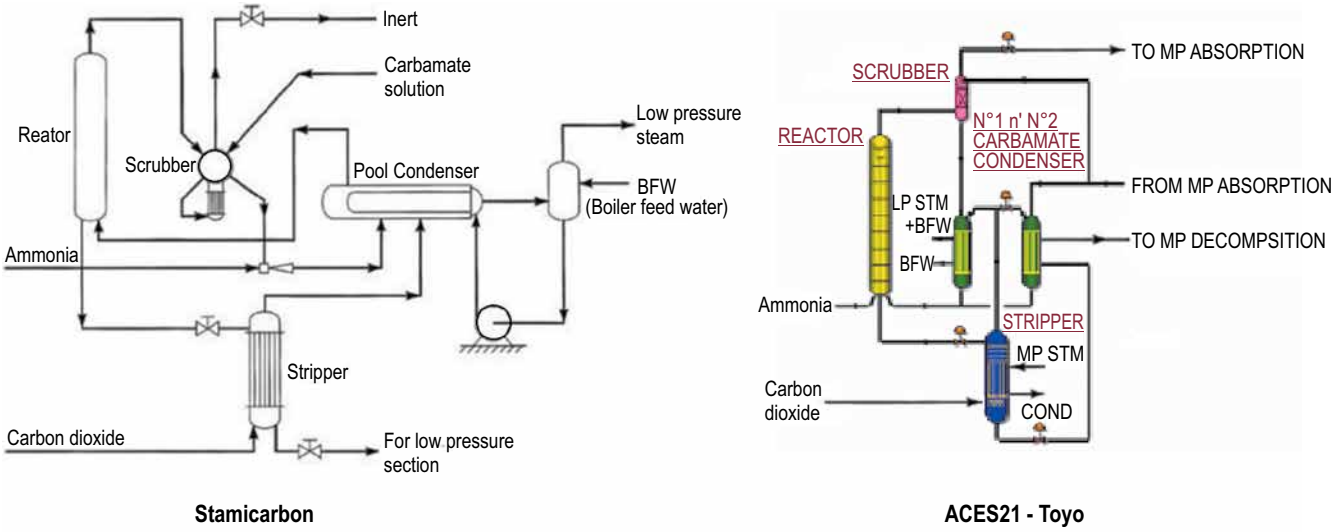

and biuret – and the top one – with unreacted NH_3 and CO_2 [4].

Scrubber

Finally, the scrubber has the function of condensing the gaseous output of the Reactor and forming $NH_2CO_2NH_4$, to send it back to the process to be dehydrated and form the product of interest in the process, urea [4].

Comparison of Thermodynamics Models

After reviewing the functioning of ammonia and urea production plants, the research focused on finding thermodynamic models that better define the studied systems. For this, the main references used were Gudjonsdottir (2016), Chinda (2019), and the files and reports of the Aspen Plus software.

According to Chinda (2019), for example, for the urea synthesis unit explained in this study, the most appropriate thermodynamic model to represent the system, as it can predict non-ideal systems with high efficiency and accuracy, is the SR-POLAR model, used by authors such as Rasheed (2011) and Chinda herself [10].

As for the ammonia process, the aspen plus reports shows that the most appropriate thermodynamic model to define the system is the RKS - BM. In addition, he also reports the use of the NRTL electrolyte method, together with the RKS - BM, to perform the calculations of the liquid and vapor properties in the CO_2 removal unit.

Another interesting approach is that of the author Gudjonsdottir, who performed a comparison between different models to assess their performance in an NH_3-CO_2-H_2O system. Some of the models analyzed were: E-NRTL, E-NRTL2, E-NRTL modified by Que and Chen (2011), extended UNIQUAC, among others [11]. Among the author's conclusions we have: The E-NRTL model modified by Que and Chen (2011) is accurate for CO2 partial pressures at low temperatures (10-40ºC) and also presents better results for NH_3 partial pressure when compared to E-NRTL2; Its computational time is also better when compared to extended UNIQUAC, for example; The modified model of Que and Chen (2011) has an action limit, referring to the concentration - by weight - of NH_3 of 30% [11].

Conclusion

We concluded that it was possible to gather important data about the functioning of each stage

of the ammonia and urea production processes, the types of available technologies, simulation strategies, as well as important information about thermodynamic models used in both processes and for NH_3-CO_2-H_2O systems in general.

The collected data can be used to start simulation attempts of an integrated Ammonia-urea plant, to facilitate future improvement procedures, intensifications, and optimizations.

References

1. Garcês LH, Pessoa FLP. Simulação, otimização e intensificação do processo de produção de amônia. Salvador, 2021.
2. Sunny A, Solomon PA, Aparna K. Syngas production from regasified liquefied natural gas and its simulation using Aspen HYSYS. Journal of Natural Gas Science and Engineering 2016;30:176-181.
3. Silva EL. Amônia – Propriedades e usos., Available at:https://educacao.uol.com.br/disciplinas/quimica/amonia-propriedades-e-usos.htm
4. Bispo AS, Pessoa FLP, Souza ALB. Simulação da seção de síntese de ureia (Stamicarbon) –uma estratégia diferente. Anais do II Congresso Brasileiro Interdisciplinar em Ciência e Tecnologia (CoBICET), August 30, 2021.
5. Kojima Y, Morikawa H, Machfudz M. Development of the ACES 21 process. 2000.
6. Pattabathula V, Richardson J. Introduction to Ammonia Production. CEP – Back to Basics. American Institute of Chemical Engineers (AIChE) 2016:69–75.
7. Christensen PV. Design and Operation of large capacity ammonia plants. 4th Conference for Development and Integration of Petrochemical Industries in the Arab States. May 7–8, 2001 – Bahrain.
8. Hamidepour M, Msotoufi N, Sotudeh-Gharebagh R. Modeling the synthesis section of an industrial urea plant. Chemical Engineering Journal 2005;106:249-260.
9. Chinda RC. Simulação da seção de síntese de uma unidade de produção de ureia – processo Stamicarbon. Rio de Janeiro, 2015.
10. Chinda RC. Process intensification applied to urea production process. Rio de Janeiro, 2019.
11. Gudjondottir V, Ferreira CI. Comparison of models for calculation of the thermodynamic properties of NH_3-CO_2-H_2O mixture. 16th International Refrigeration and Air Conditioning Conference at Purdue, 2016:1–10.

Study of Measurement Systems for Determination of Polycyclic Aromatic Hydrocarbons in Vehicle Environmental Samples

Juliana Carla Santos da Silva[1*], Lilian Lefol Nani Guarieiro[1], Valéria Loureiro da Silva[1]
[1]SENAI CIMATEC University Center; Salvador, Bahia, Brazil

Polycyclic aromatic hydrocarbons (PAHs) are organic compounds with two or more aromatic rings. Their emission sources are anthropogenic, such as burning fossil fuels in vehicles. Due to their properties, these compounds are toxic in nature and have potential carcinogens, requiring attention to their detection in the environment. Several studies have already been conducted for construction-detection systems, nevertheless, the methods are expensive and complex. The objective of this work was to identify these measurement possibilities already used to propose a new, simpler, and cheaper system for determining PAHs. So, we carried out a literature review survey to build the necessary theoretical foundation for the proposed system development.
Keywords: Polycyclic Aromatic Hydrocarbons. Permanent Organic Pollutants. Measurement System. Vehicle Pollution.

Introduction

The exponential growth of the automotive industry in recent decades has increased concerns related to the impact of this large number of vehicles on urban air pollution. The emission of pollutants by vehicles is mainly caused by the burning of fossil fuels such as diesel or gasoline, and among the main pollutants emitted are polycyclic aromatic hydrocarbons (PAHs) [1]. These are organic compounds characterized by two or more condensed aromatics rings in their chain, and they come from the incomplete burning of organic matter [2]. Research studies indicate a strong correlation between the levels of PAH in the air and urban vehicle traffic [1,3,4] among these vehicles, those powered by diesel presented themselves as the source of PAHs [4].

As for the physicochemical nature of PAHs, they are chemically stable compounds, and many of them can be transported over long distances, being able to adhere to particulate material. In addition, when excited in the ultraviolet and visible spectrum, they present the phenomenon of fluorescence, which can be used for their detection [5]. Human exposure to these pollutants occurs through ingestion, inhalation, and through the skin, and during their metabolic process in the human and animal body, they interact with DNA, which could result in a tumor [6].

Due to their properties and interaction with the human body, they have been categorized by the US Environmental Protection Agency as priority pollutants and classified by the International Agency for Research on Cancer (IARC) as potentially carcinogenic compounds to humans and animals [2,6]. Because of the toxic nature of PAHs, several methods of detection of these compounds in samples have been studied over the years, however, the most commonly used methods apply expensive and time-consuming techniques, such as High-Performance Liquid Chromatography (HPLC), Gas Chromatography with Flame Ionizer Detector (GC - DIC) and fluorescence spectrophotometry [2].Therefore, this article aims to study the existing measurement systems and alternatives that could be used in an alternative simple, practical, and fast PAH detection system for vehicle samples.

Materials and Methods

A literature review survey was carried out in scientific databases such as Google Scholar,

Received on 13 December 2021; revised 25 February 2022.
Address for correspondence: Juliana Carla Santos da Silva. Av. Orlando Gomes, 1845 - Piatã, Salvador - BA- Brazil. Zipcode: 41650-010. E-mail: juliana.silva@aln.senaicimatec.edu.br. DOI 10.34178/jbth.v5i1.203.

Science Direct, SciELO, and Research Gate, to select articles on the main polycyclic aromatic hydrocarbons, their characteristics, and their main physicochemical properties followed by a literature survey of methods for detection and identification of existing PAHs. And finally, at the beginning of the construction and characterization stage of the measurement system, we did a theoretical foundation for the construction of the proposed new measurement system.

Results and Discussion

Classification of PAHs

Growing emission of these toxic pollutants, the International Association for Research on Cancer (IARC) carried out experimental procedures and classified 19 main PAHs according to their carcinogenic potential, dividing them into groups (Table 1). Group 1 is a human carcinogen substance; group 2A: probably carcinogenic substance; group 2B: possibly carcinogenic substance; group 3: non-carcinogenic substance and group 4: probably non-carcinogenic [7].

PAHs in-Vehicle Samples

In 2020, in Brazil, it is estimated that there were approximately 107 million vehicles spread across the national territory according to the National Department of Transit (Departamento Nacional de Trânsito – DENATRAN) [8]. Additionally, according to the National Association of Vehicle Manufacturers (Associação Nacional dos Fabricantes de

Table 1. Classification of some PAHs according to the groups established by the IARC [2].

HPA	Classification
Anthracene	Group 3
Benzo [a] anthracene	Group 2B
Benzo [b] fluoranthene	Group 2B
Benzo [j] fluoranthene	Group 2B
Benzo [k] fluoranthene	Group 2B
Benzo [g, h, i] fluoranthene	Group 3
Benzo [c] fenanthrene	Group 2B
Benzo [a] pyrene	Group 1
Benzo [e] pyrene	Group 3
Chrysene	Group 2B
Coronene	Group 3
Dibenzo [a,c] anthracene	Group 3
Dibenzo [a,h] anthracene	Group 2
Dibenzo [a,j] anthracene	Group 3
Fluoranthene	Group 3
Fluorene	Group 3
Indeno [1,2,3-cd] pyrene	Group 2B
Naphthalene	Group 3
Pyrene	Group 3

Veículos Automotores-ANFAVEA) [9], more than 2 million vehicles were produced in the country in 2019. All of these vehicles, before being launched on the market, undergo a rigorous process of analysis and inspection regarding their emissions to control and minimize their environmental impact. Although the vehicle emission control is targeted at regulated pollutants, the study, and control of non-regulated pollutant emissions, such as PAHs, is also relevant, due to their toxic and harmful nature to human beings. In a survey on air pollutants carried out in Portugal, the emissions of 16 HPAs classified by the United States Environment Protection Agency (USEPA) as priority pollutants were analyzed for 40 days in a row. This research concluded that in the urban area, the main source of PAHs was emissions from diesel-powered vehicles [4].

Other studies and surveys showed that in vehicular samples, it was mainly observed the presence of pyrene, naphthalene, phenanthrene, fluoranthene, and chrysene (Figure 1), with concentrations ranging from 1.133 to 5.801 mg km-1 [1,10].

PAH Detection Methods

Due to their carcinogenic potential, PAHs have long been the subject of study in the scientific community, not only regarding their properties but also regarding their detection methods. Table 2 shows the main detection methods for these compounds. All of them are well-founded methods, with proven accuracy and effectiveness. However, their complexity and cost limit the frequency of analyses. Fluorescence applied in the detection of PAHs The phenomenon of fluorescence is characterized by the emission of light by a substance when excited through energy absorption. Nowadays, the fluorescence detection methodology is widely used in the scientific community due to its high selectivity and low complexity [5]. Lakowicz (2006) describes fluorescence as follows: Fluorescence detection is highly sensitive, and there is no longer the need for the expense and difficulties of handling radioactive tracers for most biochemical measurements. There has been dramatic growth in the use of fluorescence for cellular and molecular imaging. Fluorescence imaging can reveal the localization and measurements of intracellular molecules, sometimes at the level of single-molecule detection. The PAHs have this property and as seen in Table 3, there are already studies on the wavelength needed to induce the fluorescence in each of these compounds and the wavelength emitted by them during this phenomenon [11].

Conclusion

In the present study, the main properties and emission sources of polycyclic aromatic hydrocarbons were addressed, their main detection techniques already used in the scientific community, and the theoretical foundation for the construction of an alternative measurement system was initiated. For the continuation of the research, it is necessary to acquire the materials to carry out experiments and demonstrate the technical feasibility of the proposed PAH measurement system. The acquisition process is already in progress, for further work on the study and development of this system.

Figure 1. Chemical structure of PAHs [2].

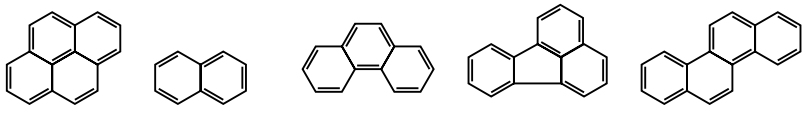

Table 2. PAH determinaton methods [2, 11-13].

Determination Method	Analysis Conditions	System Disadvantages
High Performance Liquid Chromatography (HPLC)	Most used technique for the analysis of PAHs and BaP in food	Equipment cost; complexity of the process by needing to separate the mix of PAHs.
Gas chromatography with flame ionizer detector (GC-DIC)	Allows the analysis of very complex mixtures of PAHs, widely used in oils and fats.	Equipment cost; complexity of the process by needing to separate the mix of PAHs.
Mass spectrometry	Highly sensitive and accurate analytical technique. For analysis, a preparation procedure is needed, which varies according to the sample.	In addition to the cost and complexity, as it is a highly sensitive technique, interference can significantly influence the result.
Fluorescence Spectroscopy	High sensitivity [...] without the need for any process to pre-concentrate numerous types of PAHs.	Equipment cost.
Gas chromatography with mass spectrometry (GC-MS)	Commonly used for qualitative and quantitative analysis of complex mixtures.	Equipment cost, sample preparation complexity, the analytes must be volatiles and thermally stable.

Table 3. Excitation and emission spectrum of some PAHs [11].

PAH	Excitation wavelength (energy absorption)	Maximum fluorescence emission wavelength
Pyrene	334nm	374nm
Benzo [a] pyrene	366nm	406nm
Phenanthrene	247nm	347nm
Chrysene	265nm	365nm
Benzo [a] anthracene	287nm	387nm
Dibenzo [a,h] anthracene	296nm	396nm
Benzo [k] fluoranthene	307nm	407nm
Anthracene	245nm	405nm

Acknowledgments

The CNPq Technologic Initiation Scholarship, the Foundation of Support Research of the State of Bahia (FAPESB) [grant number JCB 0033/2016]; and National Institute of Science and Technology of Energy and Environment (INCT-EA).

References

1. Guarieiro LLN, Vasconcelos PC, Solci MC. Poluentes atmosféricos provenientes da queima de combustíveis fósseis e biocombustíveis: uma breve revisão, 2011.
2. Caruso MSF, Alaburda J. Hidrocarbonetos policíclicos aromáticos-benzo (a) pireno: uma revisão. Revista do Instituto Adolfo Lutz, 2008.

3. Slezakova K, Pires JMC, Castro D et al. Impact of vehicular traffic emissions on particulate-bound PAHs: Levels and associated health risks. Atmospheric Research, 2013.
4. Slezakova K, Pires JMC, Castro D et al. PAH air pollution at a Portuguese urban area: carcinogenic risks and sources identification. Environ Sci Pollut Res, 2013.
5. Lakowucks JR Principles of fluorescence spectroscopy. Springer, 2006.
6. IARC, International Agency for Research on Cancer. Monographs on the evaluation of carcinogenic risk of chemicals to humans: Polynuclear Aromatic Compounds. 92, IARC, Lyon, 2010.
7. Toffolo G, Francischett MN, Greco R. Alguns pressupostos sobre lançamento de efluentes em recursos hídricos, 2013.
8. Ministério da Infraestrutura, Departamento Nacional de Trânsito, Frota de veículos 2020, 2020.
9. Associação Nacional dos Fabricantes de Veículos Automotores. Anuário da Indústria Automobilística Brasileira 2020, São Paulo, 2020.
10. Vieira RP, Guarieiro LLN, Pereira HBB. Representação do conhecimento sobre a emissão de HPA na queima de misturas combustíveis contendo diesel/biodiesel. SENAI CIMATEC, Salvador, 2017.
11. Rodrigues J et al. A espectroscopia de fluorescência sincronizada aplicada na análise qualitativa e quantitativa de hidrocarbonetos policíclicos aromáticos em amostras d'água. Ciência e Natura, 2014.
12. Scharf JS. Avaliação da extração assistida por ultrassom para determinação de metais em borras oleosas por espectrometria de massa com plasma acoplado, 2019.
13. CIA-FURG. Cromatografia Gasosa - GC-MS/MS. Centro Integrado de Análises – Universidade Federal do Rio Grande. Disponível em: < https://cia.furg.br/pt/cromatografia-gasosa-gc-ms-ms>. Acesso em: 20 set 2021.

Instructions for Authors

The Authors must indicate in a cover letter the address, telephone number and e-mail of the corresponding author. The corresponding author will be asked to make a statement confirming that the content of the manuscript represents the views of the co-authors, that neither the corresponding author nor the co-authors have submitted duplicate or overlapping manuscripts elsewhere, and that the items indicated as personal communications in the text are supported by the referenced person. Also, the protocol letter with the number should be included in the submission article, as well as the name of sponsors (if applicable).

Manuscripts may be submitted within designated categories of communication, including:

- Original basic or clinical investigation (original articles on topics of broad interest in the field of bioengineering and biotechnology applied to health). We particularly welcome papers that discuss epidemiological aspects of international health, clinical reports, clinical trials and reports of laboratory investigations.
- Case presentation and discussion (case reports must be carefully documented and must be of importance because they illustrate or describe unusual features or have important practice implications).
- Brief reports of new methods or observations (short communications brief reports of unusual or preliminary findings).
- State-of-the-art presentations (reviews on protocols of importance to readers in diverse geographic areas. These should be comprehensive and fully referenced).
- Review articles (reviews on topics of importance with a new approach in the discussion). However, review articles only will be accepted after an invitation of the Editors.
- Letters to the editor or editorials concerning previous publications (correspondence relating to papers recently published in the Journal, or containing brief reports of unusual or preliminary findings).
- Editor's corner, containing ideas, hypotheses and comments (papers that advance a hypothesis or represent an opinion relating to a topic of current interest).
- Innovative medical products (description of new biotechnology and innovative products applied to health).
- Health innovation initiatives articles (innovative articles of technological production in Brazil and worldwide, national policies and directives related to technology applied to health in our country and abroad).

The authors should checklist comparing the text with the template of the Journal.

Supplements to the JBTH include articles under a unifying theme, such as those summarizing presentations of symposia or focusing on a specific subject. These will be added to the regular publication of the Journal as appropriate, and will be peer reviewed in the same manner as submitted manuscripts.

Statement of Editorial Policy

The editors of the Journal reserve the right to edit manuscripts for clarity, grammar and style. Authors will have an opportunity to review these changes prior to creation of galley proofs. Changes in content after galley proofs will be sent for reviewing and could be required charges to the author. The JBTH does not accept articles which duplicate or overlap publications elsewhere.

Peer-Review Process

All manuscripts are assigned to an Associate Editor by the Editor-in-Chief and Deputy Editor, and sent to outside experts for peer review. The Associate Editor, aided by the reviewers' comments, makes a recommendation to the Editor-in-Chief regarding the merits of the manuscript. The Editor-in-Chief makes a final decision to accept, reject, or request revision of the manuscript. A request for revision does not guarantee ultimate acceptance of the revised manuscript.

Manuscripts may also be sent out for statistical review ou *ad hoc* reviewers. The average time from submission to first decision is three weeks.

Revisions

Manuscripts that are sent back to authors for revision must be returned to the editorial office by 15 days after the date of the revision request. Unless the decision letter specifically indicates otherwise, it is important not to increase the text length of the manuscript in responding to the comments. The cover letter must include a point-by-point response to the reviewers and Editors comments, and should indicate any additional changes made. Any alteration in authorship, including a change in order of authors, must be agreed upon by all authors, and a statement signed by all authors must be submitted to the editorial office.

Style

Manuscripts may be submitted only in electronic form by www.jbth.com.br. Each manuscript will be assigned a registration number, and the author notified that the manuscript is complete and appropriate to begin the review process. The submission file is in OpenOffice, Microsoft Word, or RTF document file format for texts and JPG (300dpi) for figures.

Authors must indicate in a cover letter the address, telephone number, fax number, and e-mail of the corresponding author. The corresponding author will be asked to make a statement confirming that the content of the manuscript represents the views of the co-authors, that neither the corresponding author nor the co-authors have submitted duplicate or overlapping manuscripts elsewhere, and that the items indicated as personal communications in the text are supported by the referenced person.

Manuscripts are to be typed as indicated in Guide for Authors, as well as text, tables, references, legends. All pages are to be numbered with the order of presentation as follows: title page, abstract, text, acknowledgements, references, tables, figure legends and figures. A running title of not more than 40 characters should be at the top of each page. References should be listed consecutively in the text and recorded as follows in the reference list, and must follow the format of the National Library of Medicine as in Index Medicus and "Uniform Requirements for Manuscripts Submitted to Biomedical Journals" or in "Vancouver Citation Style". Titles of journals not listed in Index Medicus should be spelled out in full.

Manuscript style will follow accepted standards. Please refer to the JBTH for guidance. The final style will be determined by the Editor-in-Chief as reviewed and accepted by the manuscript's corresponding author.

Approval of the Ethics Committee

The JBTH will only accept articles that are approved by the ethics committees of the respective institutions (protocol number and/or approval certification should be sent after the references). The protocol number should be included in the end of the Introduction section of the article.

Publication Ethics

Authors should observe high standards with respect to publication ethics as set out by the International Committee of Medical Journal Editors (ICMJE). Falsification or fabrication of data, plagiarism, including duplicate publication of the authors' own work without proper citation, and misappropriation of the work are all unacceptable practices. Any cases of ethical misconduct are treated very seriously and will be dealt with in accordance with the JBTH guidelines.

Conflicts of Interest

At the point of submission, each author should reveal any financial interests or connections, direct or indirect, or other situations that might raise the question of bias in the work reported or the conclusions, implications, or opinions stated - including pertinent commercial or other sources of funding for the individual author(s) or for the associated department(s) or organizations(s), and personal relationships. There is a potential conflict of interest when anyone involved in the publication process has a financial or other beneficial interest in

the products or concepts mentioned in a submitted manuscript or in competing products that might bias his or her judgment.

Material Disclaimer

The opinions expressed in JBTH are those of the authors and contributors, and do not necessarily reflect those of the SENAI CIMATEC, the editors, the editorial board, or the organization with which the authors are affiliated.

Privacy Statement

The names and email addresses entered in this Journal site will be used exclusively for the stated purposes of this journal and will not be made available for any other purpose or to any other party.

Brief Policies of Style

Manuscript	Original	Review	Birief Comunication	Case Report	Editorial ; Letter to the Editor; Editor' s Corner	Innovative Medical Products	State-of-the-Art	Health Innovation Initiatives
Font Type	Times or Arial	Times or Arial	Times or Arial	Times or Arial	Times or Arial	Times or Arial	Times or Arial	Times or Arial
Number of Words – Title	120	90	95	85	70	60	120	90
Font Size/Space-Title	12; double space	12; double space	12; double space	12; double space	12; double space	12; double space	12; double space	12; double space
Font Size/Space-Abstracts/Key Words and Abbreviations	10; single space	10; single space	10; single space	10; single space	-	-	10; single space	10; single space
Number of Words – Abstracts/Key Words	300/5	300/5	200/5	250/5	-	-	300/5	300/5
Font Size/Space-Text	12; Double space	12; Double space	12; Double space	12; Double space	12; Double space	12; Double space	12; Double space	12; Double space
Number of Words – Text	5,000 including spaces	5,500 including spaces	2,500 including spaces	1,000 including spaces	1,000 including spaces	550 including spaces	5,000 including spaces	5,500 including spaces
Number of Figures	8 (title font size 12, double space)	3 (title font size 12, double space)	2 (title font size 12, double space)	2 (title font size 12, double space)	-	2 (title font size 12, double space)	8 (title font size 12, double space)	8 (title font size 12, double space)
Number of Tables/Graphic	7 title font size 12, double space	2 title font size 12, double space	2(title font size 12, double space)	1(title font size 12, double space)	-	-	7 title font size 12, double space	4 title font size 12, double space
Number of Authors and Co-authors*	15	10	5	10	3	3	15	10
References	20 (font size 10,single space	30(font size 10,single space	15 (font size 10,single space)	10 (font size 10,single space)	10 (font size 10,single space	5(font size 10,single space	20 (font size 10,single space	20

*First and last name with a sequencing overwritten number. Corresponding author(s) should be identified with an asterisk; Type 10, Times or Arial, single space. Running title of not more than 40 characters should be at the top of each page. References should be listed consecutively in the text. References must be cited on (not above) the line of text and in brackets instead of parentheses, e.g., [7,8]. References must be numbered in the order in which they appear in the text. References not cited in the text cannot appear in the reference section. References only or first cited in a table or figures are numbered according to where the table or figure is cited in the text. For instance, if a table is placed after reference 8, a new reference cited in table 1 would be reference 9.1 would be reference 9.

Checklist for Submitted Manuscripts

❑1. Please provide a cover letter with your submission specifying the corresponding author as well as an address, telephone number and e-mail.

❑2. Submit your paper using our website www.jbth.com.br. Use Word Perfect/Word for Windows, each with a complete set of original illustrations.

❑3. The entire manuscript (including tables and references) must be typed according to the guidelines instructions.

❑4. The order of appearance of material in all manuscripts should be as follows: title page, abstract, text, acknowledgements, references, tables, figures/graphics/diagrams with the respective legends.

❑5. The title page must include a title of not more than three printed lines (please check the guidelines of each specific manuscript), authors (no titles or degrees), institutional affiliations, a running headline of not more than 40 letters with spaces.

❑6. Acknowledgements of persons who assisted the authors should be included on the page preceding the references.

❑7. References must begin on a separate page.

❑8. References must be cited on (not above) the line of text and in brackets instead of parentheses, e.g., [7,8].

❑9. References must be numbered in the order in which they appear in the text. References not cited in the text cannot appear in the reference section. References only or first cited in a table or figures are numbered according to where the table or figure is cited in the text. For instance, if a table is placed after reference 8, a new reference cited in table 1 would be reference 9.

❑10. Reference citations must follow the format established by the "Uniform Requirements for Manuscripts Submitted to Biomedical Journals" or in "Vancouver Citation Style".

❑11. If you reference your own unpublished work (i.e., an "in press" article) in the manuscript that you are submitting, you must attach a file of the "in press" article and an acceptance letter from the journal.

❑12. If you cite unpublished data that are not your own, you must provide a letter of permission from the author of that publication.

❑13. Please provide each figure in high quality (minimum 300 dpi: JPG or TIF). Figure must be on a separate file.

❑14. If the study received a financial support, the name of the sponsors must be included in the cover letter and in the text, after the author's affiliations.

❑15. Provide the number of the Ethics Committees (please check the guidelines for authors).